School of Neutron Scattering Francesco Paolo Ricci
International School of Neutron Science and Instrument
Erice July 28th – August 4th 2015

Triple-Axis Neutron Spectrometer

Kazuhisa Kakurai

Quantum Beam Science Center, Japan Atomic Energy Agency (JAEA)
Tokai, Ibaraki 319-1195, Japan
&
Center for Emergent Matter Science, RIKEN, Wako, Saitama 351-0198, Japan
&
Jülich Centre for Neutron Science, Maier-Leibnitz-Zentrum, Garching, Germany

Acknowledgement: Helmholtz Gesellschaft for awarding the International fellowship

Main Facilities of JAEA for Quantum Beam Science &Technology

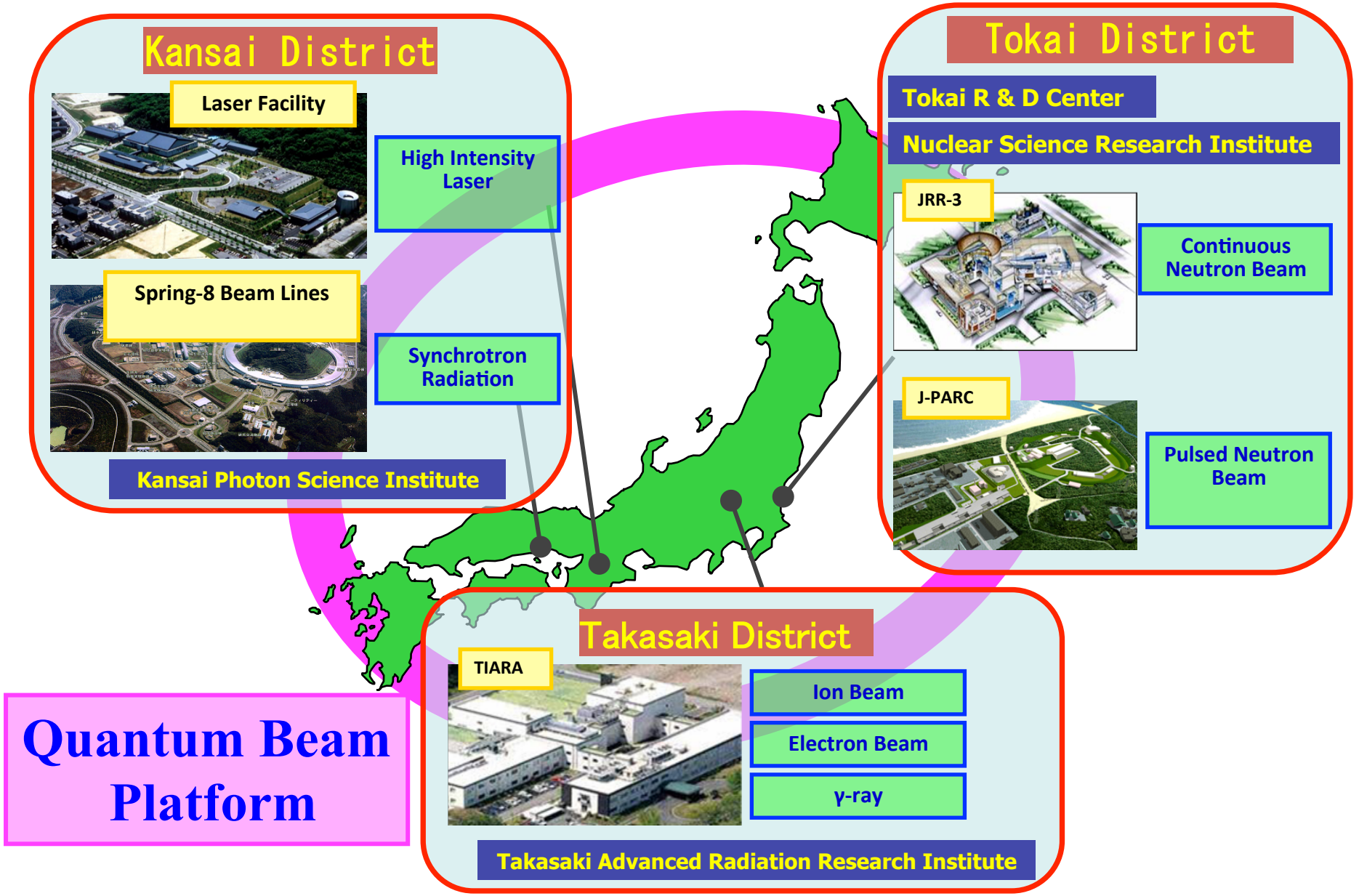

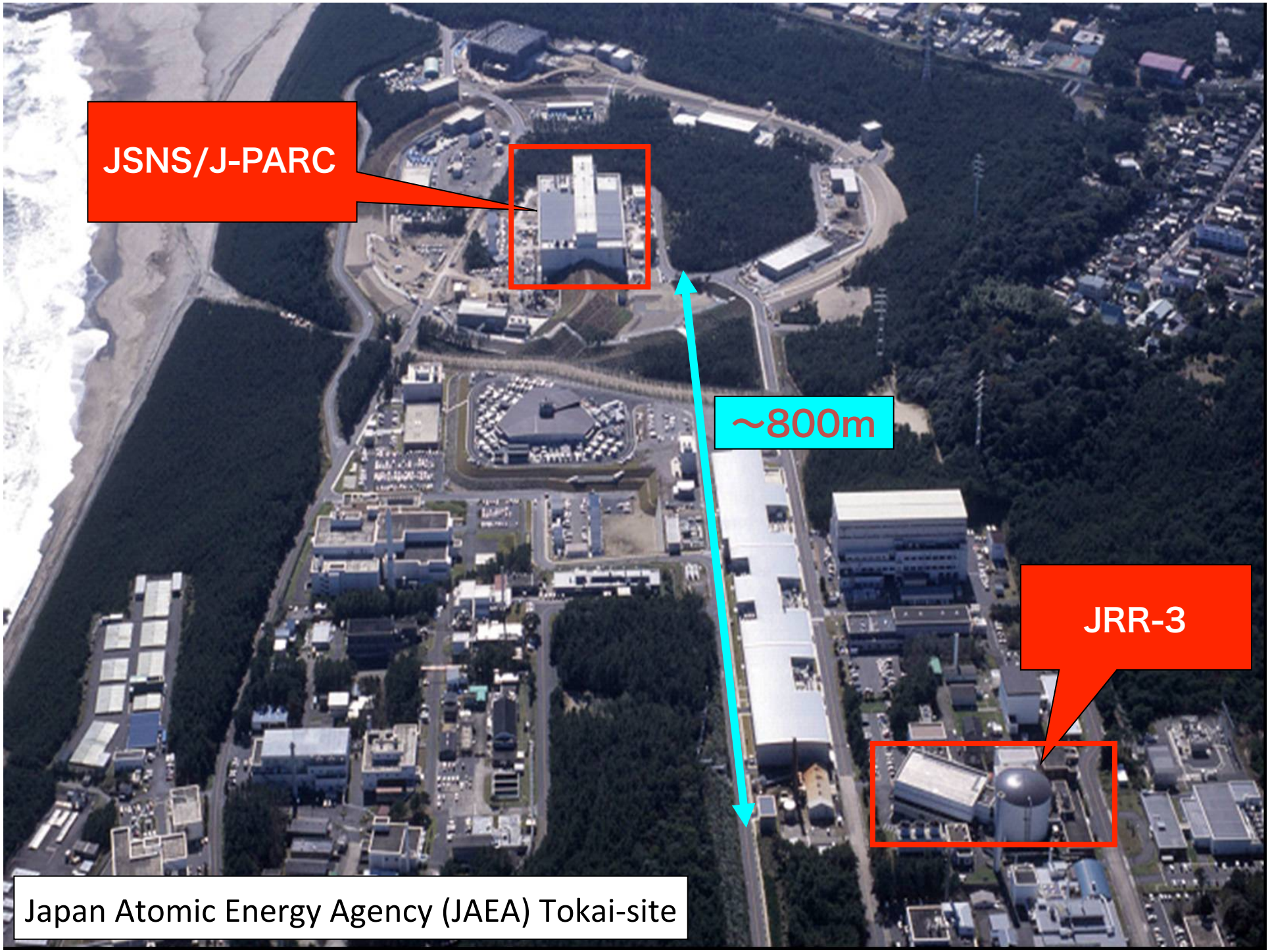
JSNS/J-PARC
~800m
JRR-3
Japan Atomic Energy Agency (JAEA) Tokai-site

JRR-3

1962 Construction,1990 Refurbishment

- thermal power 20MW, with CNS
- neutron flux 3×10^{14} n/s.cm^2

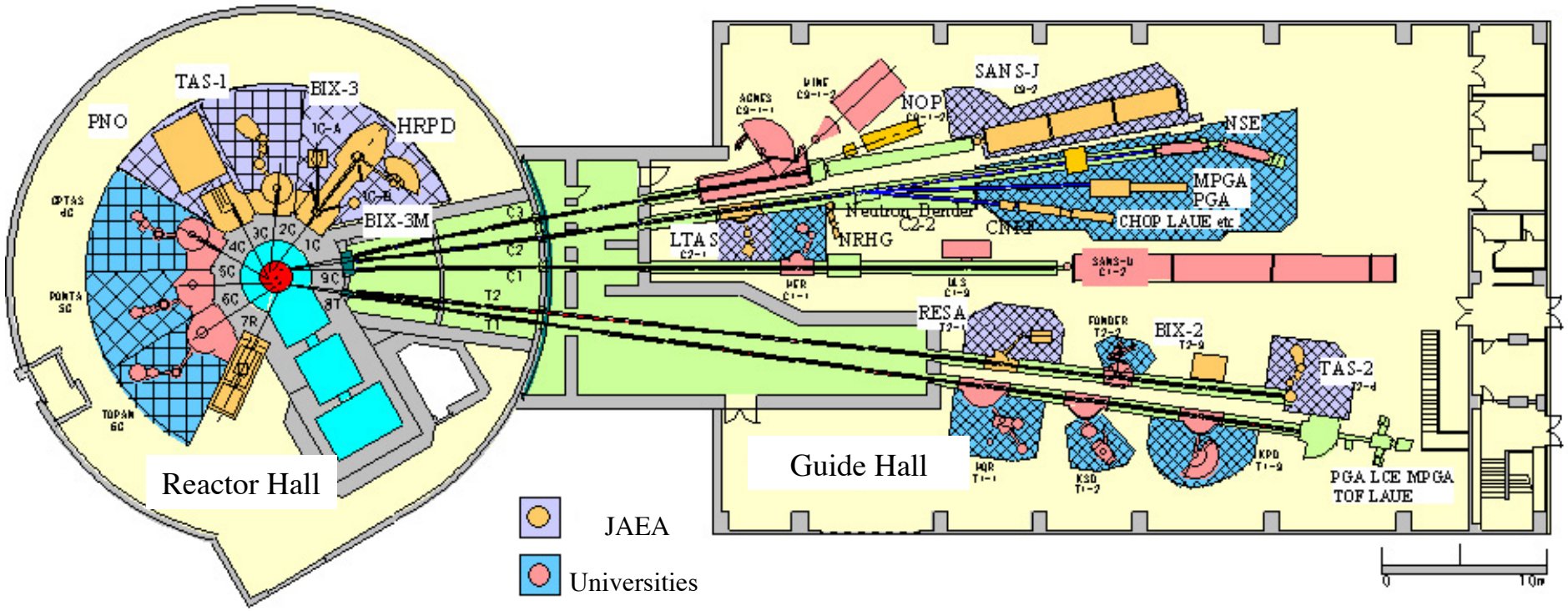

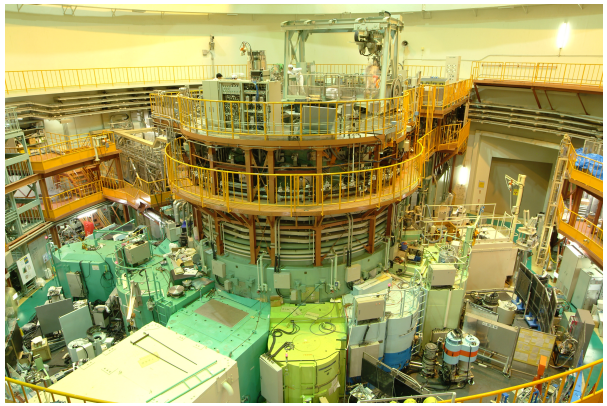

Neutron Beam Instruments

- Diffractometer and Spectrometer : 30
  (Universities 14 +JAEA 16)
- Radiography : 2 (JAEA)
- Prompt gamma analysis : 2 (JAEA)

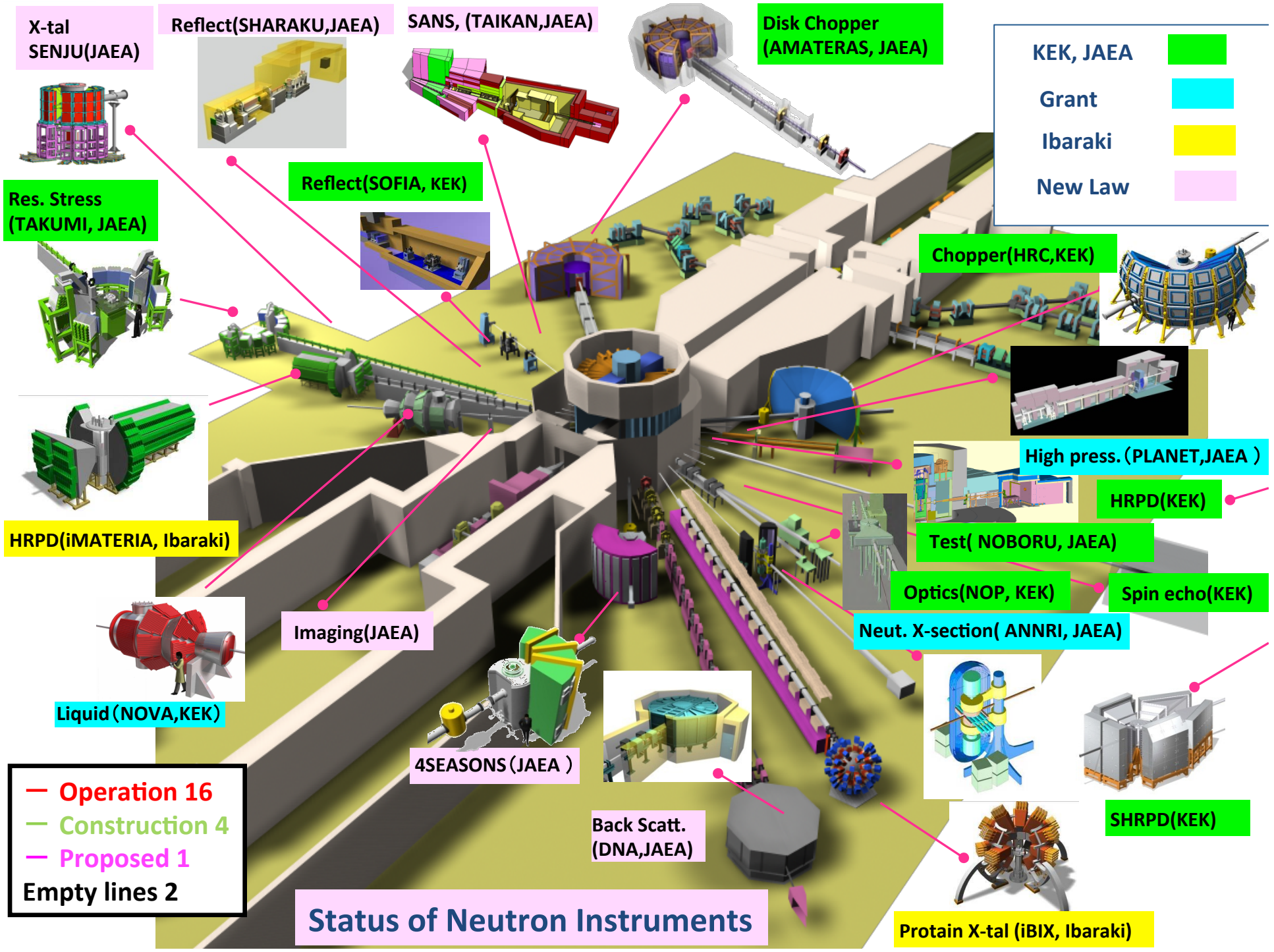
X-tal
SENJU(JAEA)
Reflect(SHARAKU,JAEA)
SANS, (TAIKAN,JAEA)
Disk Chopper
(AMATERAS, JAEA)
KEK, JAEA
Grant
Ibaraki
New Law
Reflect(SOFIA, KEK)
Res. Stress
(TAKUMI, JAEA)
Chopper(HRC,KEK)
High press.（PLANET,JAEA ）
HRPD(KEK)
HRPD(iMATERIA, Ibaraki)
Test(NOBORU, JAEA)
Optics(NOP, KEK)
Spin echo(KEK)
Neut. X-section(ANNRI, JAEA)
Imaging(JAEA)
Liquid（NOVA,KEK）
4SEASONS（JAEA ）
Back Scatt.
(DNA,JAEA)
SHRPD(KEK)
Protain X-tal (iBIX, Ibaraki)
— Operation 16
— Construction 4
— Proposed 1
Empty lines 2
Status of Neutron Instruments

Development of Neutron Beam Techniques at JRR-3

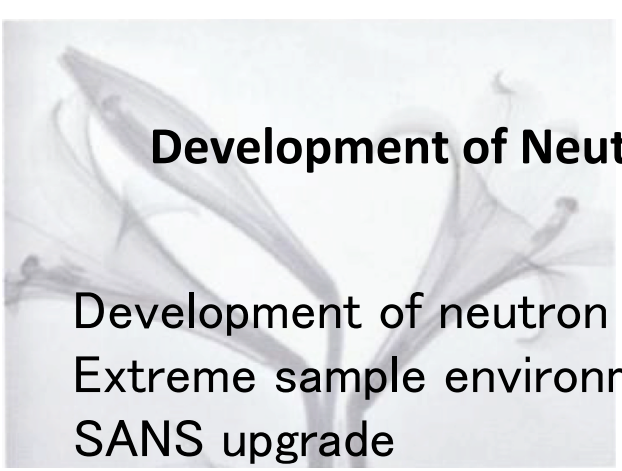

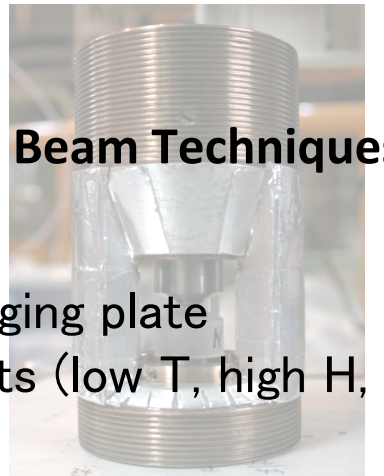

Development of neutron imaging plate
Extreme sample environments (low T, high H, high P)
SANS upgrade
Development of neutron optics（magnetic lens、mirror、detector）
Polarized neutron upgrade（higher flux, 3-D polarization analysis）
Installation of reflectometer
LTAS upgrade
High energy transfer（Cu monochromator）

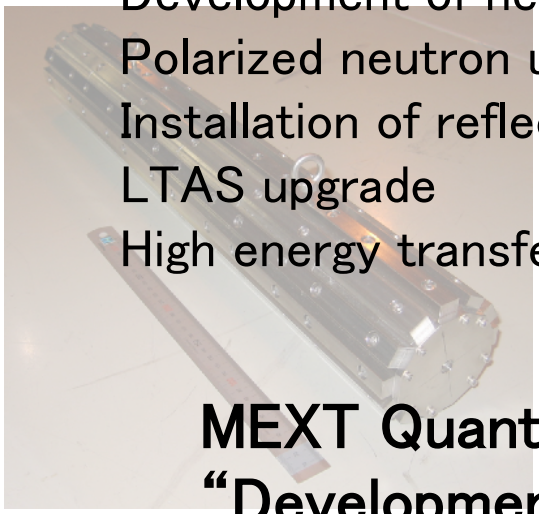

MEXT Quantum Beam Technique Development Program
“Development of Neutron Beam Fundamentals Techniques”

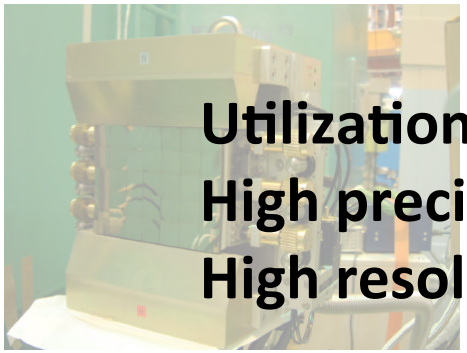

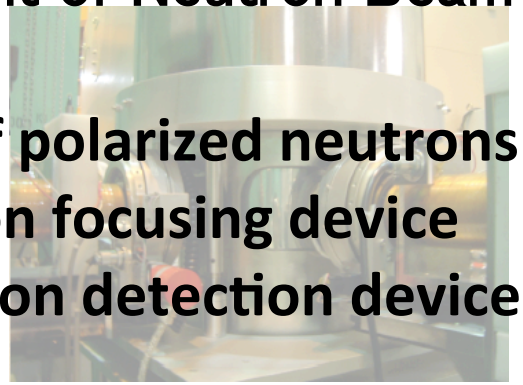

Utilization of polarized neutrons e.g. ^{3}He polarization filter
High precision focusing device
High resolution detection device

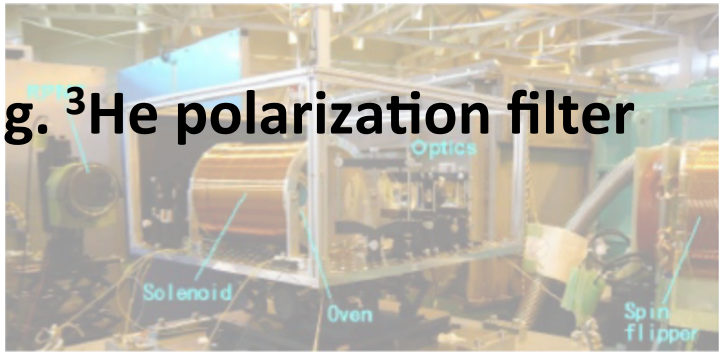

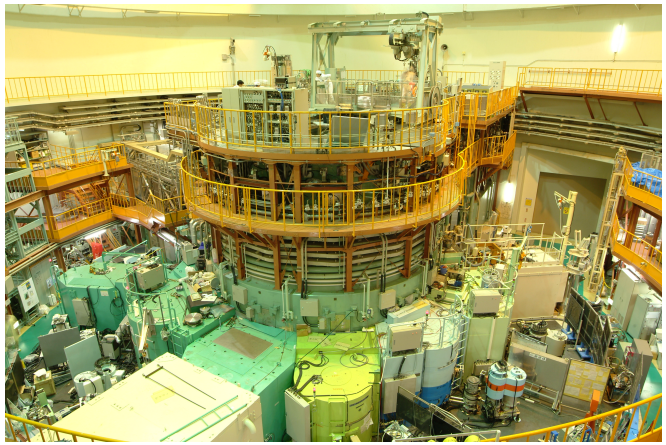

- Neutron Scattering: 25 (14 by Univ. & 11 by JAEA)
- Neutron Radiography: 2 (JAEA)
- Prompt Gamma-ray Analysis: 2 (JAEA)

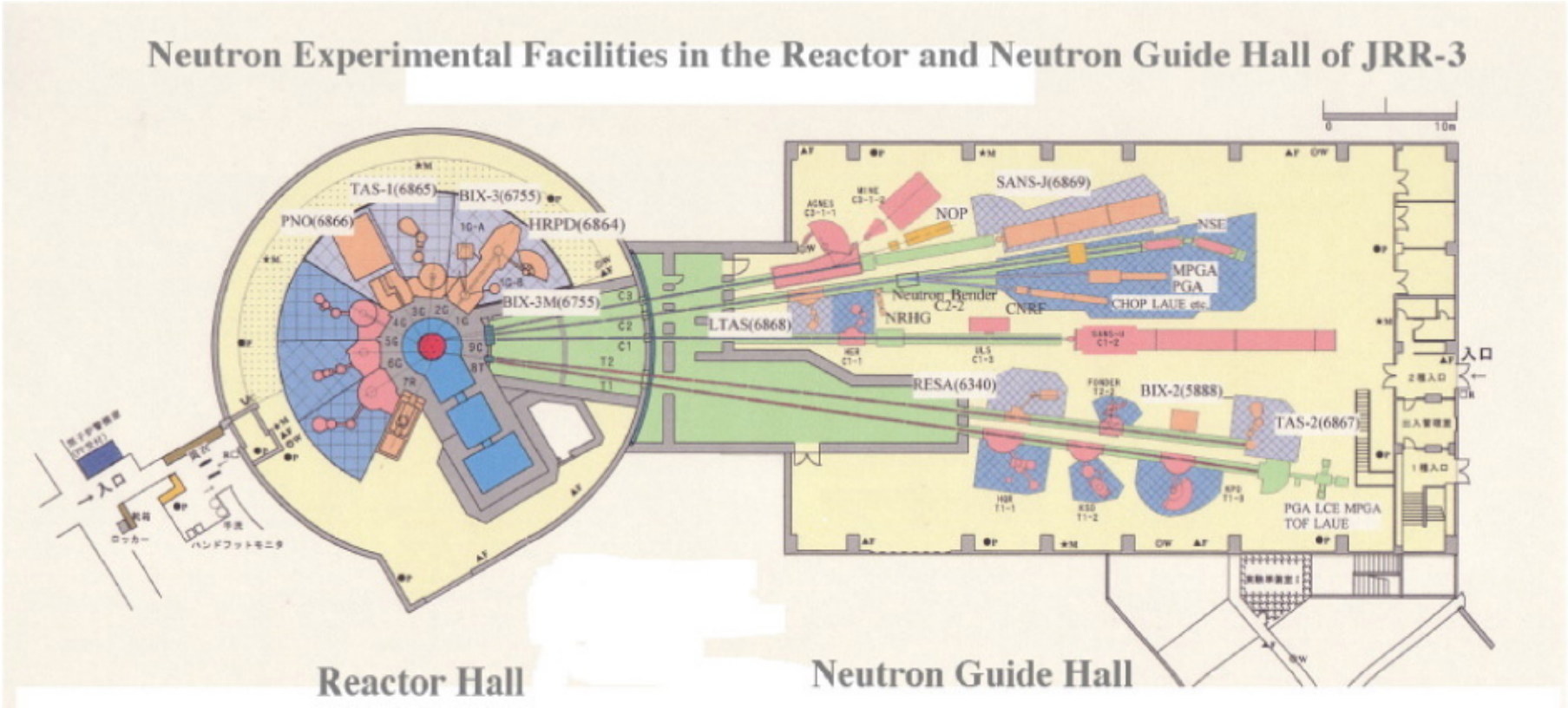

(20MW, 3×10^{14} n/(sec cm^2), CNS)

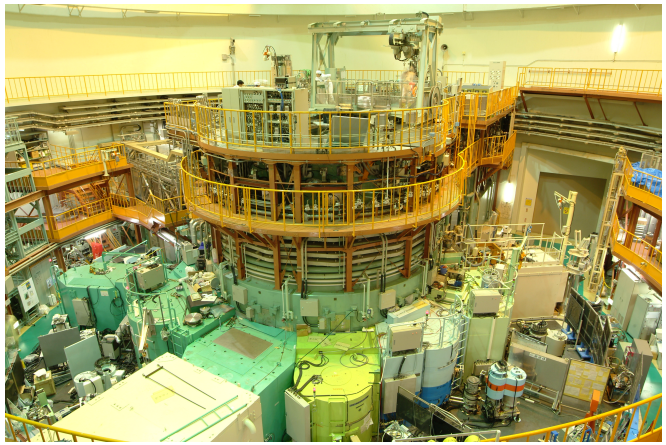

Thermal neutron triple axis instruments in the reactor hall

TAS-1(JAEA), GPTAS(ISSP), PONTA(ISSP) & TOPAN(Tohoku)

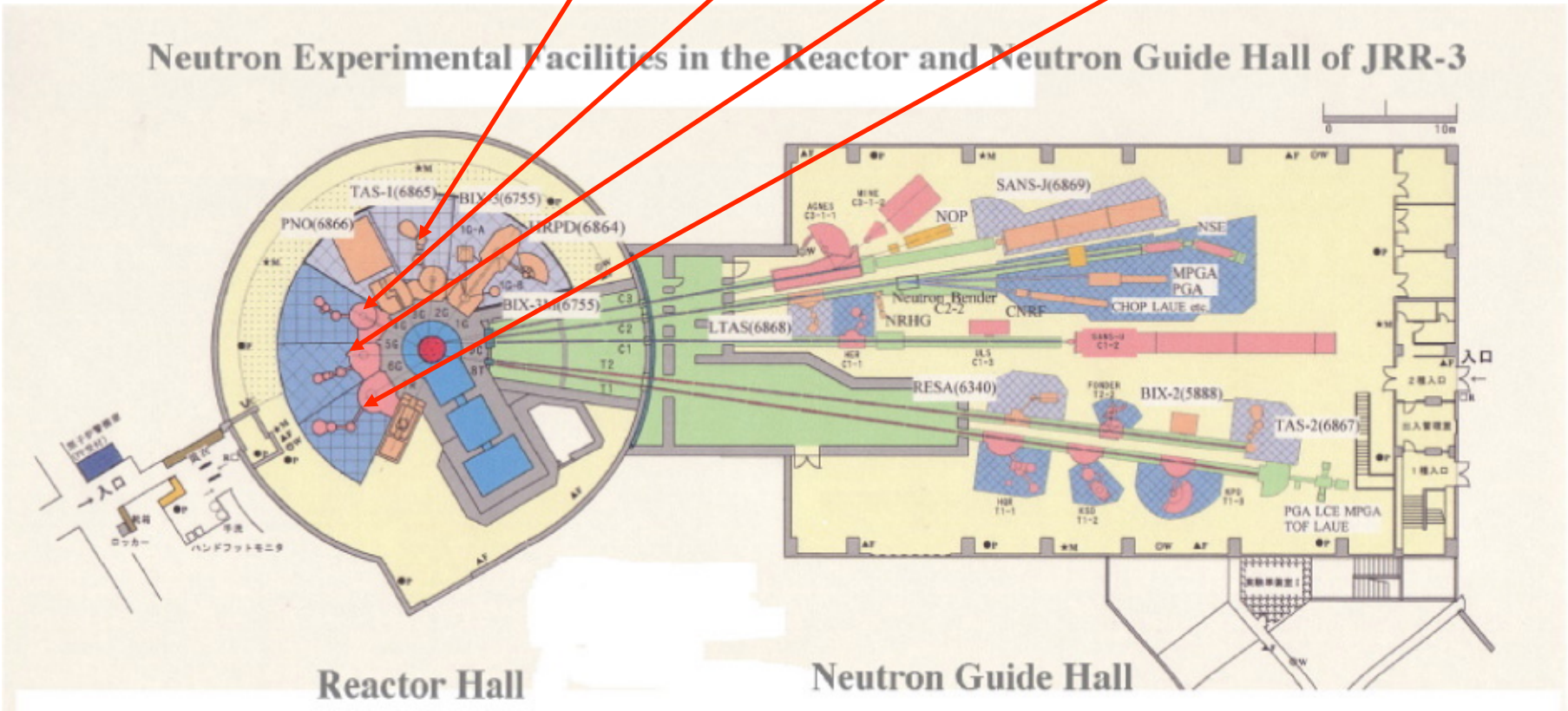

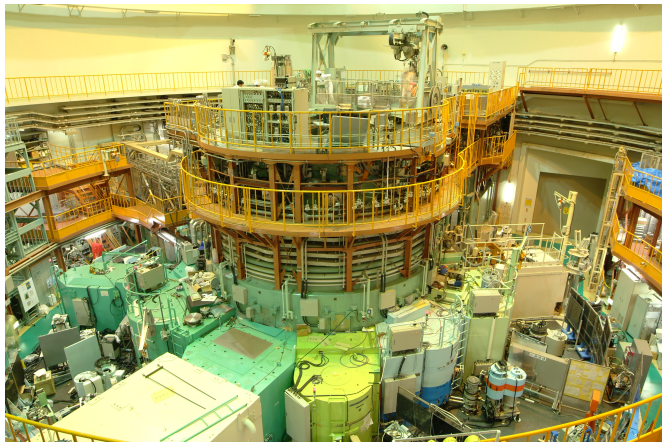

Thermal neutron triple axis instruments in the guide hall

HQR(ISSP), TAS-2(JAEA),

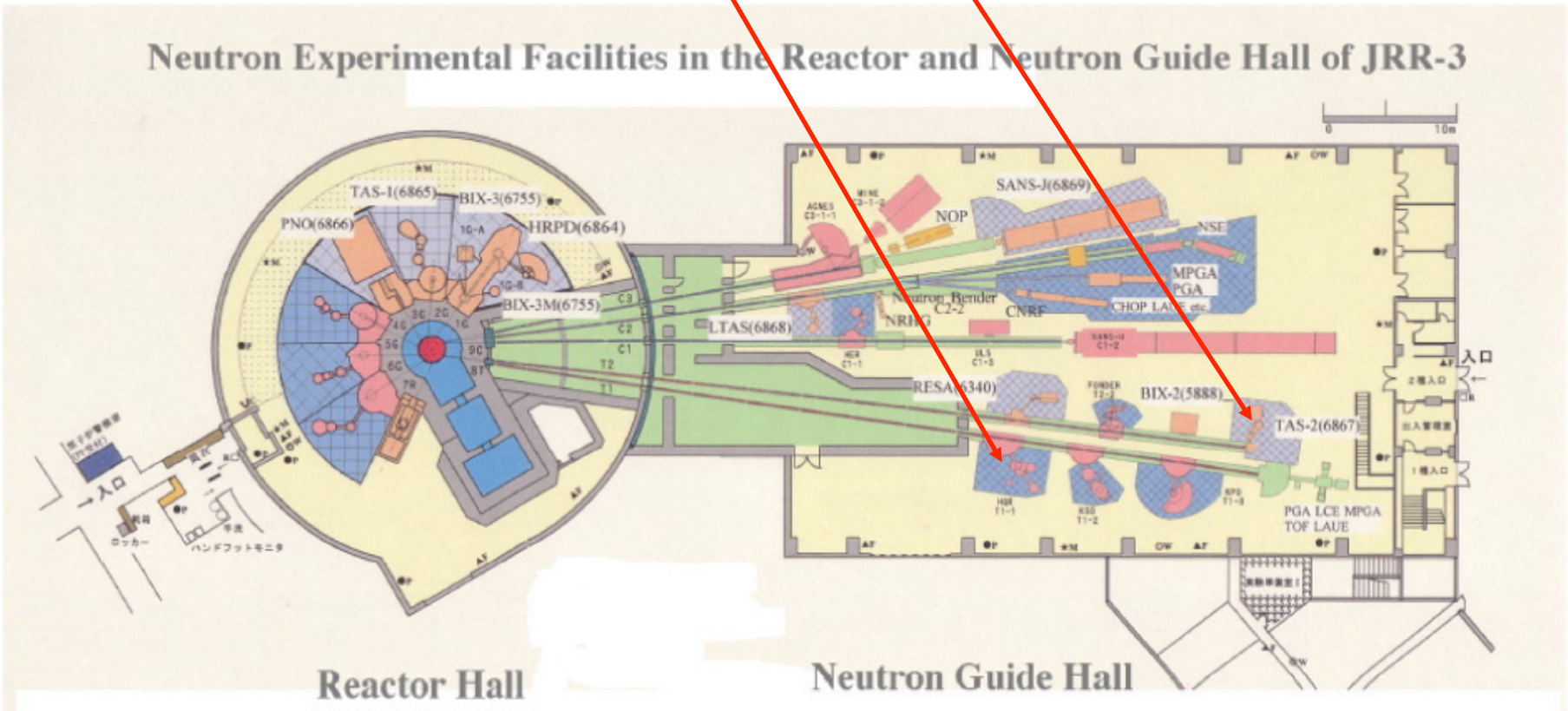

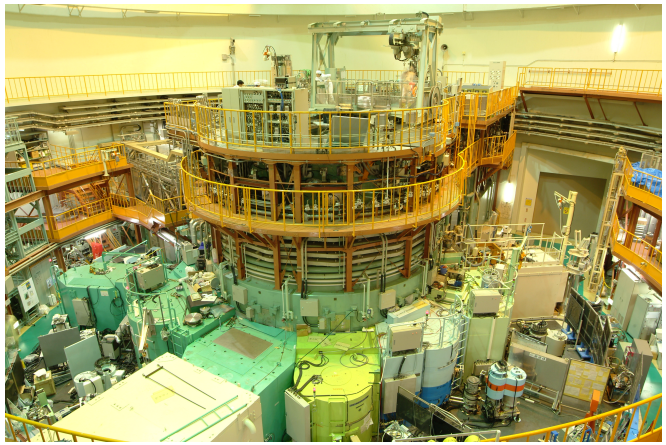

Cold neutron triple axis instruments in the guide hall

LTAS(JAEA), HER(ISSP)

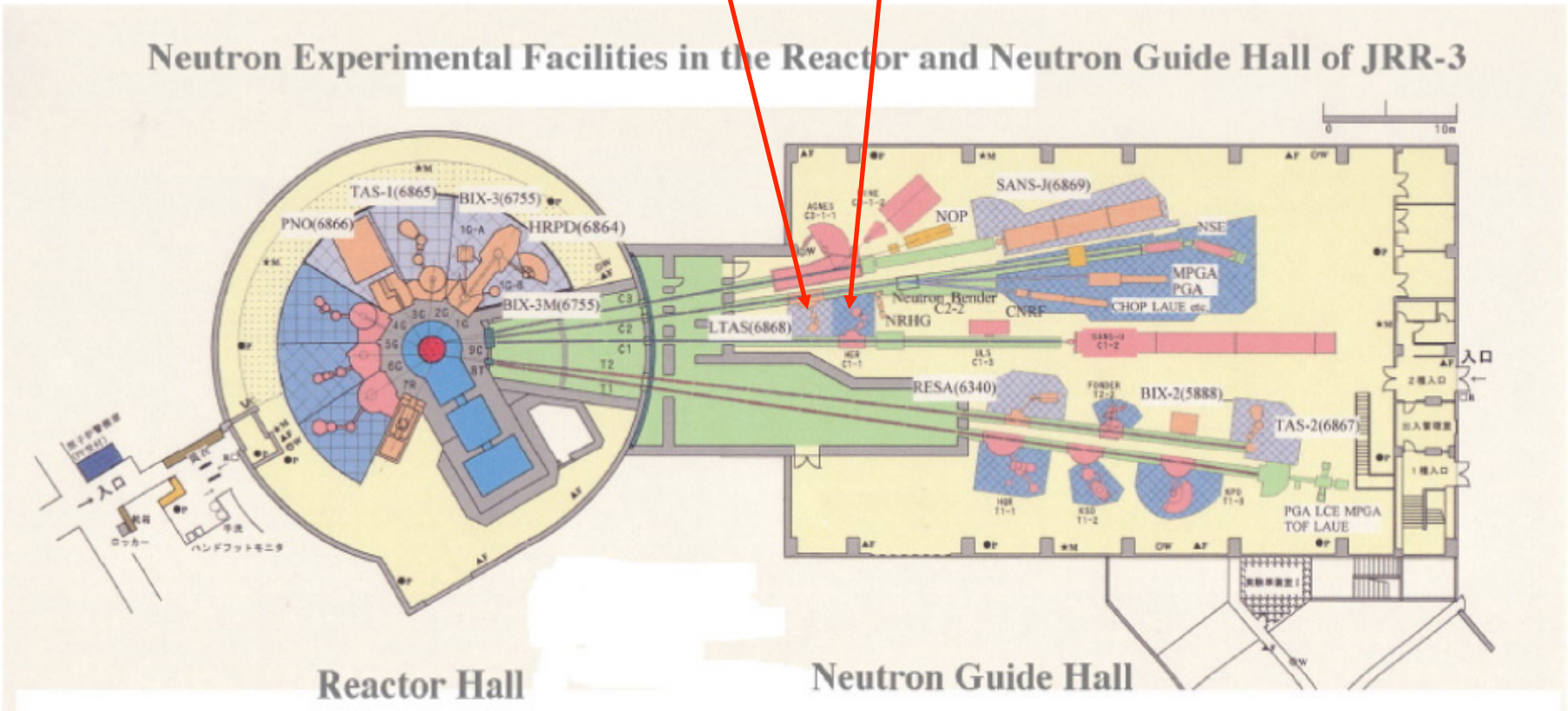


WT 25000 KG
NKK

TAS-1 at JRR-3 of JAEA

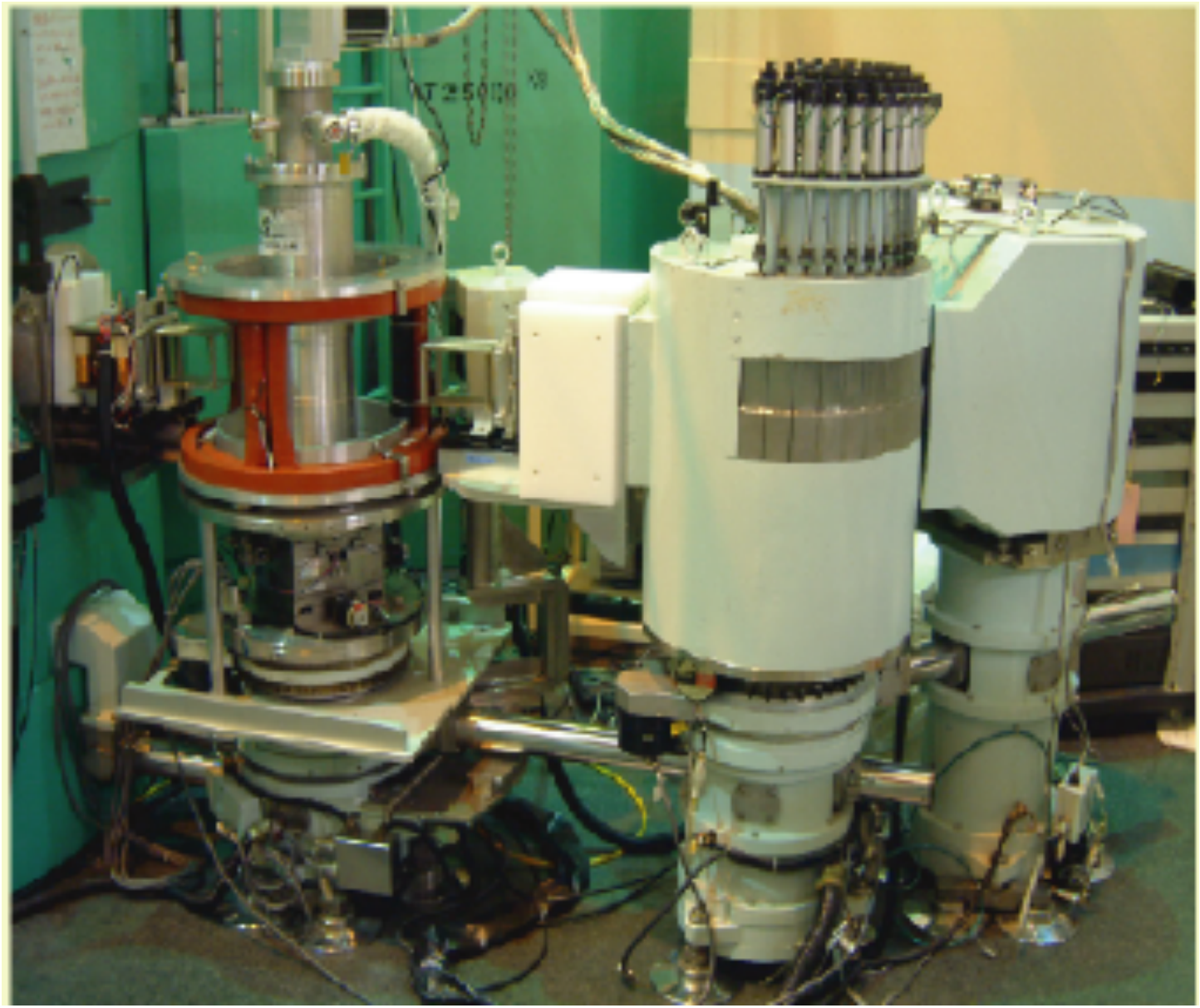

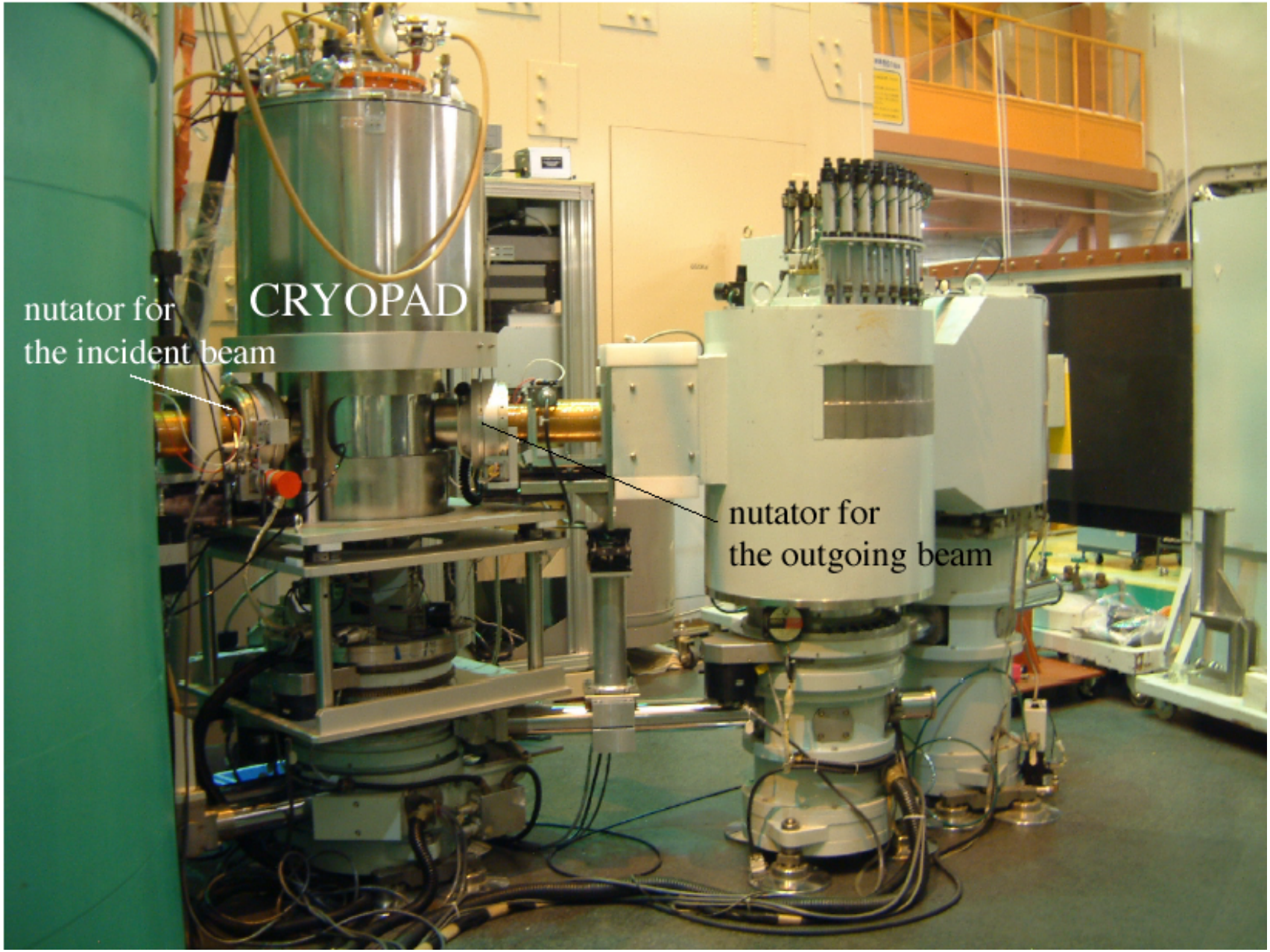
nutator for
the incident beam
CRYOPAD
nutator for
the outgoing beam

Development of Thermal Neutron Spin Echo Option for 3-Axis Spectrometer

K. Kakurai, C.M.E. Zeyen, M. Nishi, K. Nakajima, T. Sakaguchi, Y. Kawamura,

S. Watanabe, Y. Endoh; ISSP, ILL and Tohoku Univ.

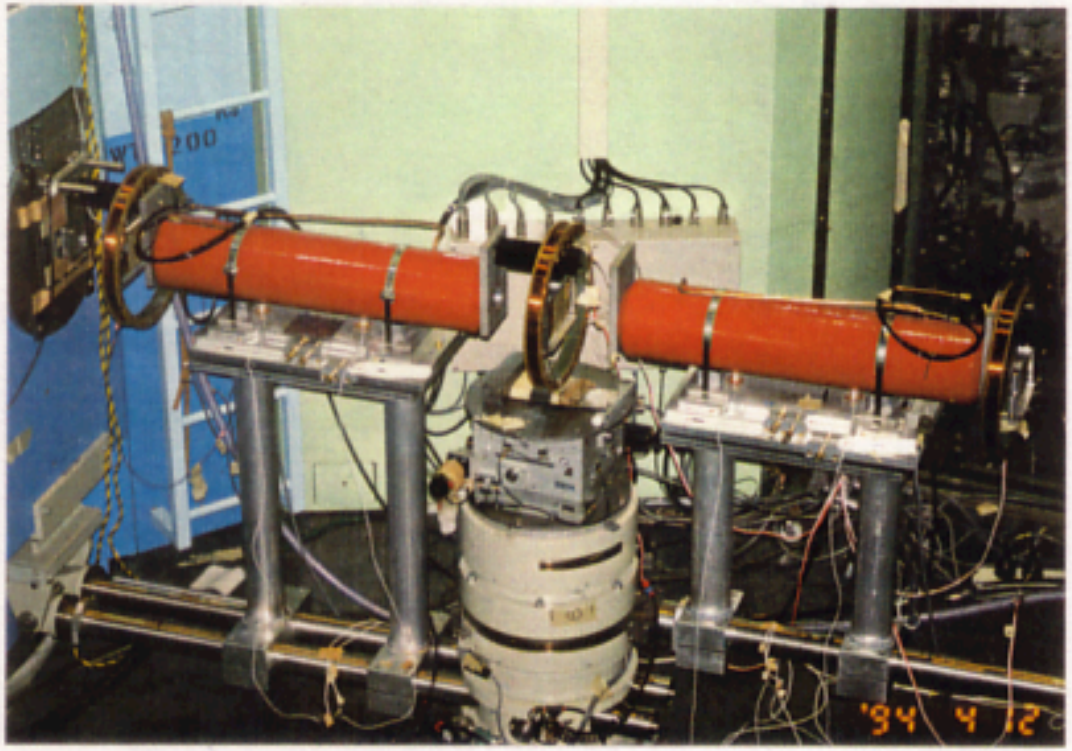

Energy resolution of $\Delta E/E_i \sim 10^{-5}$

Outline

- Recap of triple axis spectrometry
- Magnetic excitations in quasi-1-dimensional magnet and quantum magnet

Outline

- Recap of triple axis spectrometry
- Magnetic excitations in quasi-1-dimensional magnet and quantum magnet

Brockhouse and Shull: 1994 Nobel Prize in Physics

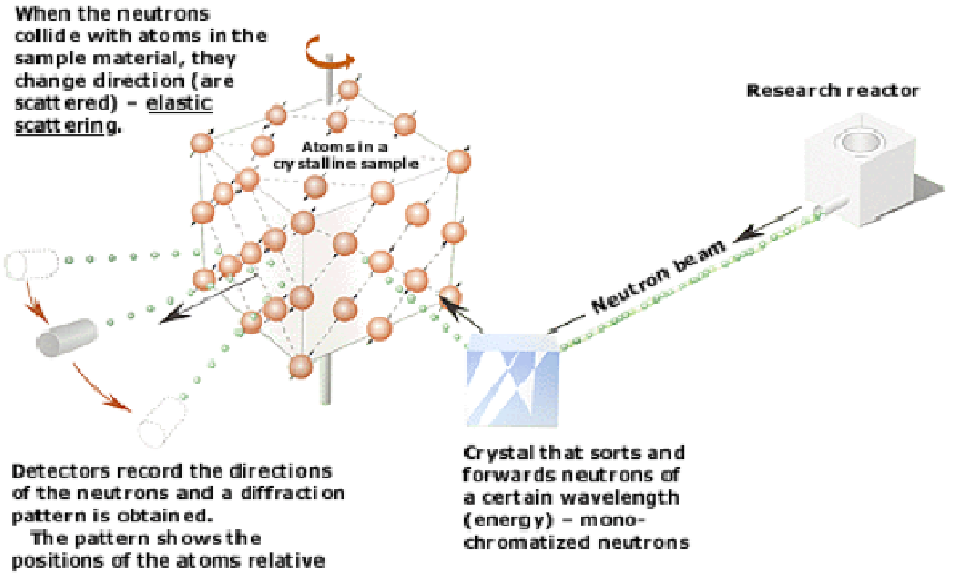

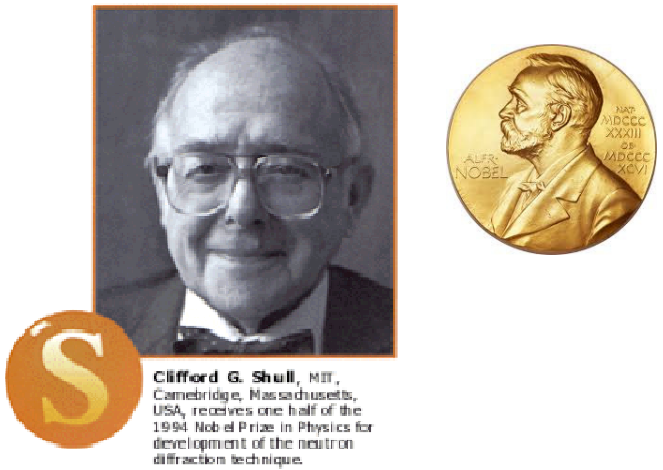

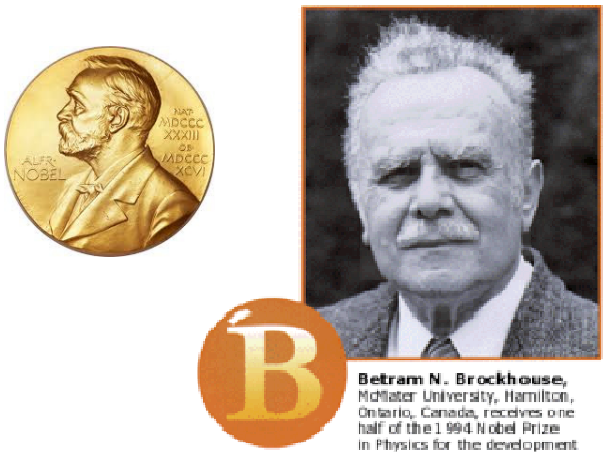

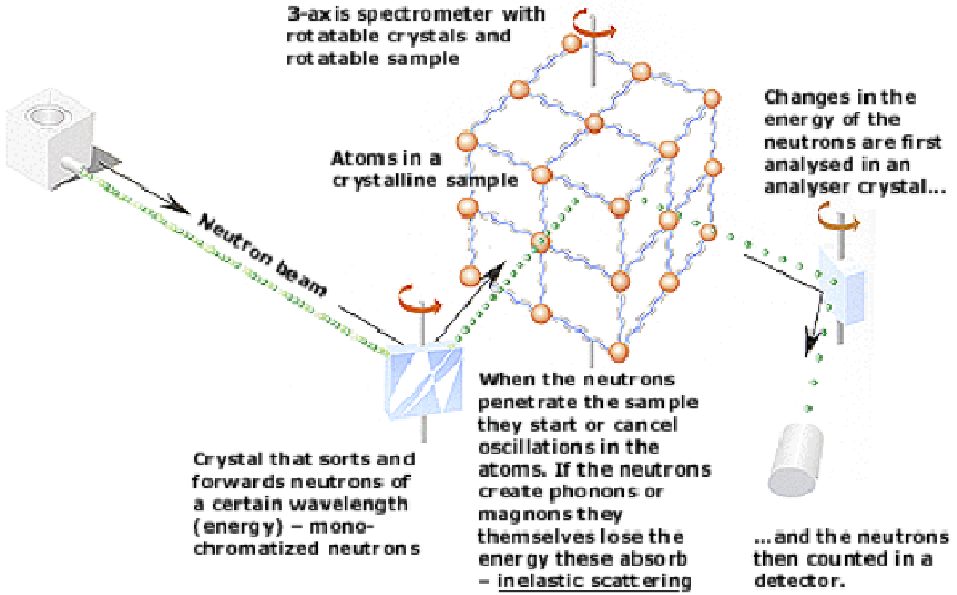

Brockhouse's Triple Axis Spectrometer

$| \mathbf{k}_i | = 2\pi / \lambda_i$

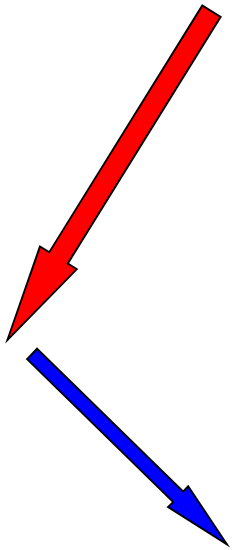

$| \mathbf{k}_f | = 2\pi / \lambda_f$

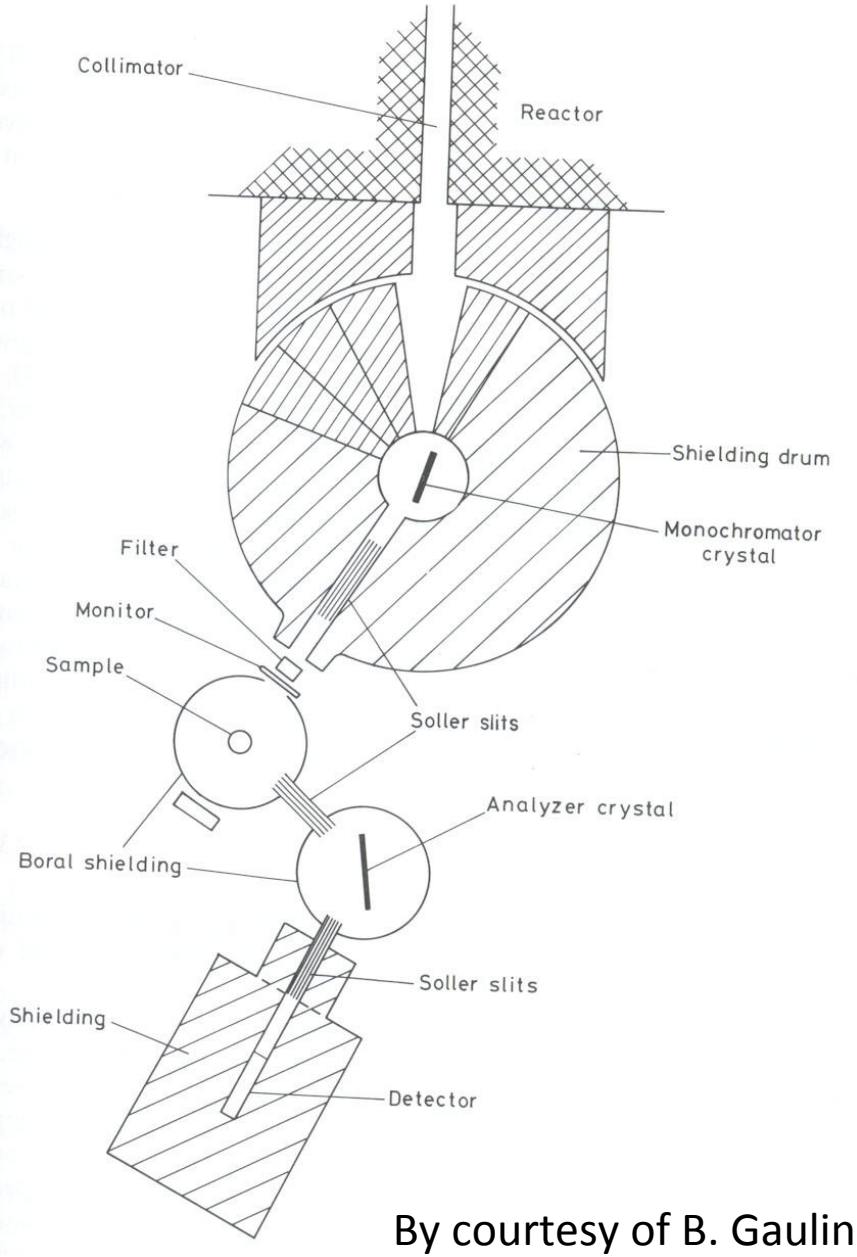

By courtesy of B. Gaulin

Momentum Transfer:

$$Q = k_f - k_i$$

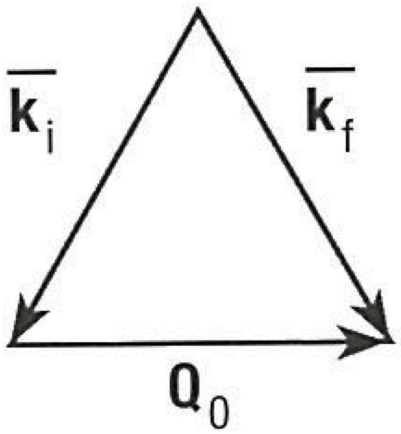

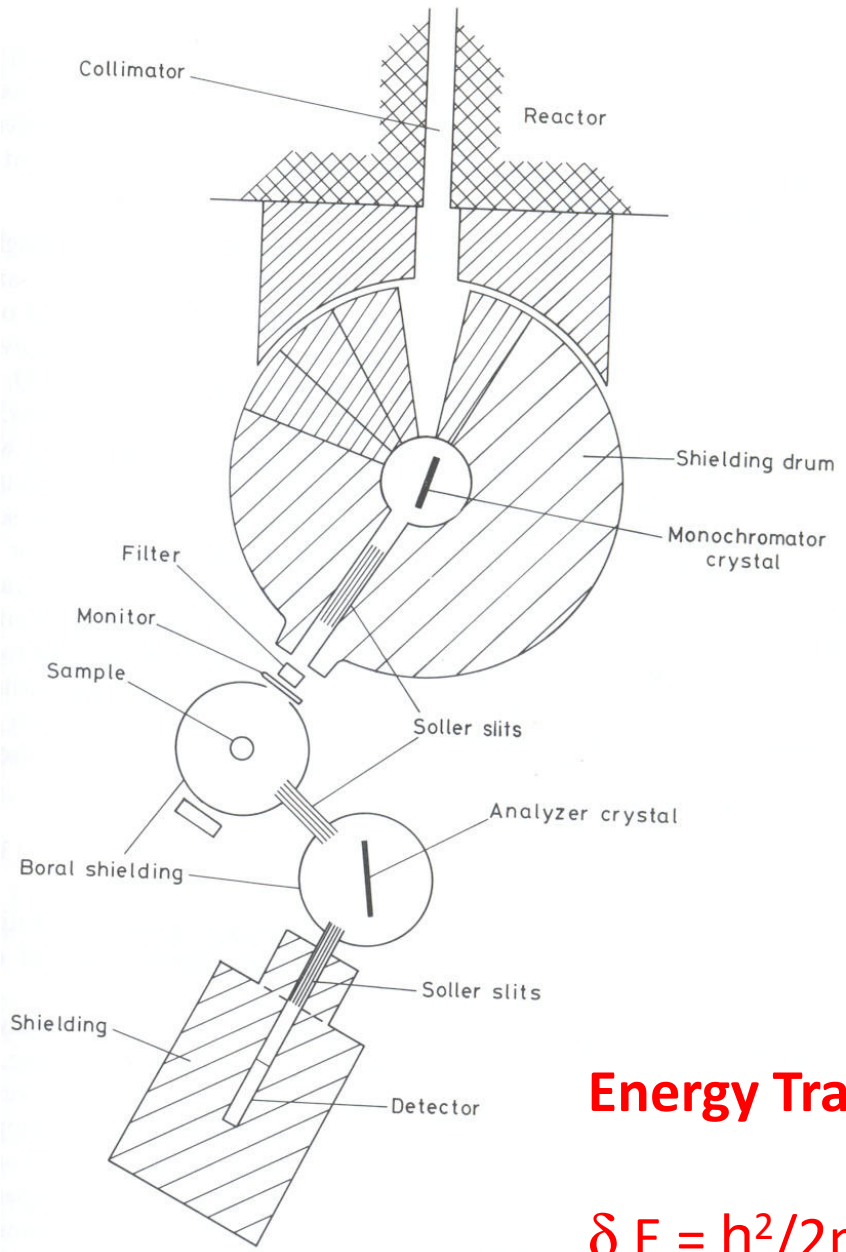

Energy Transfer:

$$\delta E = h^2/2m\ (k_i^2 - k_f^2)$$

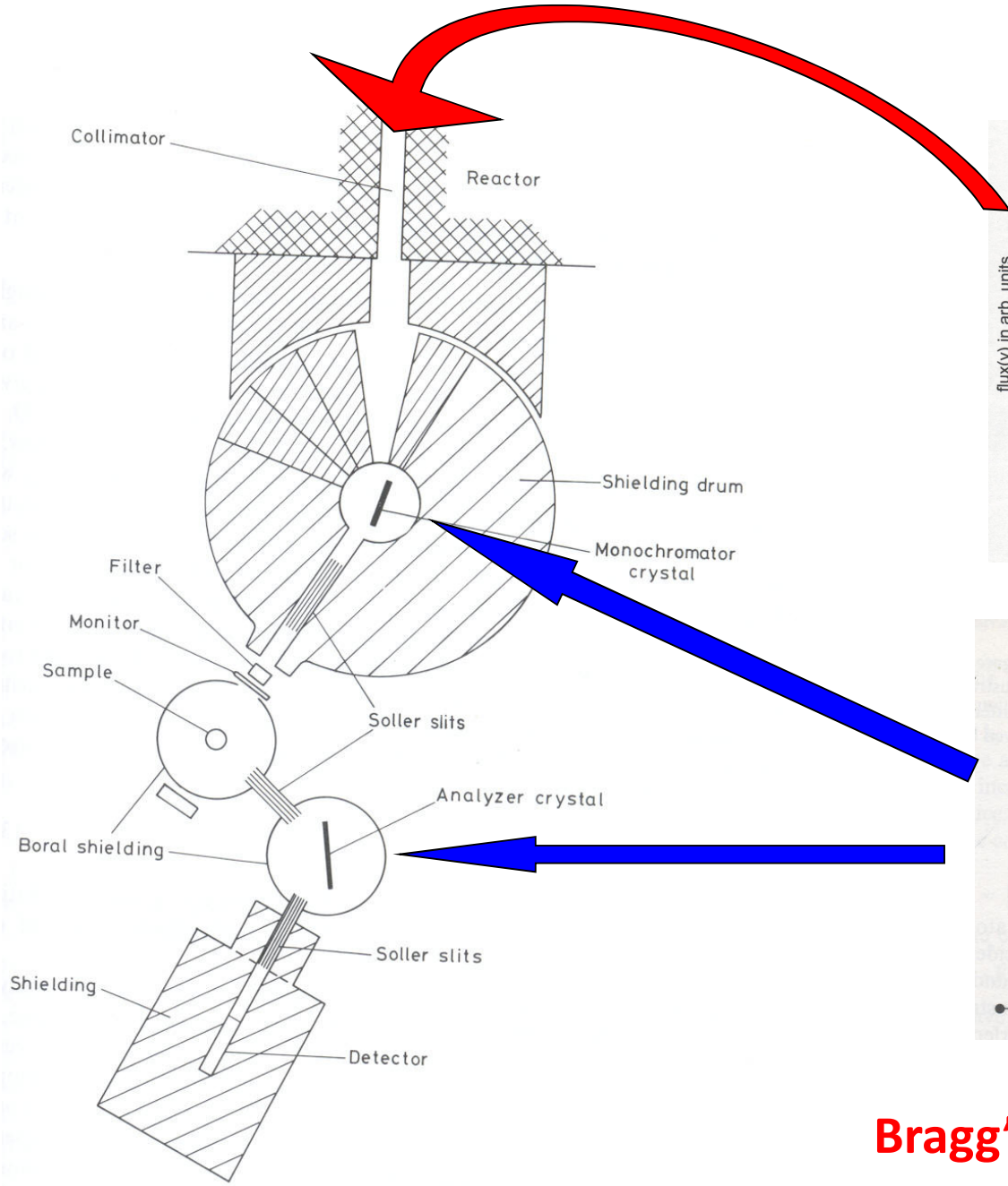

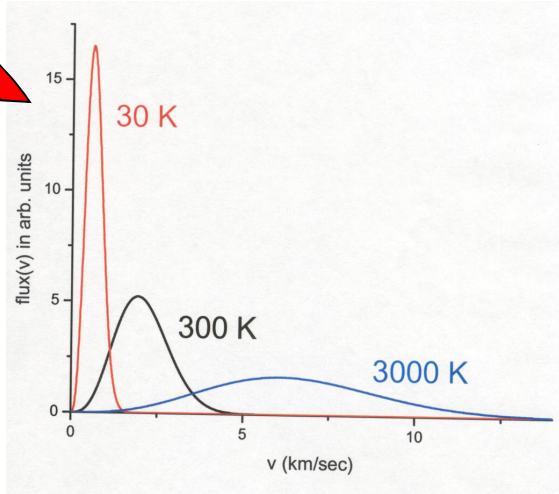

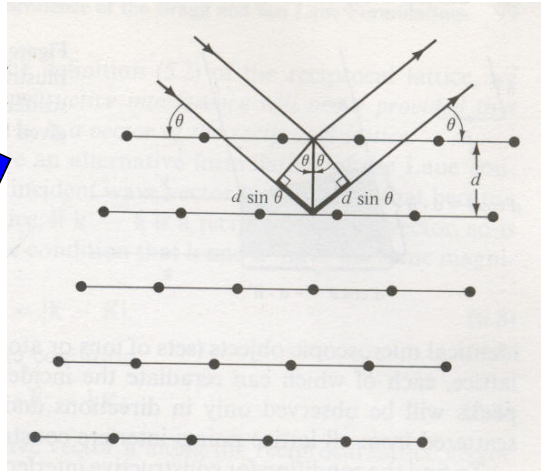

Bragg's Law: $n\lambda = 2d \sin(\theta)$

By courtesy of B. Gaulin

Soller collimators

Define beam directions to
+/- 0.3, 0.5, 0.75 etc. degrees

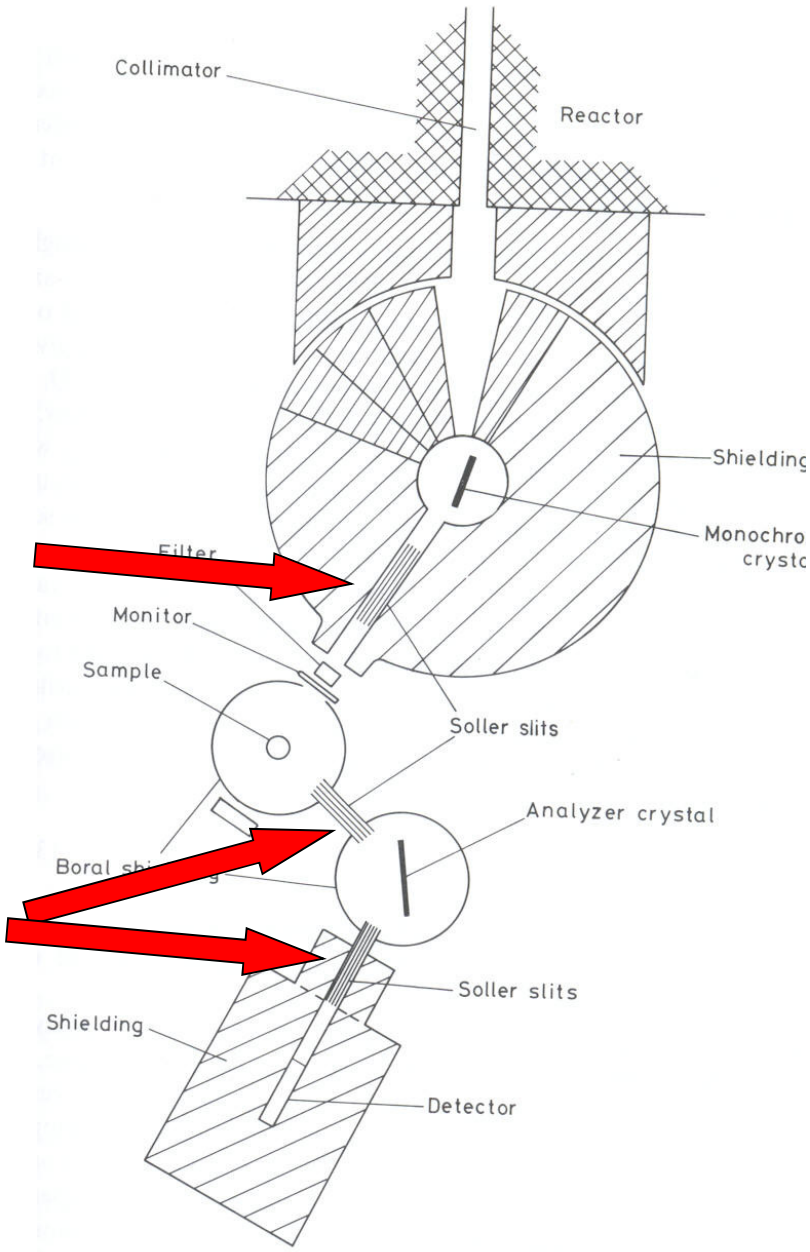

Single crystal monochromators

Bragg reflection and harmonic contamination

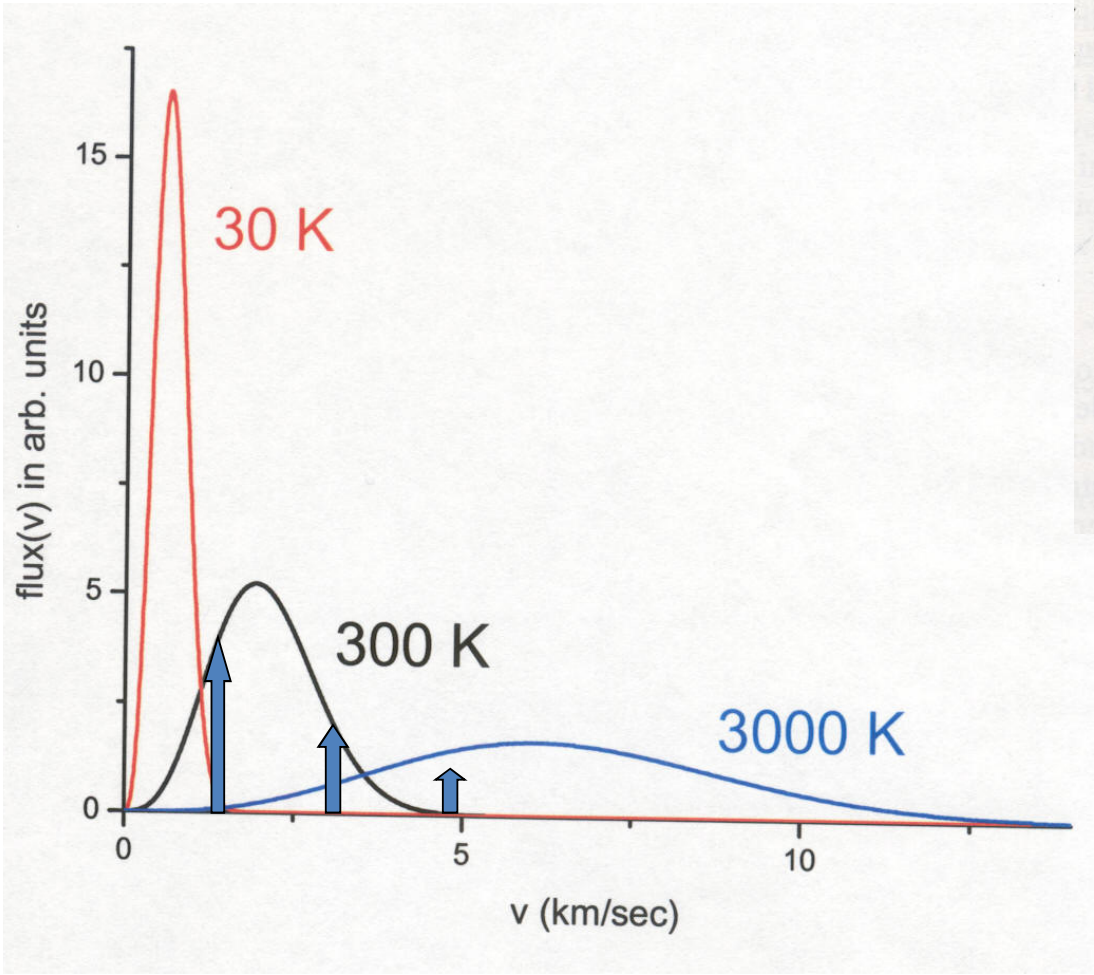

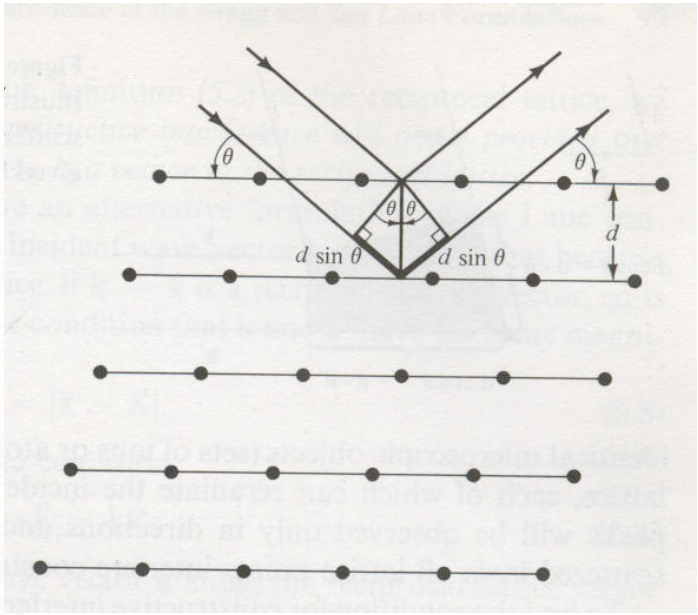

$n\lambda = 2d \sin(\theta)$

λ , $\lambda/2$, $\lambda/3$, etc.

By courtesy of B. Gaulin

Filters:

Remove λ /n from incident or scattered beam, or both

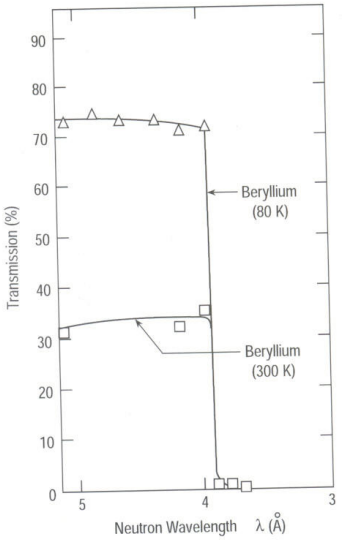

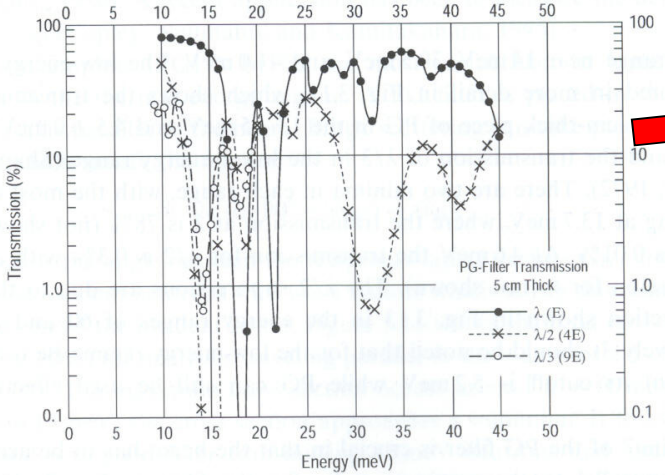

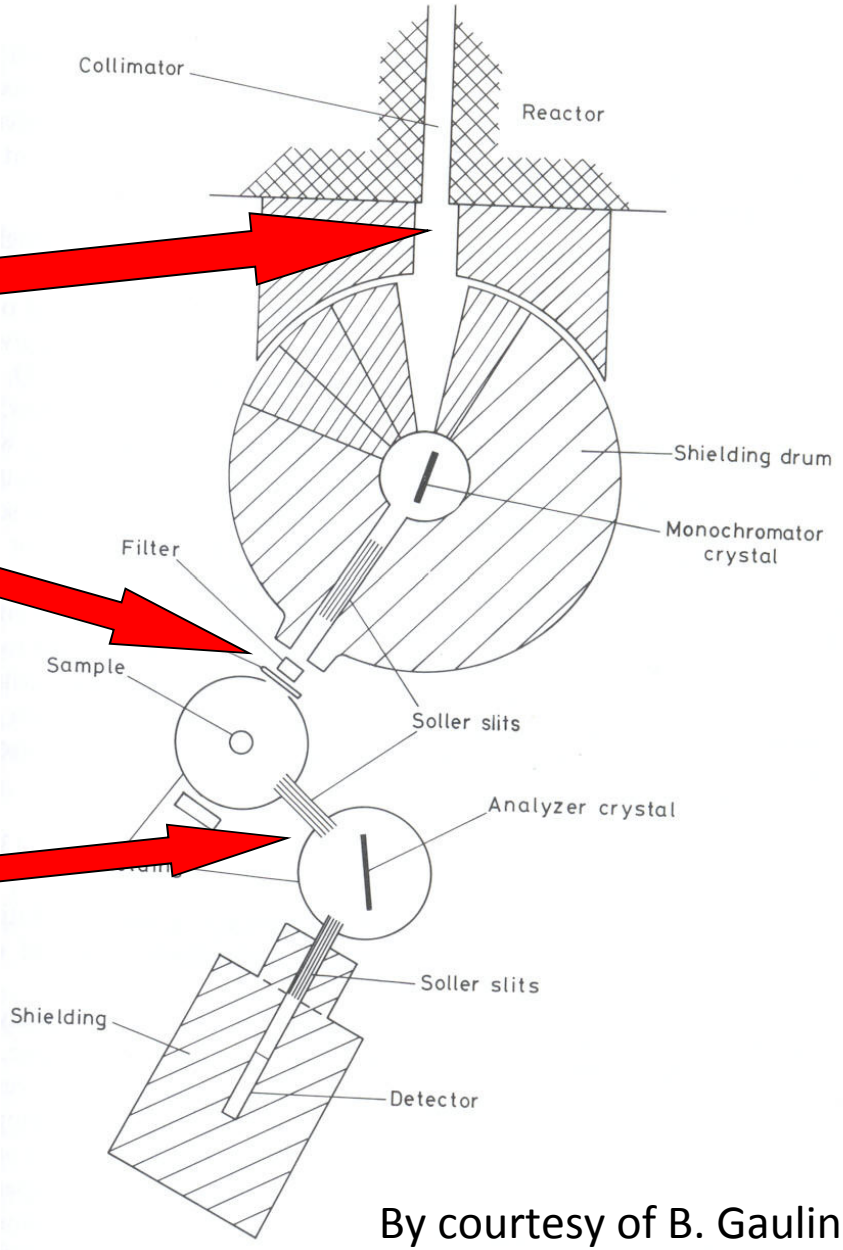

By courtesy of B. Gaulin

Higher-Order-Filter Velocity Selector for Thermal Neutrons

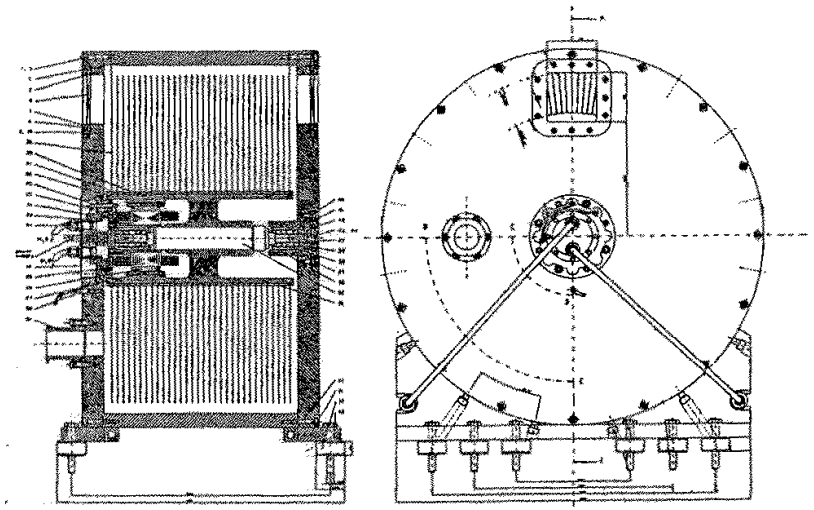

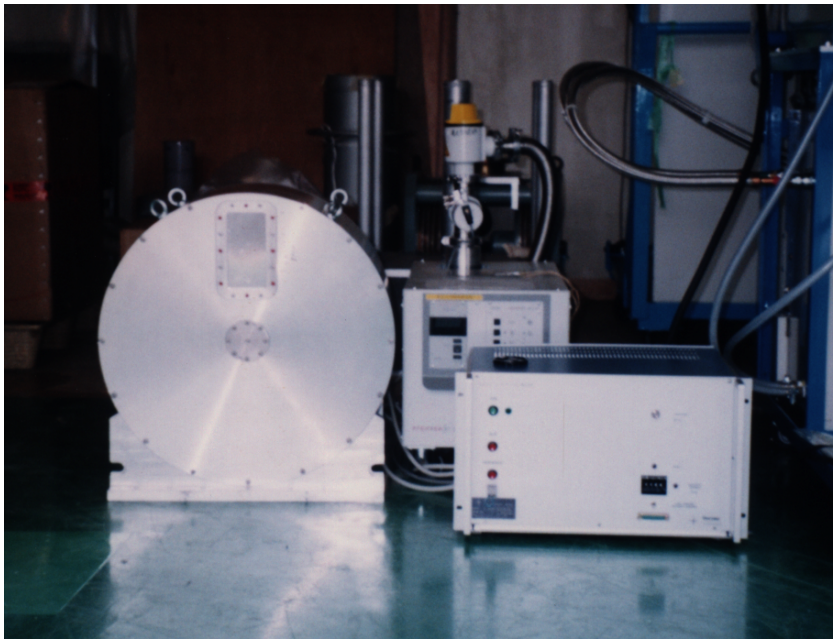

Rotor length: 250 mm
Rim radius: 235 mm
Selector screw: 5.507 degree
Radius of beam center: 206.5 mm
No. of spokes: 160
Max. rpm: 13200
Effective beam cross section: 50 x 50 mm^2

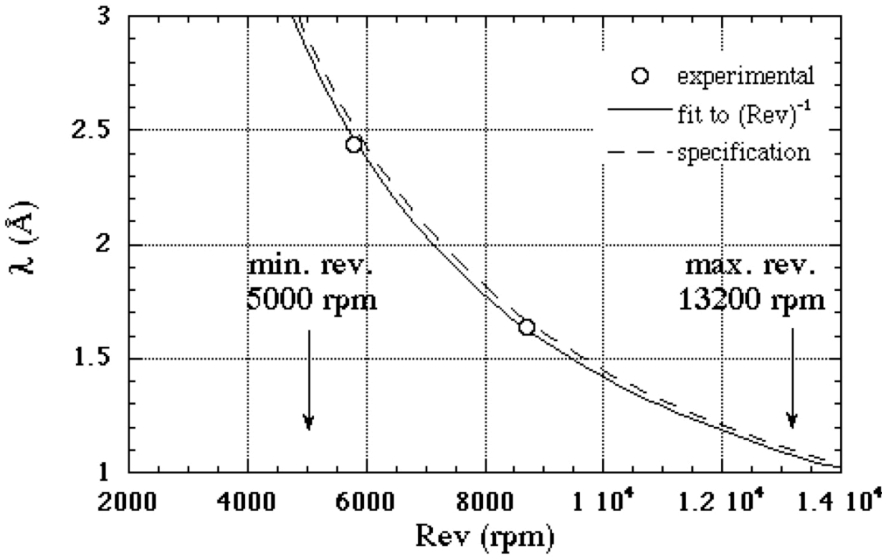

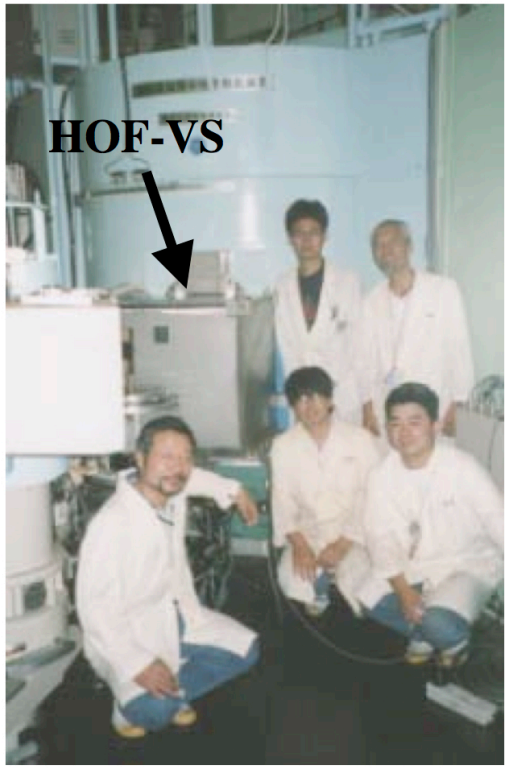

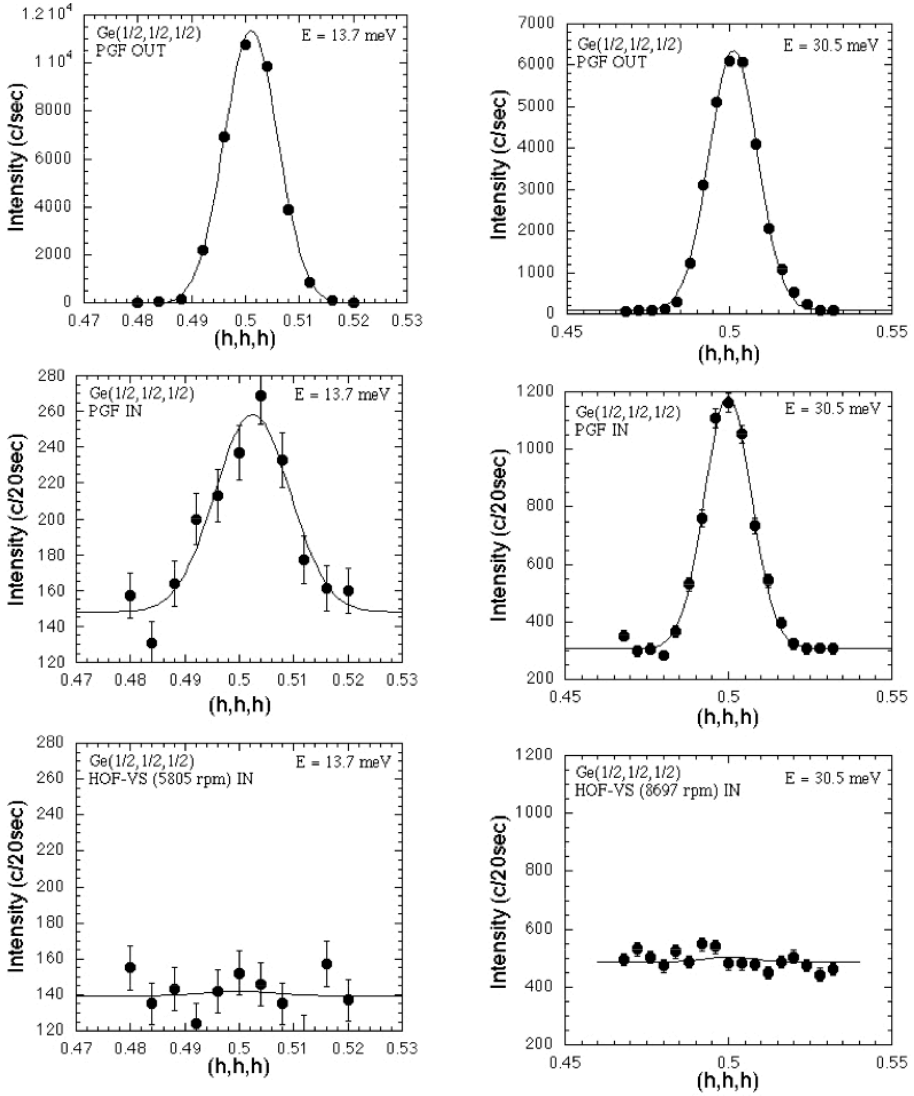

	PGF	HOF-VS
at 13.7 meV	5×10^{-4}	$<5\times10^{-5}$
at 30.5 meV	7×10^{-3}	$<2\times10^{-4}$

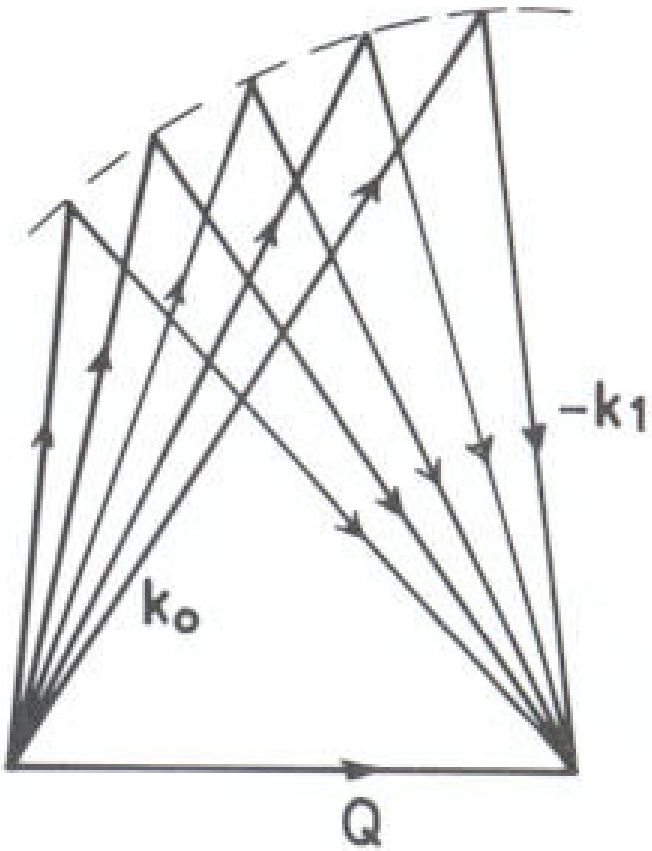

Constant k_f (ii)

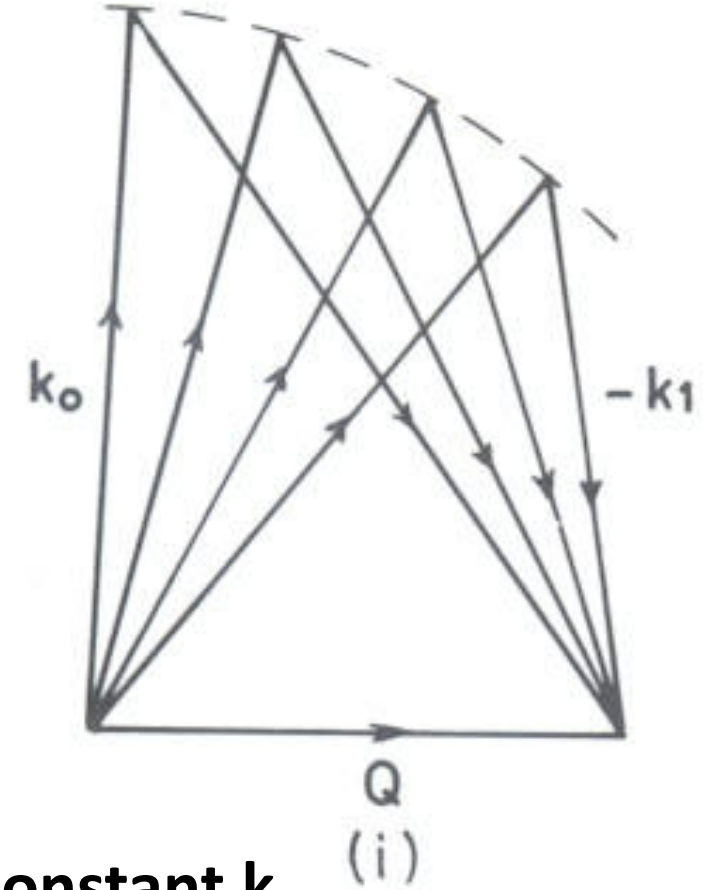

Constant k_i (i)

Two different ways of performing constant-Q scans

By courtesy of B. Gaulin

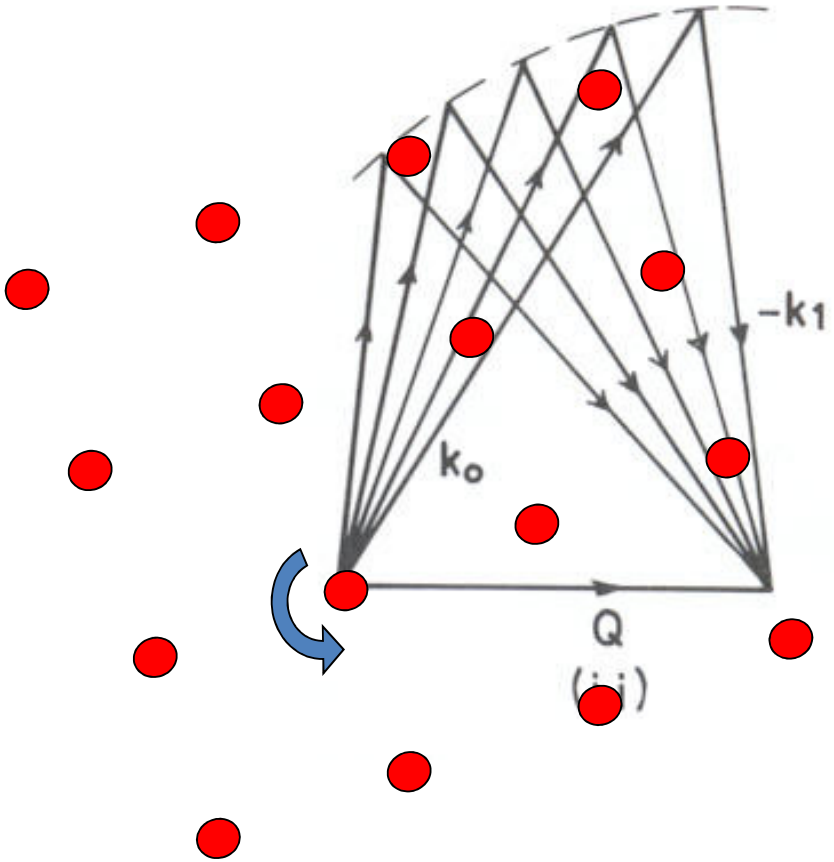

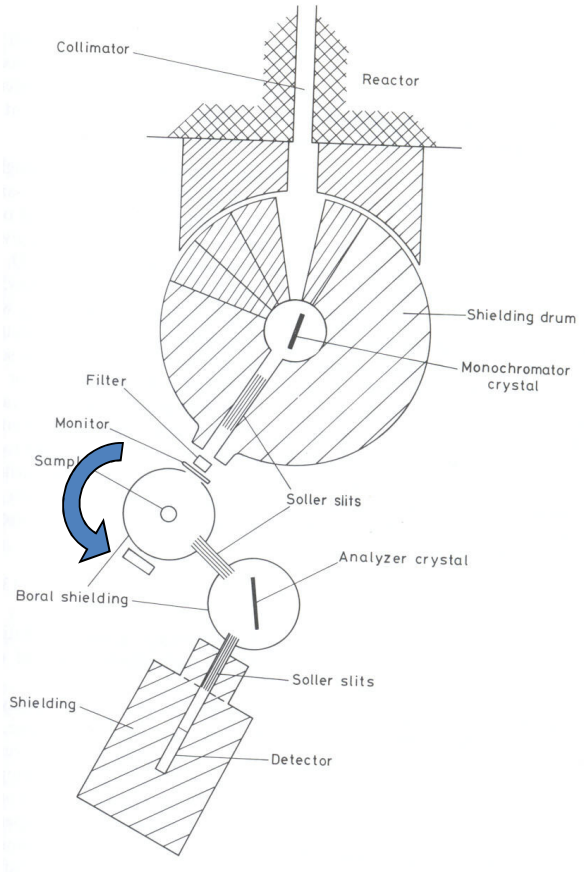

By courtesy of B. Gaulin

Spurious peaks in the inelastic spectrum

$$E_i(n_{\mathrm{M}}) = n_{\mathrm{M}}^2 E_i,$$

$$E_f(n_{\mathrm{A}}) = n_{\mathrm{A}}^2 E_f.$$

$$E_i(n_{\mathrm{M}}) = E_f(n_{\mathrm{A}}),$$

$$\begin{aligned} \hbar\omega &= E_i - E_f \\ &= \left(1 - \frac{n_{\mathrm{M}}^2}{n_{\mathrm{A}}^2}\right) E_i \end{aligned}$$

- **Bragg – incoherent – Bragg**
  - Eg. $k_i - 2k_f$
    - $\hbar\omega$ = 41.1 meV
    - E_f = 13.7 meV
      E_i = 54.8 meV
      $4E_f$ = 54.8 meV
    - Incoherent elastic scattering visible from analyzer $\lambda/2$
- **incoherent – Bragg – Bragg**
  - Sample 2θ in Bragg condition for k_f-k_f
  - Even for inelastic config, weak incoherent from mono

n_{M}	n_{A} =	1	2	3	4
1		0	**3/4**	**8/9**	**15/16**
2		−3	0	5/9	3/4
3		−8	−5/4	0	7/16
4		−15	−3	−7/9	0

- **incoherent – Bragg – Bragg**
  - Sample 2θ in Bragg condition for k_f-k_f
  - Even for inelastic config, weak incoherent from mono

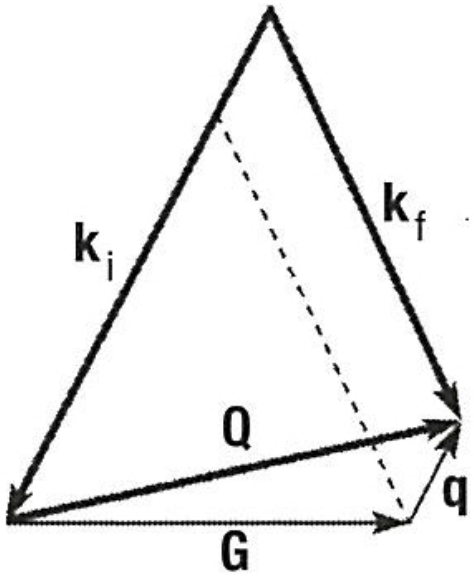

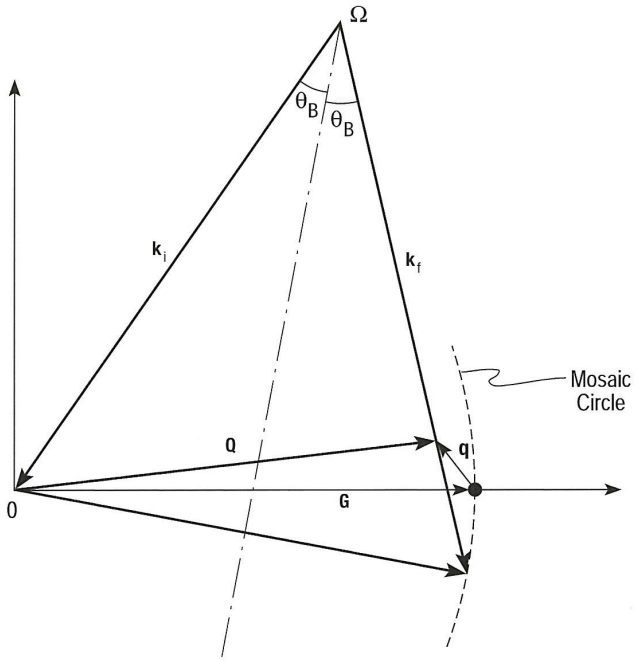

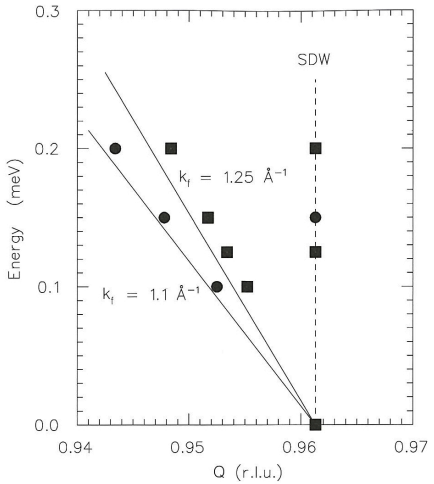

Fig. 6.6. Positions of peaks measured in constant-E scans near a $(Q_0, 0, 0)$ incommensurate magnetic peak corresponding to spin-wave-density (SDW) order in Cr metal at room temperature. The measurements were performed by Uemura, Grier, and Shirane (1982) at the H9 spectrometer at the HFBR. [r.l.u. = reciprocal-lattice

Reference from

Triple-axis techniques

Shirane, Shapiro, Tranquada, "Neutron scattering with a triple-axis spectrometer", Cambridge, 2002.

Detectors

- **Gas Detectors**
- n + ^{3}He → ^{3}H + p + 0.764 MeV
- Ionization of gas
- e^- drift to high voltage anode
- High efficiency

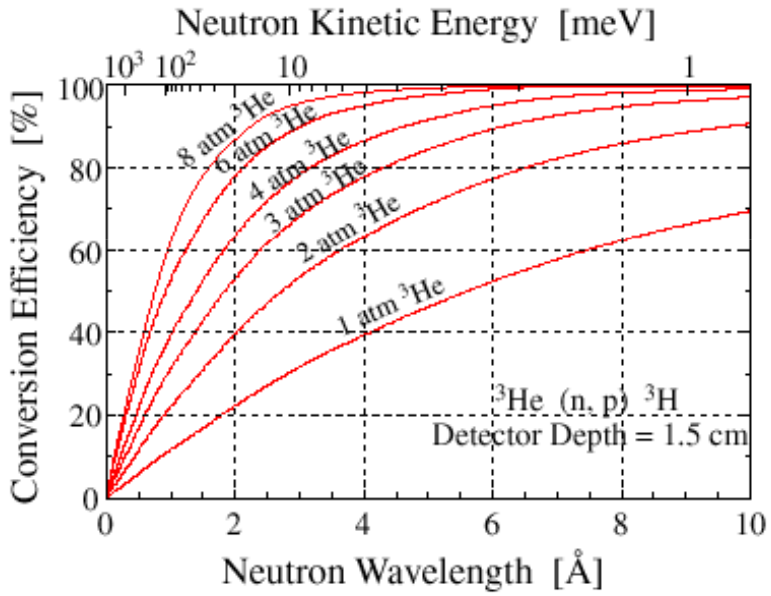

- **Beam monitors**
- Low efficiency detectors for measuring beam flux

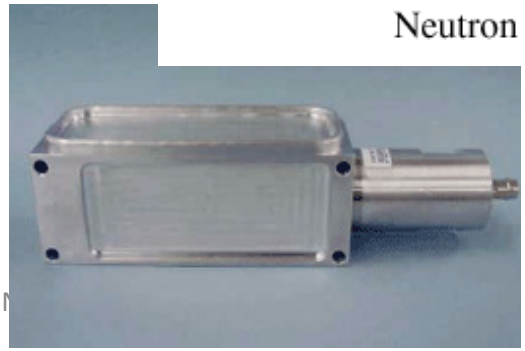

By courtesy of B. Gaulin

Resolution

- **Resolution ellipsoid**
  - Beam divergences
  - Collimations/distances
  - Crystal mosaics/sizes/angles

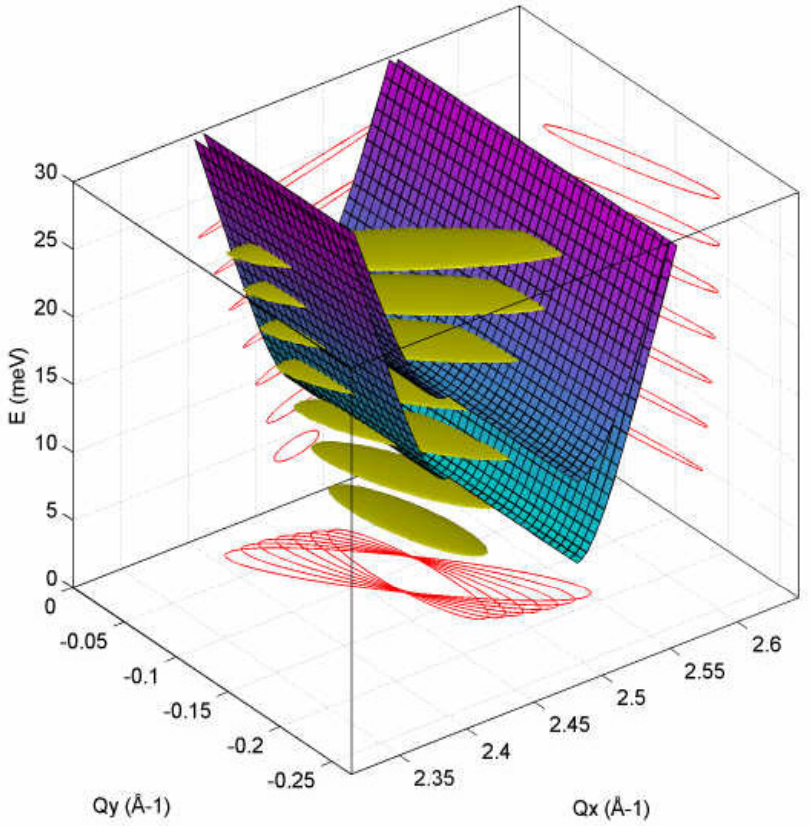

- **Resolution convolutions**

$$\mathrm{I}(\mathbf{Q}_0,\omega_0) = \int \mathrm{S}(\mathbf{Q}_0,\omega_0) R(\mathbf{Q}-\mathbf{Q}_0,\omega-\omega_0)\, d\mathbf{Q}\, d\omega$$

By courtesy of B. Gaulin

Resolution focusing

- **Optimizing peak intensity**
- **Match slope of resolution to dispersion**

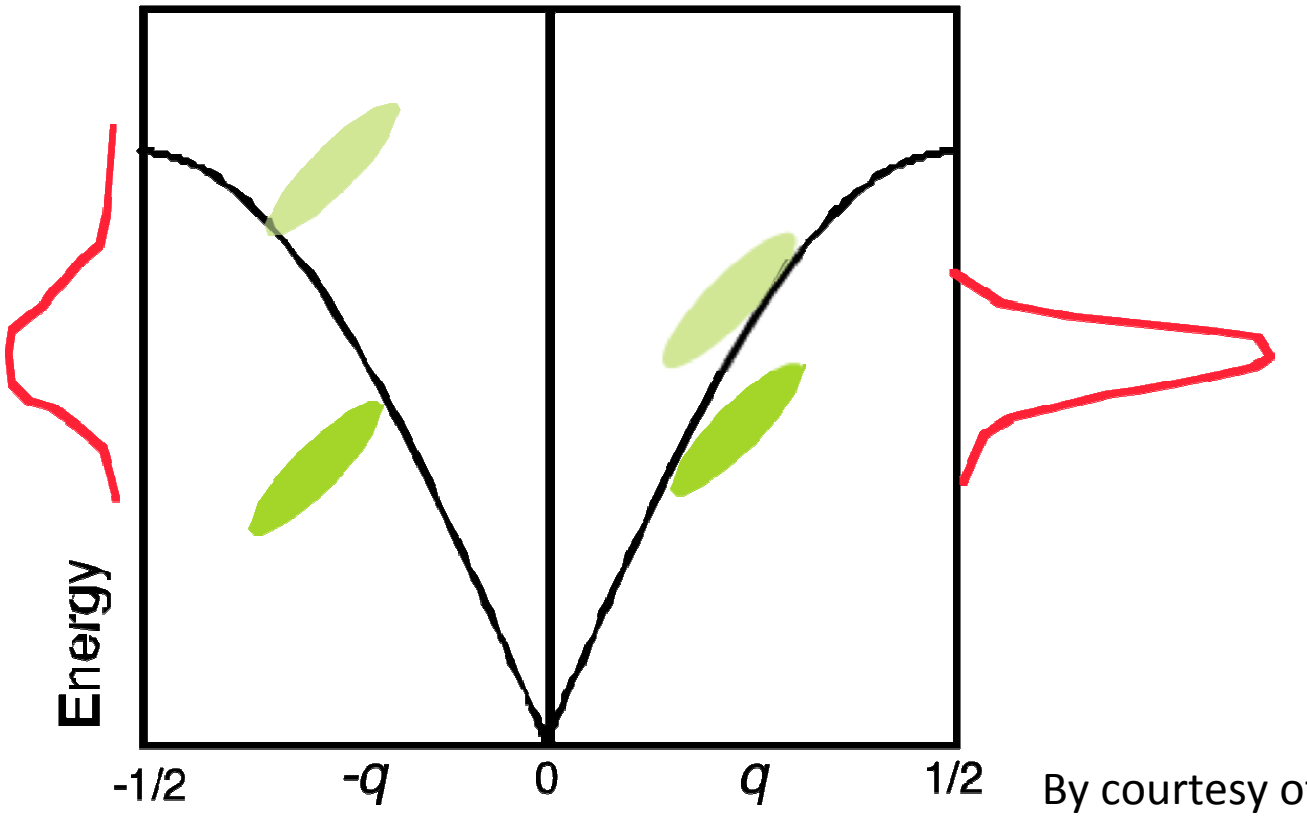

By courtesy of B. Gaulin

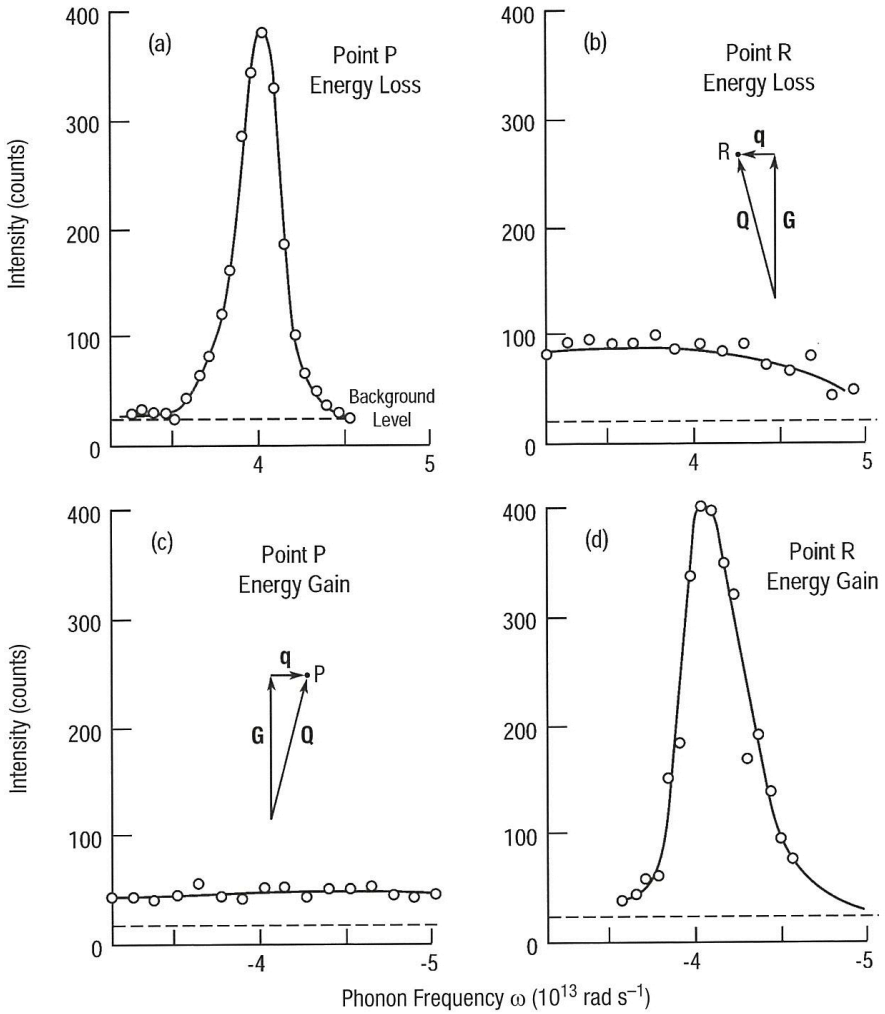

Fig. 4.4. Constant-**Q** scans of a transverse phonon propagating along a [111] direction in MgO measured for (a, b) energy gain and (c, d) energy loss at (a, d) focused and (b, c) unfocused positions using a right-handed spectrometer (from Peckham, Saunderson, and Sharp, 1967).

Reference from

Shirane, Shapiro, Tranquada, "Neutron scattering with a triple-axis spectrometer", Cambridge, 2002.

References

General neutron scattering

G. Squires, “Intro to theory of thermal neutron scattering”, Dover, 1978.

S. Lovesey, “Theory of neutron scattering from condensed matter”, Oxford, 1984.

R. Pynn, http://www.mrl.ucsb.edu/~pynn/.

Polarized neutron scattering

Moon, Koehler, Riste, Phys. Rev **181**, 920 (1969).

Triple-axis techniques

Shirane, Shapiro, Tranquada, “Neutron scattering with a triple-axis spectrometer”, Cambridge, 2002.

Time-of-flight techniques

B. Fultz, http://www.cacr.caltech.edu/projects/danse/ARCS_Book_16x.pdf

RITA-II@PSI

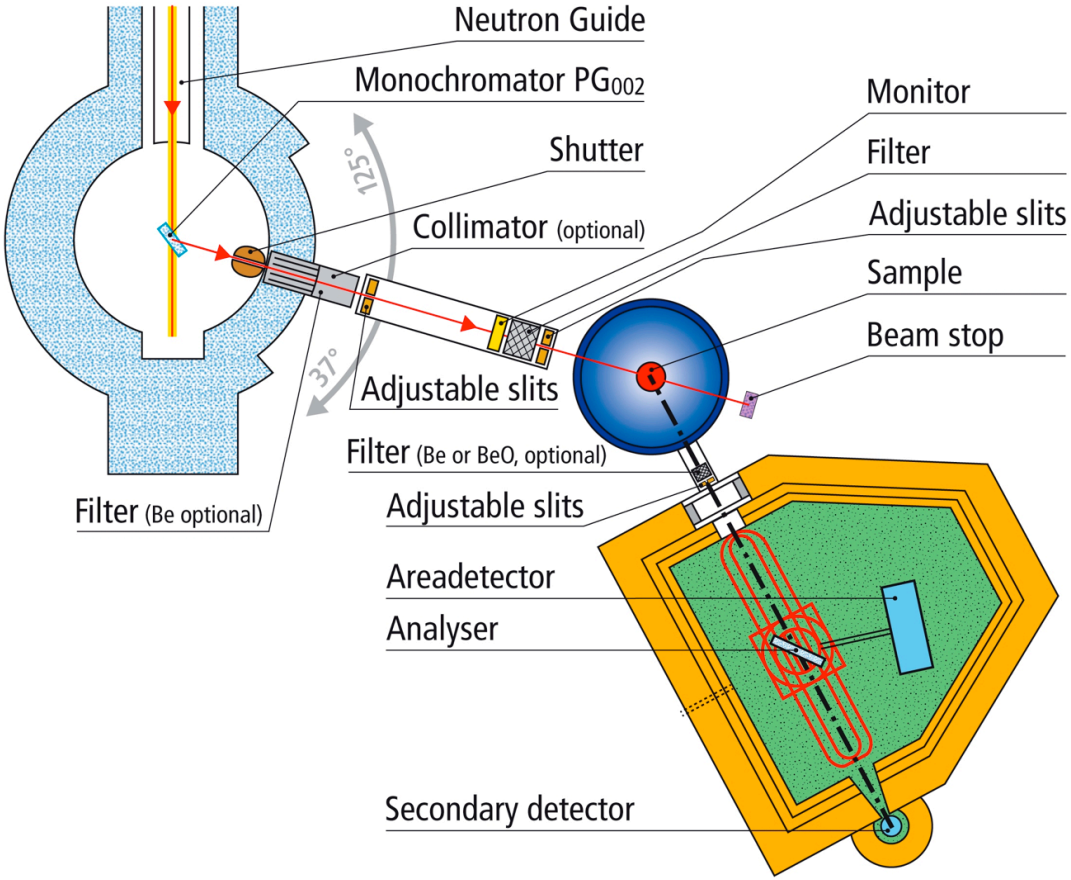
Neutron Guide
Monochromator PG002
Shutter
Collimator (optional)
Filter (Be optional)
125°
37°
Monitor
Filter
Adjustable slits
Sample
Beam stop
Adjustable slits
Filter (Be or BeO, optional)
Adjustable slits
Areadetector
Analyser
Secondary detector

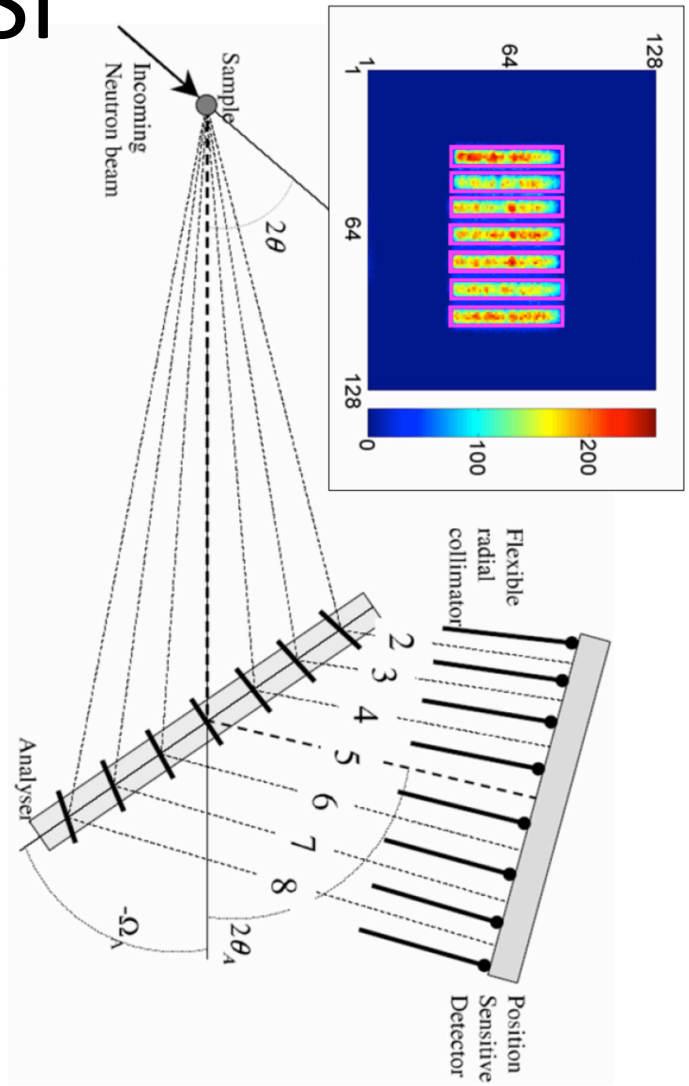
Incoming
Neutron beam
Sample
2θ
1
64
128
0
100
200
Flexible
radial
collimator
2
3
4
5
6
7
8
Analyser
-Ω_A
2θ_A
Position
Sensitive
Detector

FlatCone option@ILL

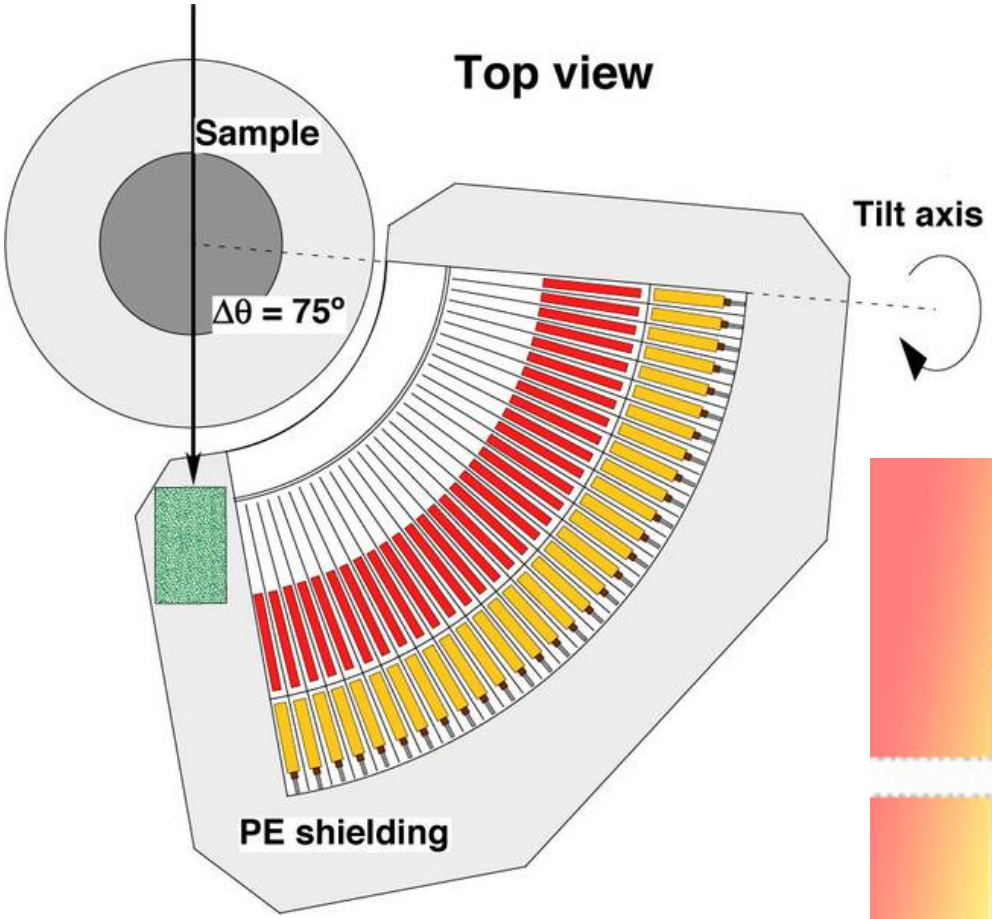

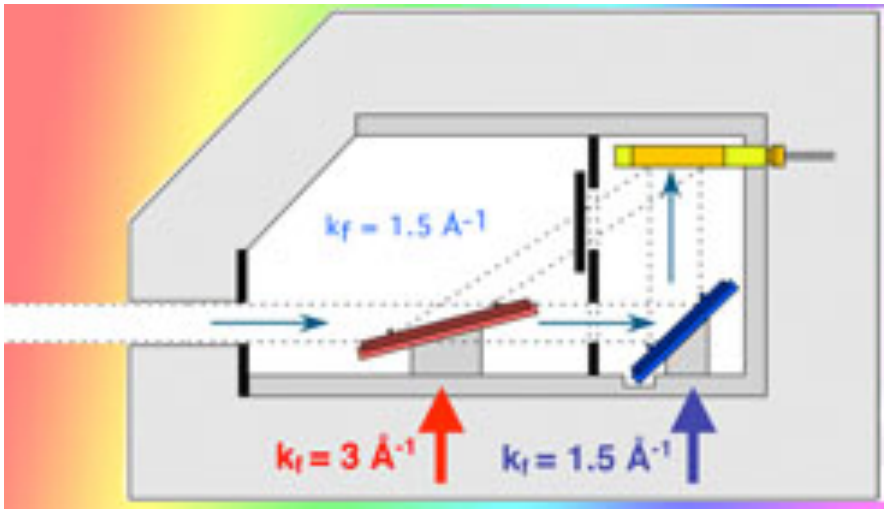

CAMEA concept

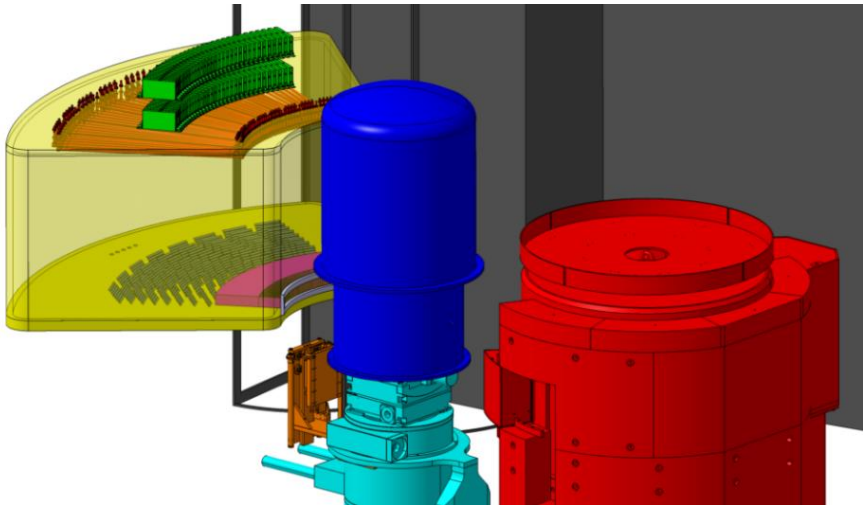

For PSI

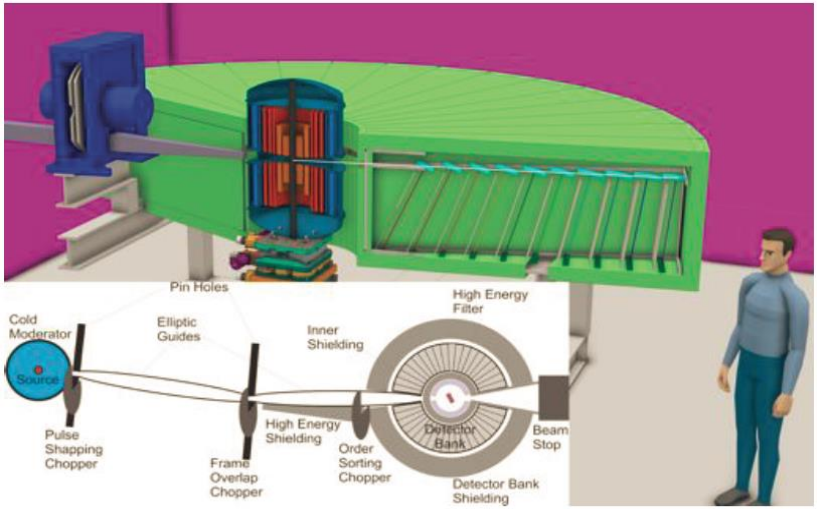

For ESS

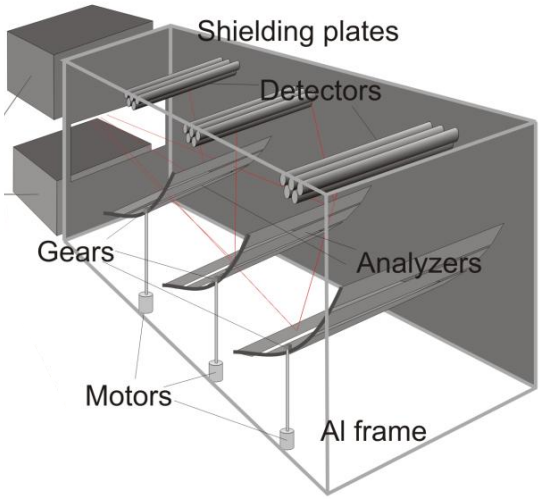

MACS-II@NIST

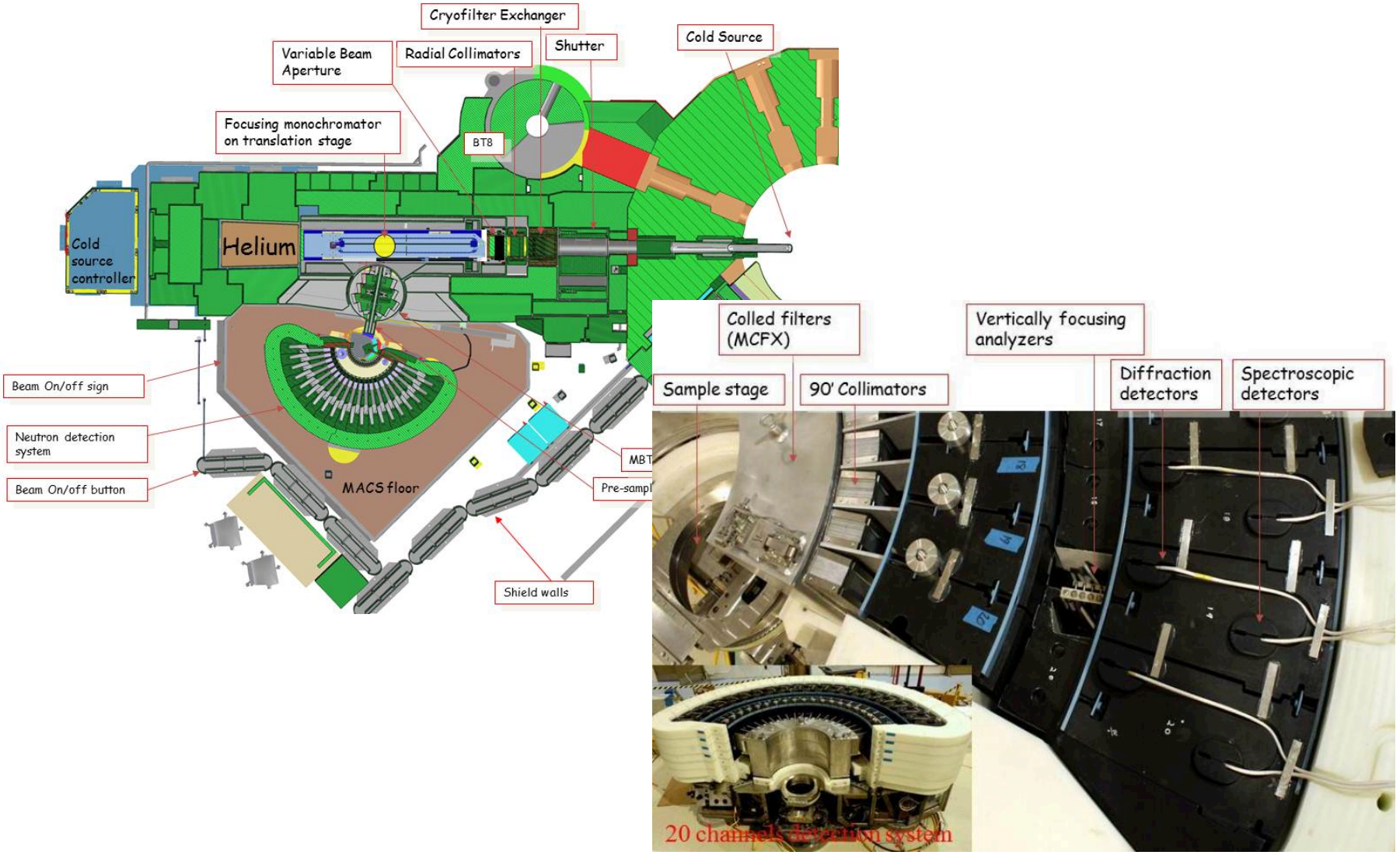
Cryofilter Exchanger
Variable Beam Aperture
Radial Collimators
Shutter
Cold Source
Focusing monochromator on translation stage
BT8
Cold source controller
Helium
Beam On/off sign
Neutron detection system
Beam On/off button
MACS floor
MBT
Pre-sampl
Shield walls
Colled filters (MCFX)
Vertically focusing analyzers
Sample stage
90' Collimators
Diffraction detectors
Spectroscopic detectors
20 channels detection system

Virtual Source concept

JPSJ 82 (2013) SA026

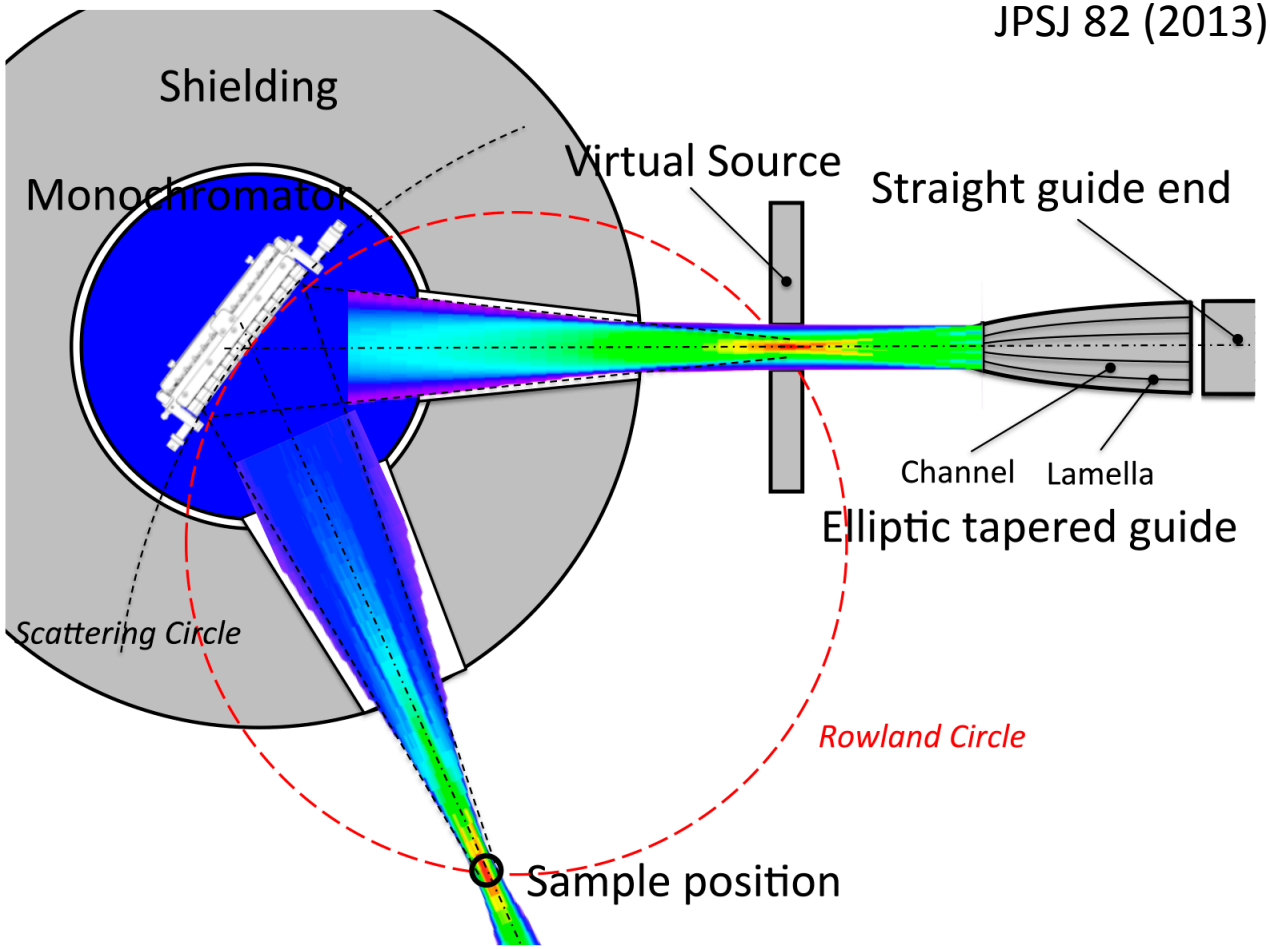

ThALES@ILL, MACS-II@NIST

Outline

- Recap of triple axis spectrometry

- Magnetic excitations in quasi-1-dimensional magnet and quantum magnet

Neutron Scattering Investigations of Low Dimensional and Quantum Magnets

Introduction

Neutron inelastic scattering is a unique tool to study the spin dynamics in
magnetic materials from microscopic point of view

$$\hbar\mathbf{k}_i + \hbar\mathbf{q} = \hbar\mathbf{k}_f, \qquad \frac{\hbar^2|\mathbf{k}_i|^2}{2M_n} = \frac{\hbar^2|\mathbf{k}_f|^2}{2M_n} + \hbar\omega,$$

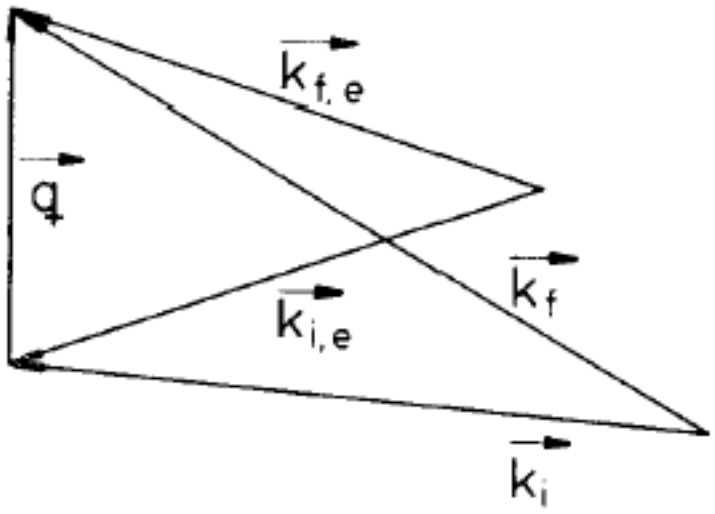

$$S(\mathbf{q},\omega) \sim \frac{d^2\sigma}{d\Omega\, d\omega} = \frac{|\mathbf{k}_f|}{|\mathbf{k}_i|}\left(1{\cdot}91\,\frac{e^2}{mc^2}\right)^2 \sum_{ij} F_j{}^*(q)F_i(q)\cdot\frac{1}{2\pi}\int dt$$
$$\times \exp(i\omega t)\,\langle S_{i\perp}(0)S_{j\perp}(t)\rangle \exp[i\mathbf{q}(\mathbf{R}_i-\mathbf{R}_j)].$$

The cross section is directly proportional to the space-time Fourier transform of the time-dependent spin pair-correlation function

A careful study of the q and ω-dependence of the scattered intensity gives directly S(q,ω) over the whole Brillouin zone
i.e. microscopic information on the magnetic exchange interactions

Direct information
on
spin Hamiltonian of the system

real space

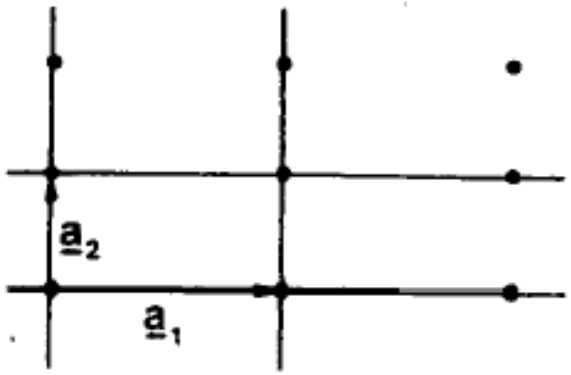

reciprocal space

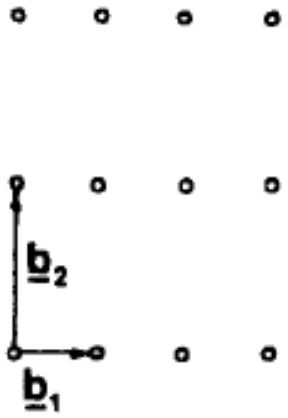

$$S(\mathbf{Q}) = N\sum_{\mathbf{G}} \delta_{\mathbf{Q},\mathbf{G}}$$

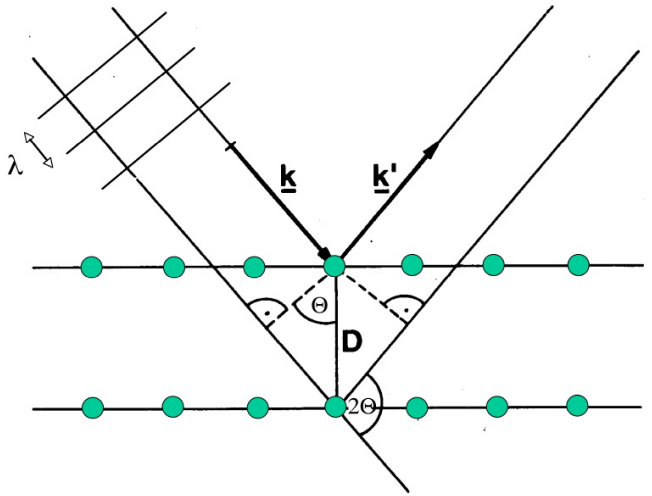

$2D\sin\theta = n\lambda$

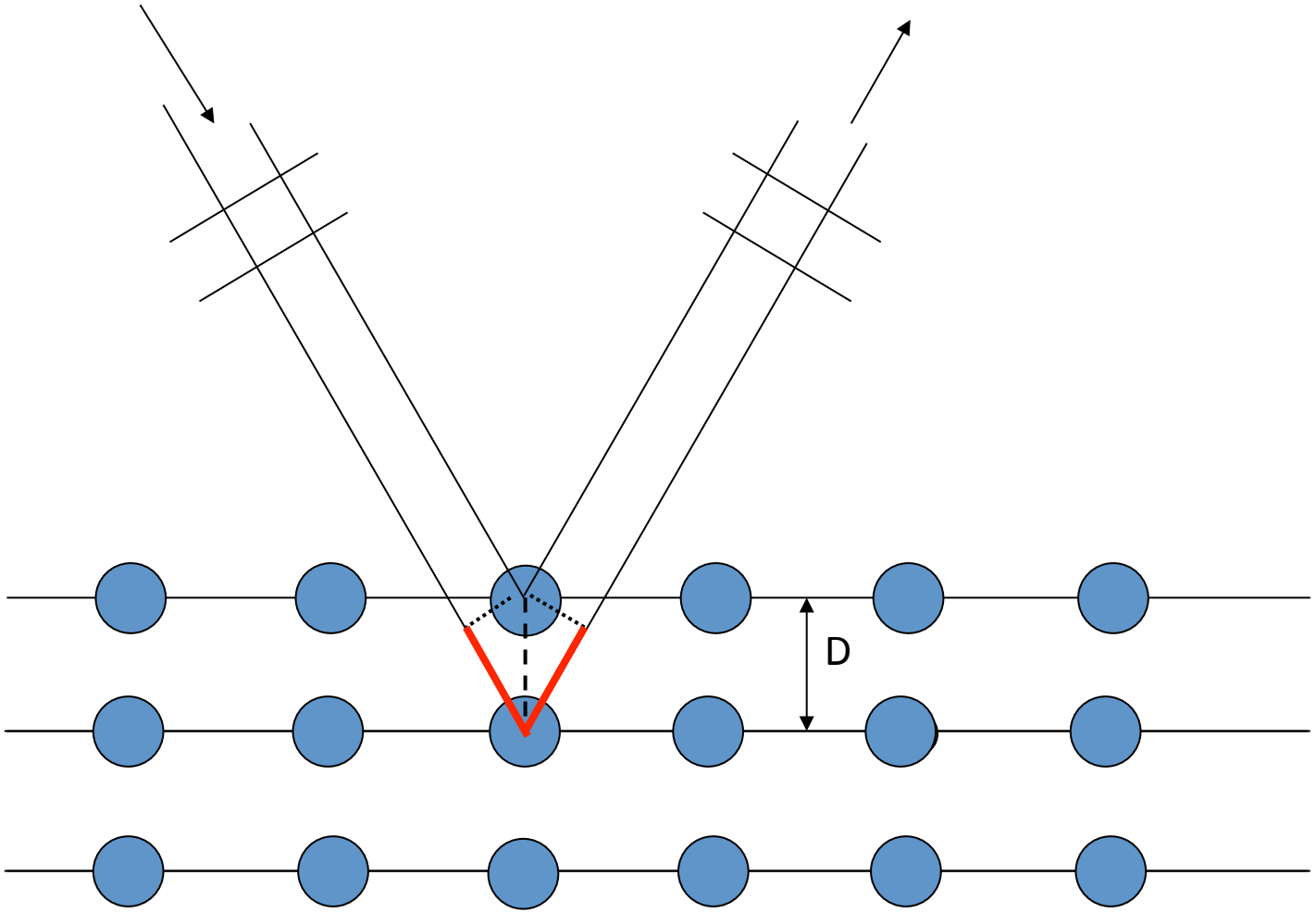

$$2D\sin\theta = n\lambda$$

Ferromagnetic material

below the Curie temperature (T_c)

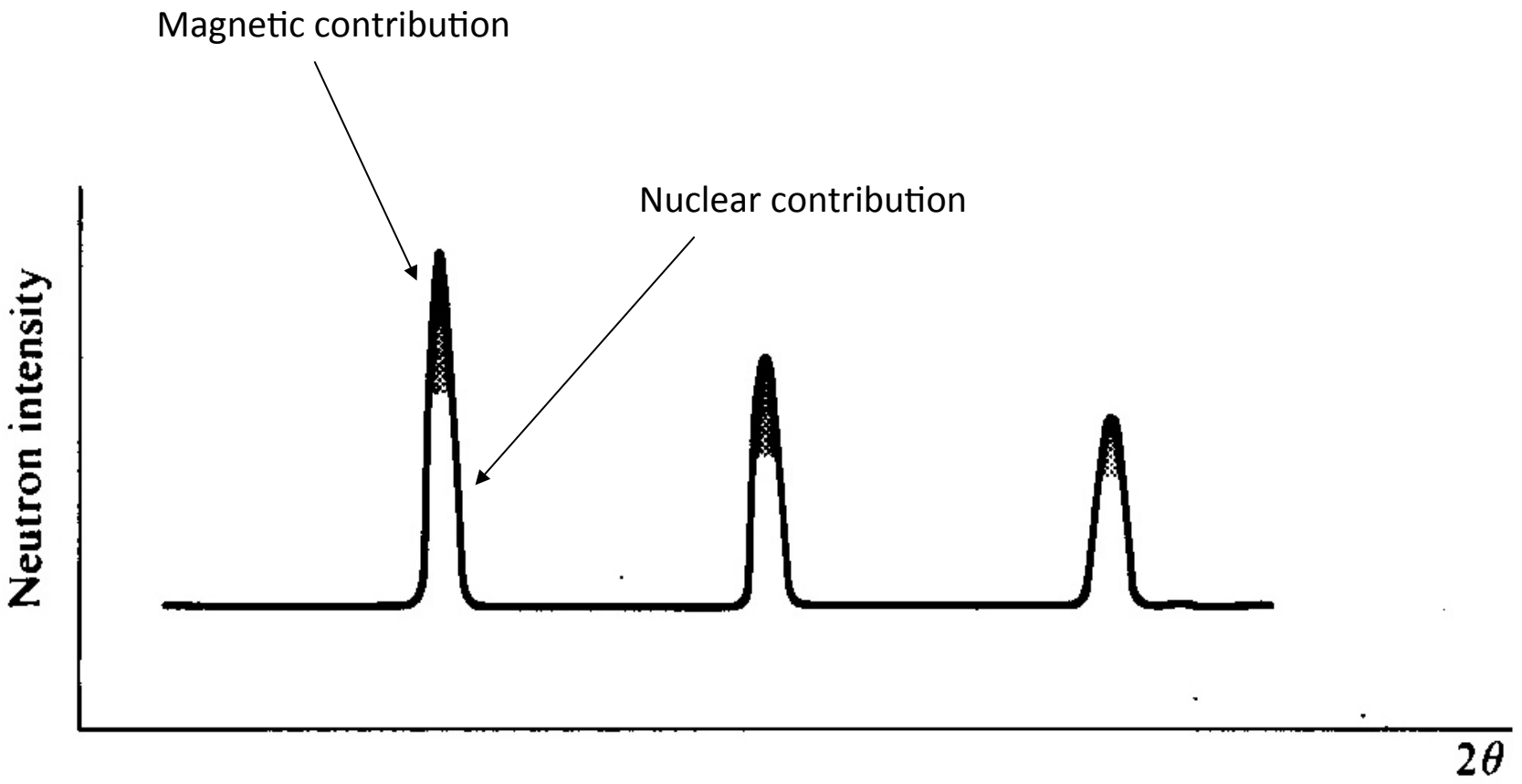

磁性イオンによる磁気散乱

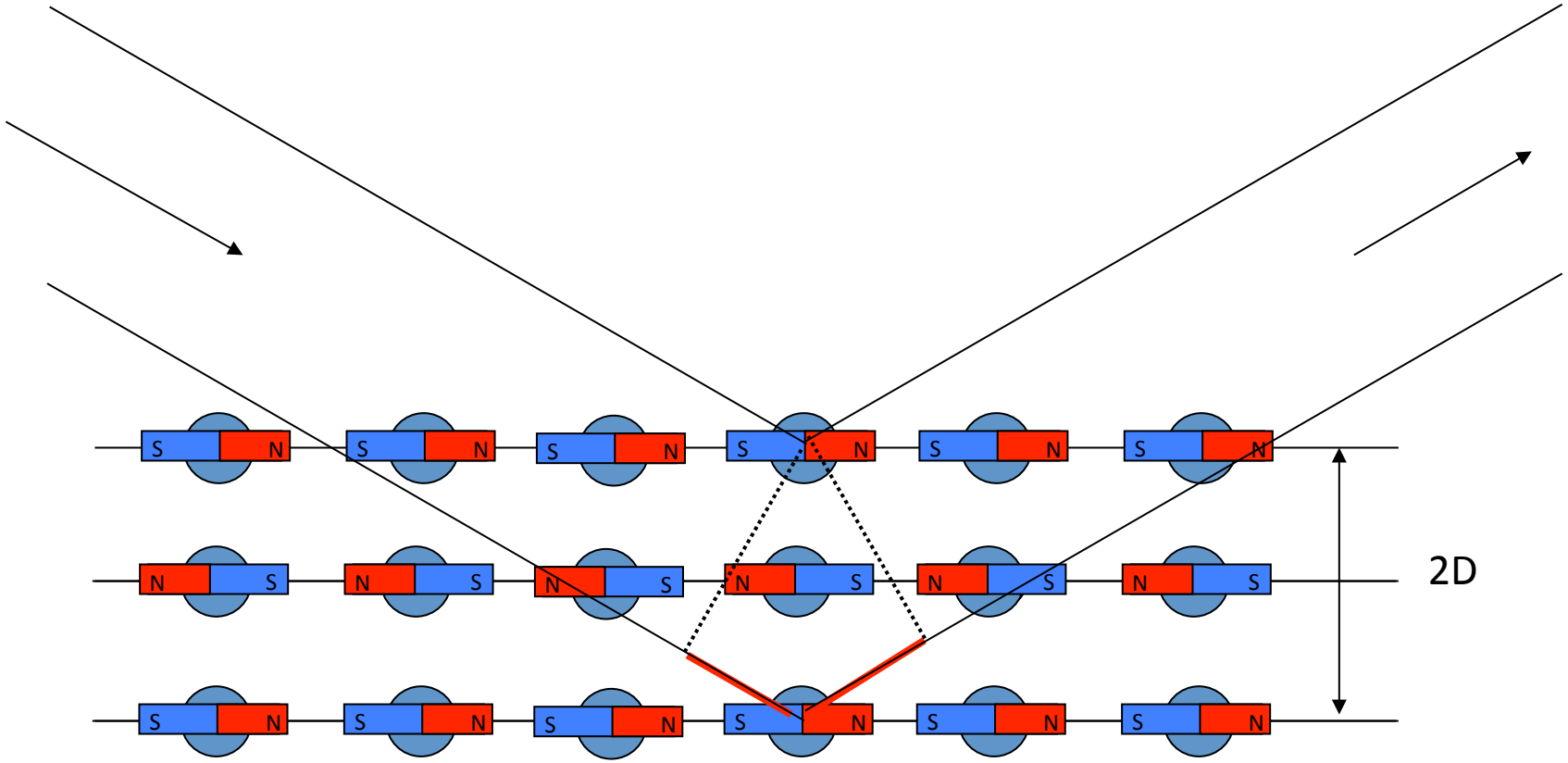

$$2(2D)\sin\theta = n\lambda$$

Antiferromagnetic material

below the Néel temperature (T_N)

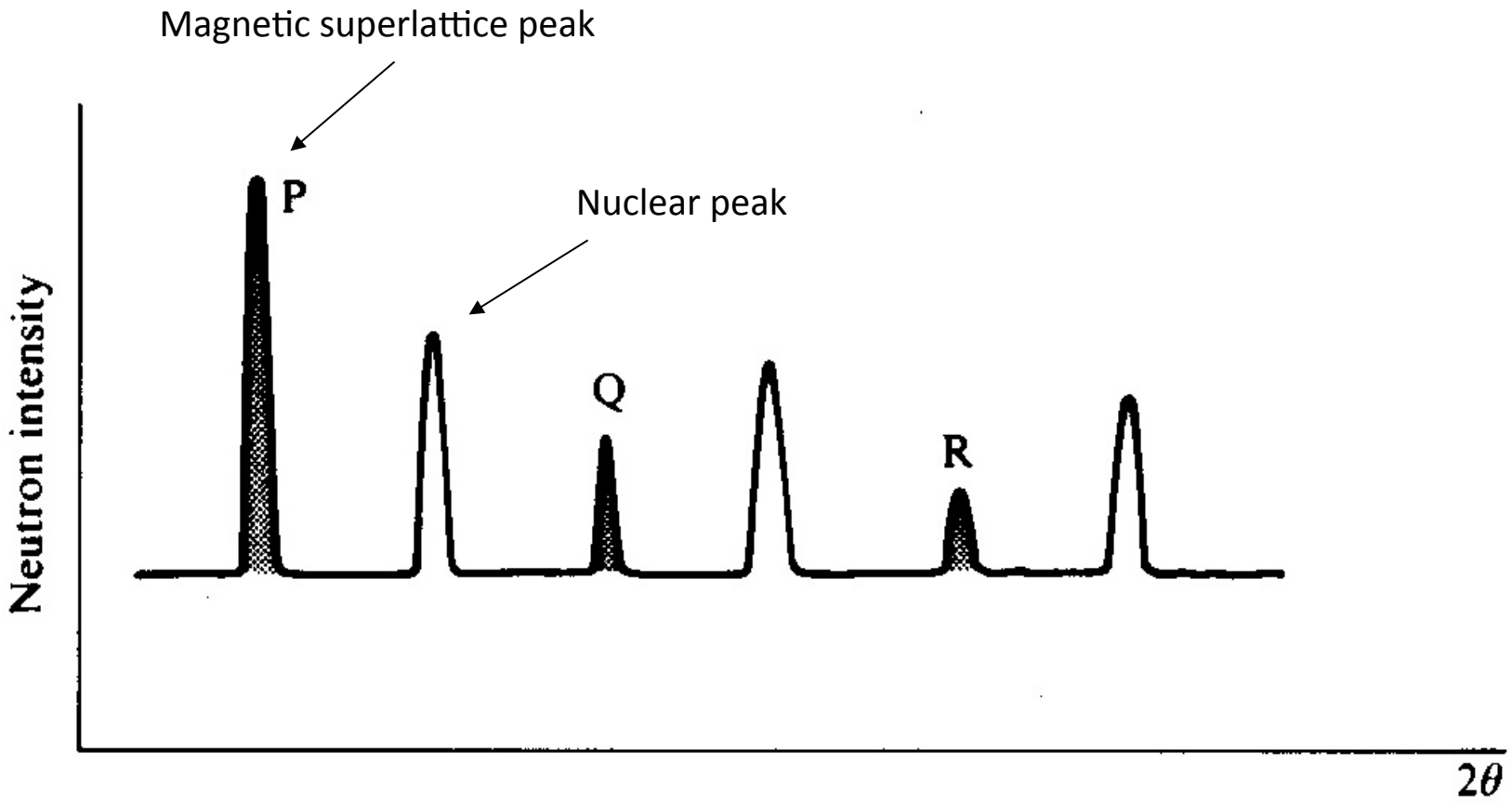

MnO

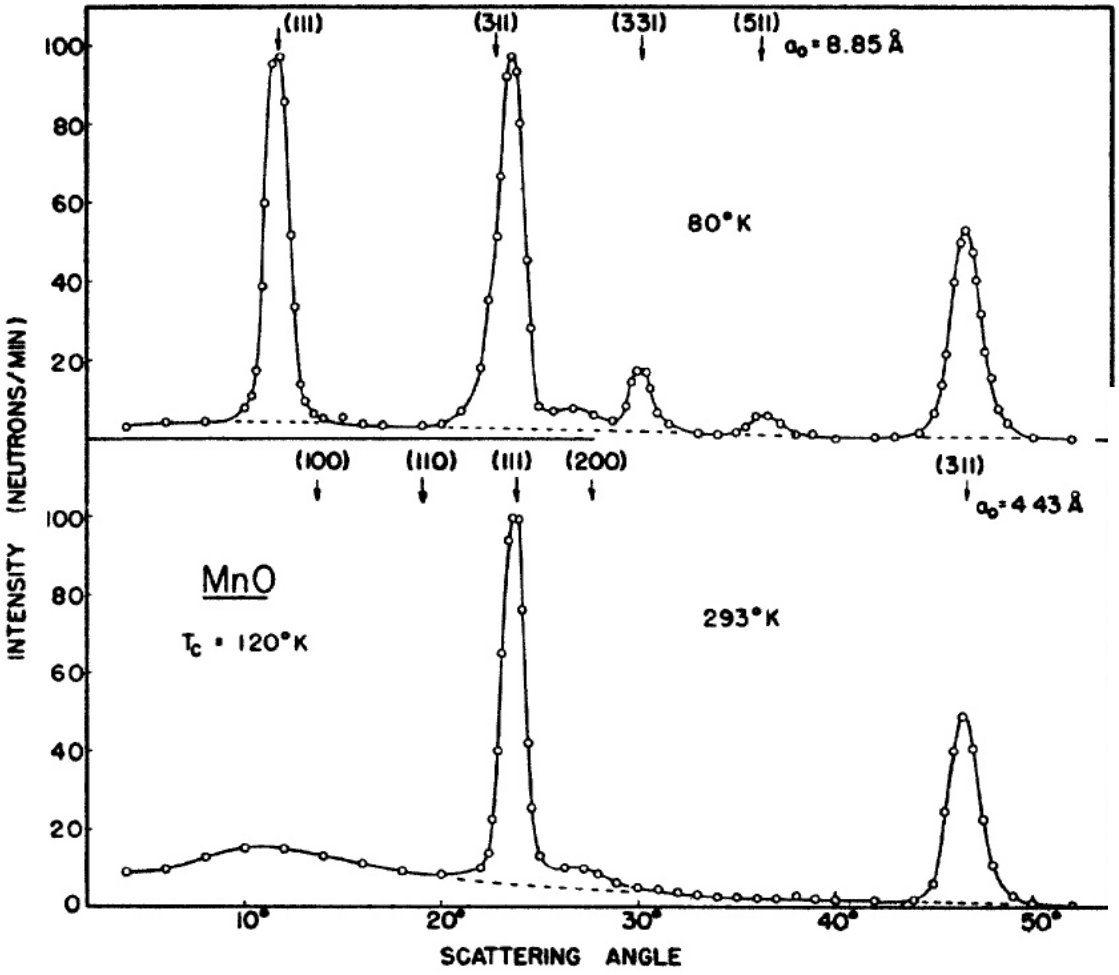

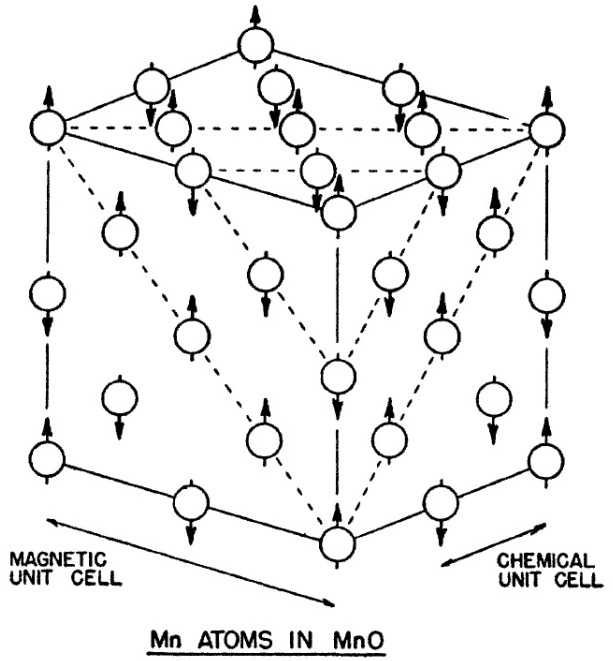

Shull et al., Phys. Rev. 83, 333 (1951)

T_N=120K

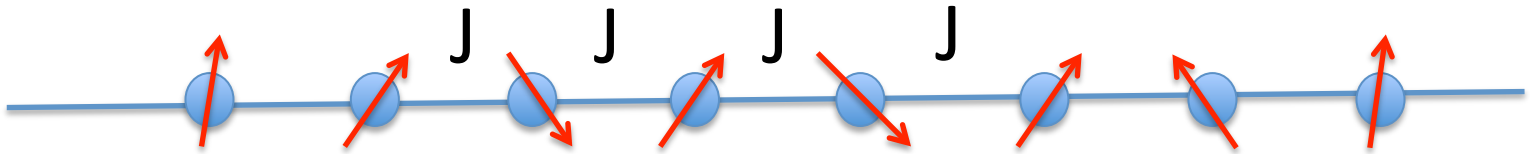

$$\mathscr{H} = -2J \sum_n \mathbf{S}_n \mathbf{S}_{n+1}$$

Examples of low-dimensional magnets

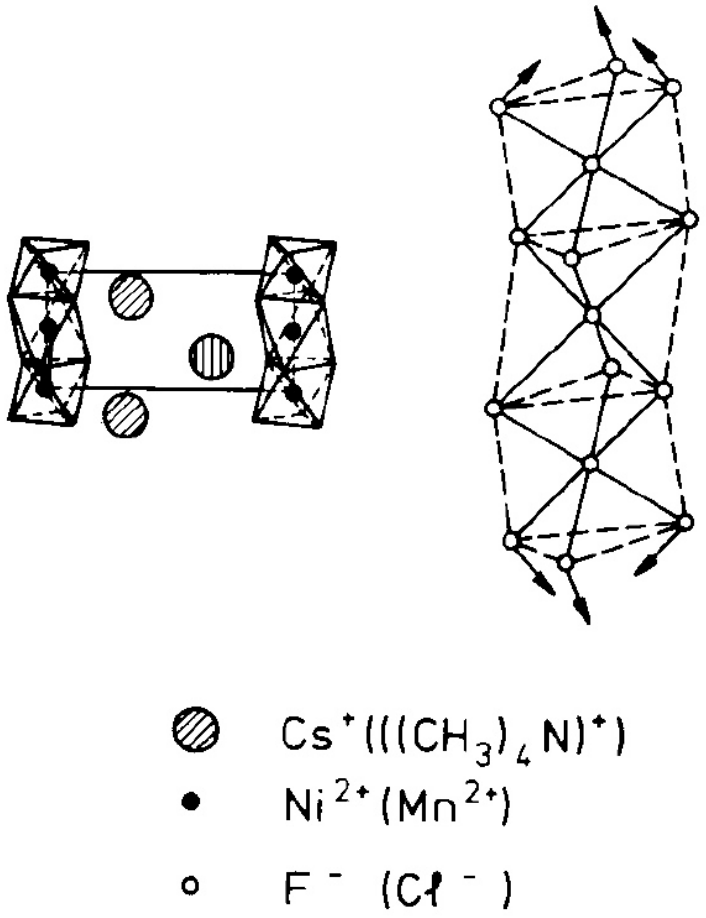

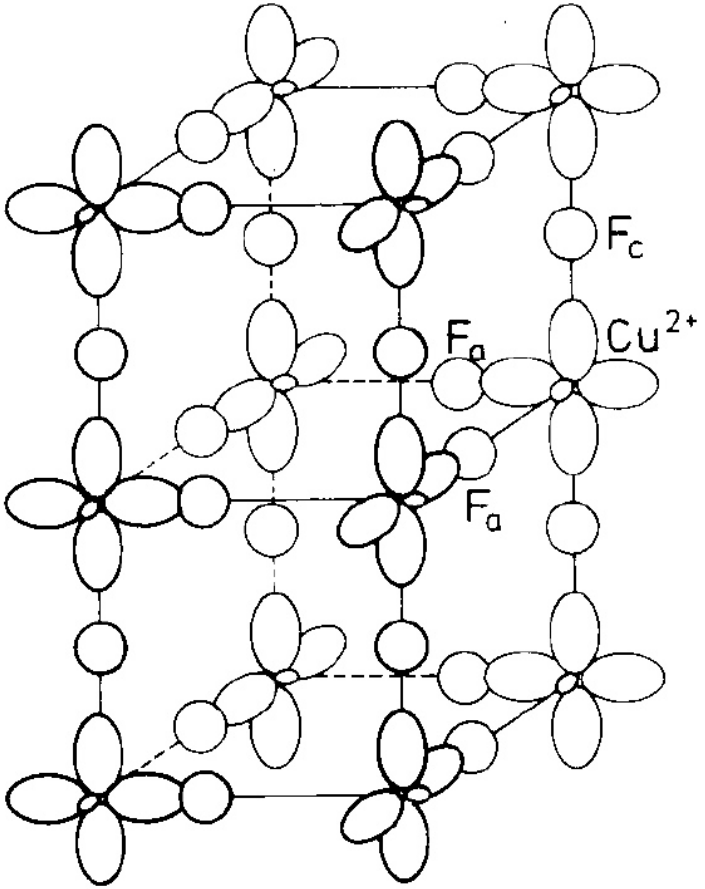

CsNiF3 , TMMC

KCuF3

Table 1. One-dimensional magnets with characteristic properties (note that, in section 4, we use $H=-J\sum \boldsymbol{S}\cdot\boldsymbol{S}$ while, in section 5, $H=-\frac{1}{2}J\sum\sigma\sigma=-2J\sum \boldsymbol{S}\cdot\boldsymbol{S}$ is used).

Substance	S	J/k (K)	T_c, T_N (K)	T_c/O_p	Model
$CuSO_4.5H_2O$	$\frac{1}{2}$	−2·9	0·03	0·02	Heisenberg
$CuSeO_4.5H_2O$	$\frac{1}{2}$	−1·6	0·045	0·056	Heisenberg
$Cu(NH_3)_4SO_4.H_2O$	$\frac{1}{2}$	−6·3	0·37	0·12	Heisenberg
$Cu(NH_3)_4SeO_4.H_2O$	$\frac{1}{2}$	−4·72	1·2	?	Heisenberg
$Cu(NH_3)_4(NO_3)_2$	$\frac{1}{2}$	−7·4	1·4	?	Heisenberg
$CuCl_2.2NC_5H_5$	$\frac{1}{2}$	−26	1·7	0·13	Heisenberg
CHAB	$\frac{1}{2}$	131·6	1·5		Heisenberg (weak x–y)
$KCuF_3$	$\frac{1}{2}$	−380	38	0·2	Heisenberg
$CsNiCl_3$	1	−16·6	4·65	0·13	Heisenberg
$RbNiCl_3$	1	−34	11·0	0·24	Heisenberg
$CsMnCl_32H_2O$	$\frac{5}{2}$	−7·2	4·89	0·12	Heisenberg
TMMC	$\frac{5}{2}$	−13	0·84	0·011	Heisenberg
$CsCuCl_3$	$\frac{1}{2}$	+?	10·4	?	Heisenberg
$(CH_3)_4NCuCl_3$	$\frac{1}{2}$	60	<2	?	Heisenberg
$((CH_3)_3NH)Cu_2Cl_7$	$\frac{1}{2}$	100	<2	?	Heisenberg
$(CH_3)_4NNiCl_3$	1	+4	1·2?	0·5?	Heisenberg
$K_3Fe(CN_6)$	$\frac{1}{2}$	−0·23	0·129	0·56	Ising
$CsCoCl_3$	$\frac{1}{2}$	−75	21·5	0·08	Ising
$(NH_4)_2MnF_5$	$\frac{1}{2}$	−12	7·5	0·08	Ising
$CsCoCl_3.2H_2O$	$\frac{1}{2}$		3·8	?	Ising
$CoCl_2.2NC_5H_5$	$\frac{1}{2}$	+11·5	3·2	0·37	Ising
$CsCoBr_3$	$\frac{1}{2}$	−78	28·3		Ising
$RbCoBr_3$	$\frac{1}{2}$		36	?	Ising
$Fe(N_2H_5)_2(SO_4)_2$	2	−2·0	6·0		Ising
$FeC_2O_4.2H_2O$	$\frac{1}{2}$	−82·6	11·7		Ising
Fe(biPy)Cl_3	$\frac{5}{2}$	−3·0	?		Ising
$RbFeCl_3.H_2O$	$\frac{1}{2}$	−39	12·0		Ising
$FeCl_2Py_2$	$\frac{1}{2}$	+25	6·6		Ising
$NiCl_2Py_2$	$\frac{1}{2}$	+21·4	6·8		Ising
$RbFeCl_3$	2		2·55	?	Planar Heisenberg
$CsNiF_3$	1	23·6	2·65	0·08	Planar Heisenberg

1-D system

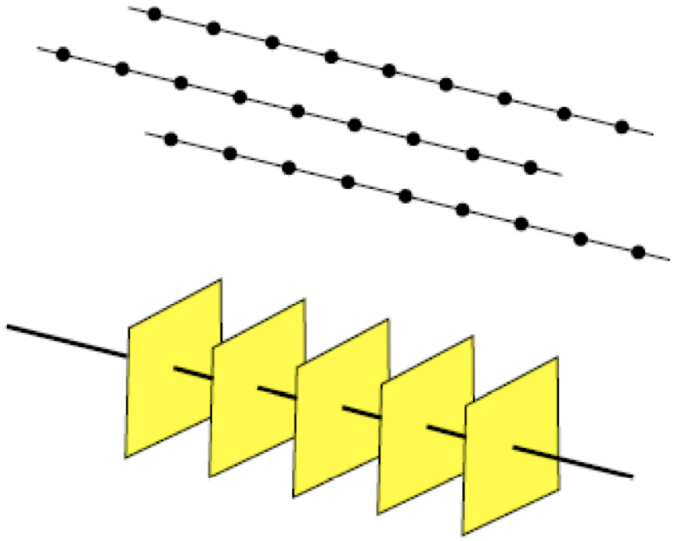

Bragg plane

2-D system

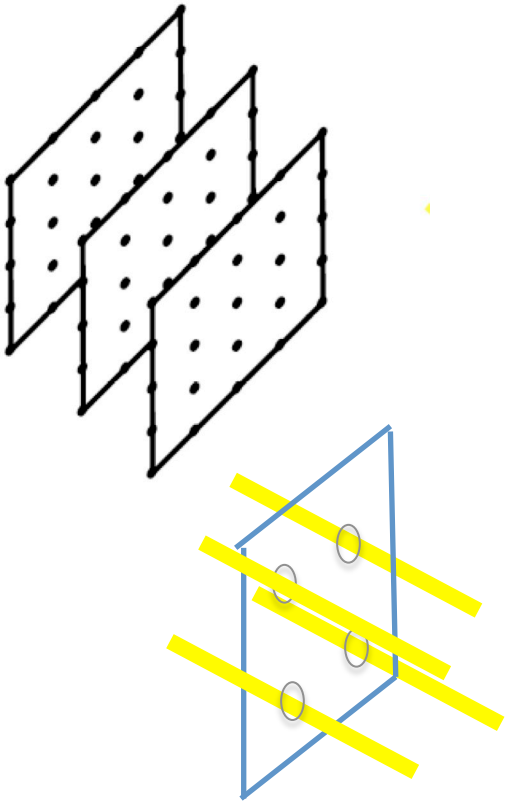

Bragg rod

J < 0 Antiferromagnetic chain

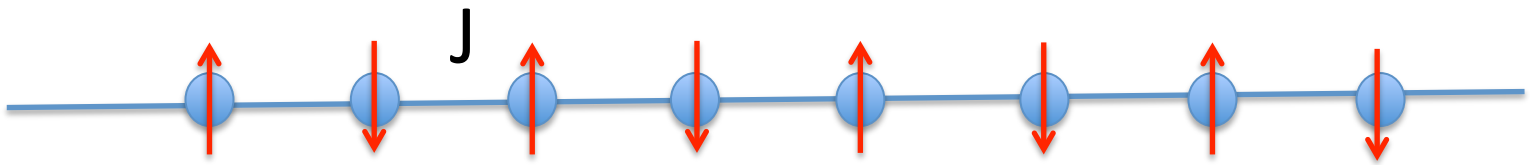

$$\mathscr{H} = -2J \sum_n \mathbf{S}_n \mathbf{S}_{n+1}$$

(ND3)4NMnCl3 (TMMC)

$$H = -2J_{nn}\vec{S}_i \cdot \vec{S}_{i+1}$$

$$\langle \vec{S}_i \cdot \vec{S}_{i+n} \rangle = u^{|n|} S(S+1)$$

$$u = \coth K - K^{-1},\ K = 2J_{nn}S(S+1)/kT$$

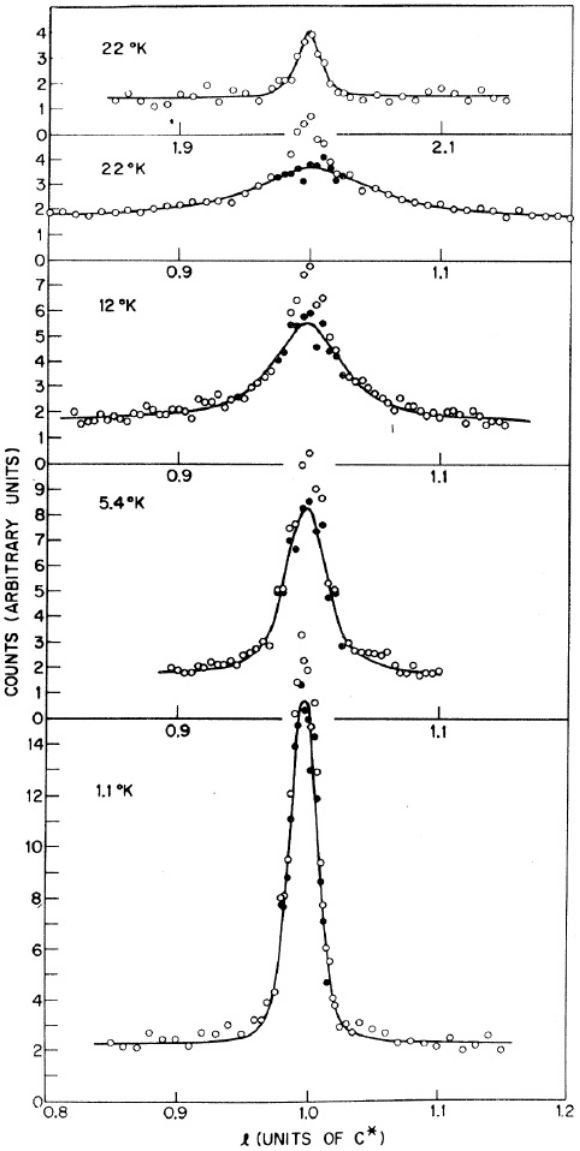

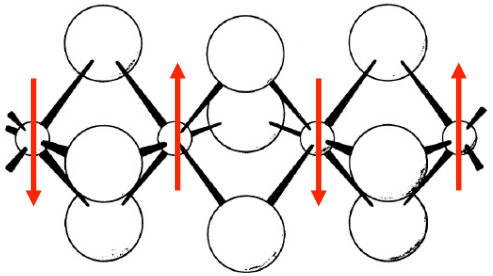

(hOℓ) ORIENTATION

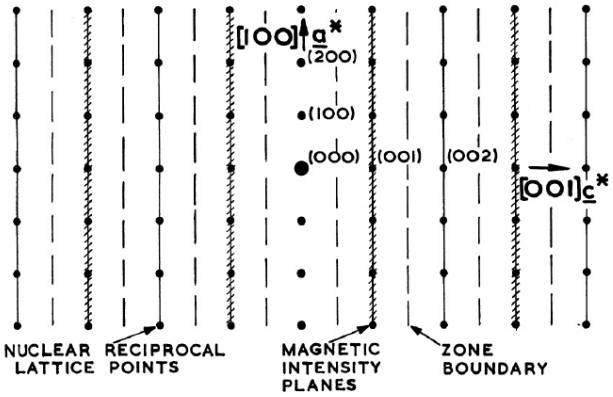

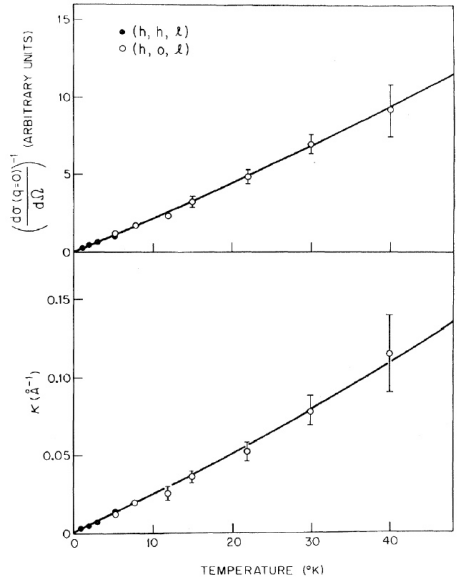

R.J. Birgeneau et al. PRL 26(1971)718

Jnn~ - 7.7K

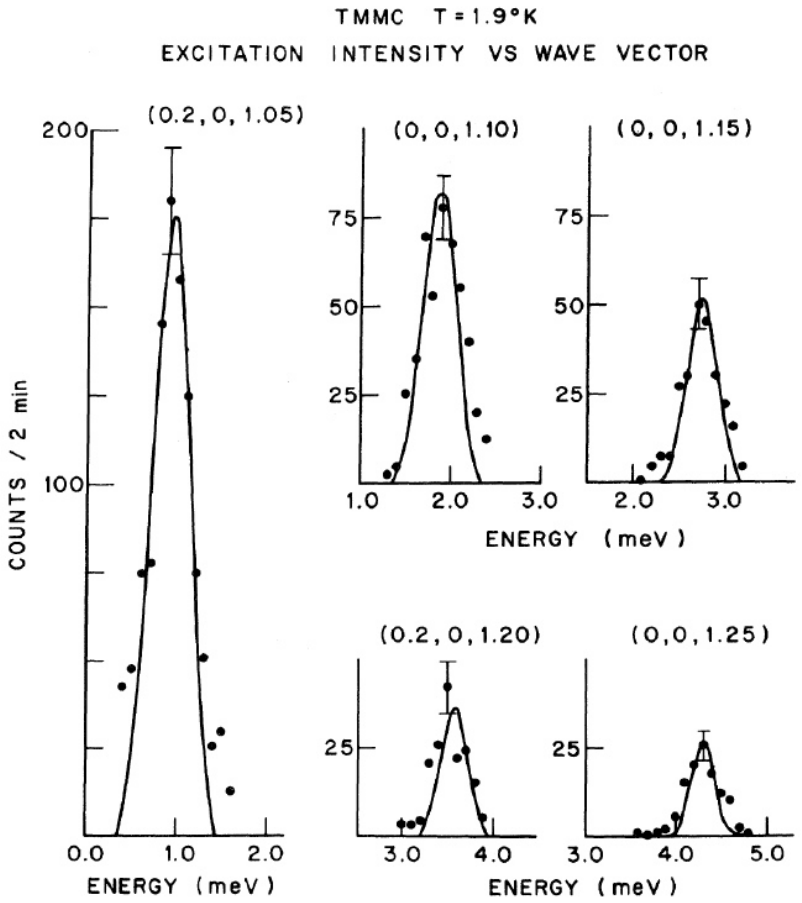

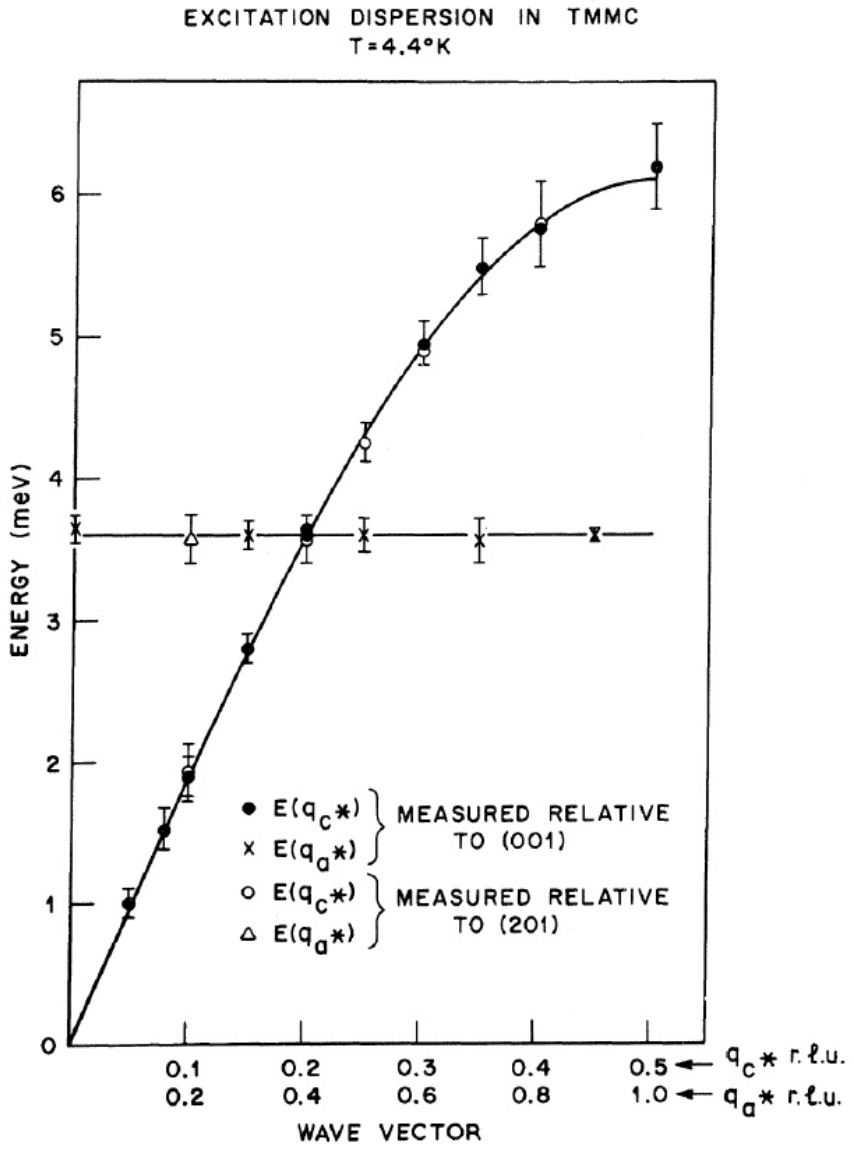

M. T. Hutchingset al. PRB5(1972)1999

J > 0 Ferromagnetic chain

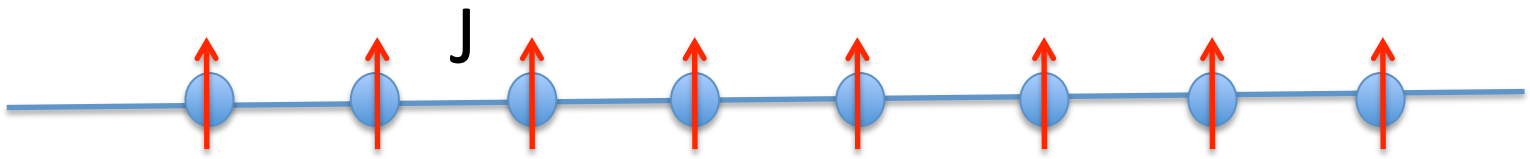

$$\mathscr{H} = -2J \sum_n \mathbf{S}_n \mathbf{S}_{n+1}$$

$CsNiF_3$ 1-D ferromagnet

M. Steiner, J. Villain and C.G. Windsor,
Advances in Physics 25(1976) 87

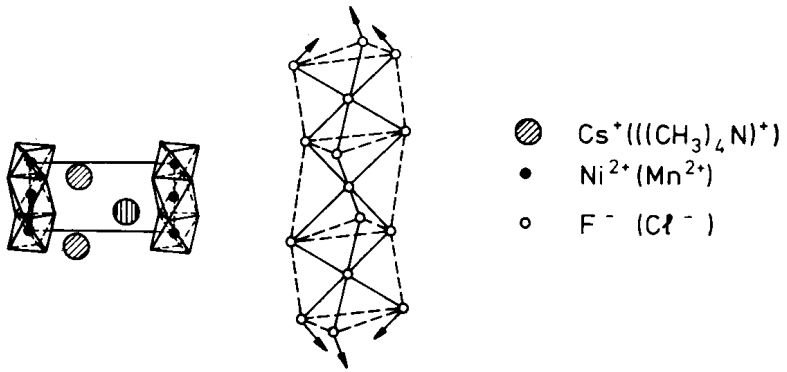

hexagonal crystal structure $P6\ 3/mmc$

$a = b = 6.21$ Å and $c = 5.2$ Å

CsNiF3 ferromagnetic chain

Steiner et al.

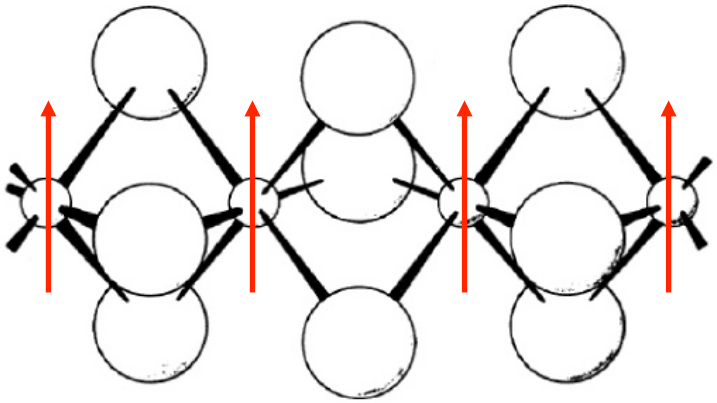

(hOℓ) ORIENTATION

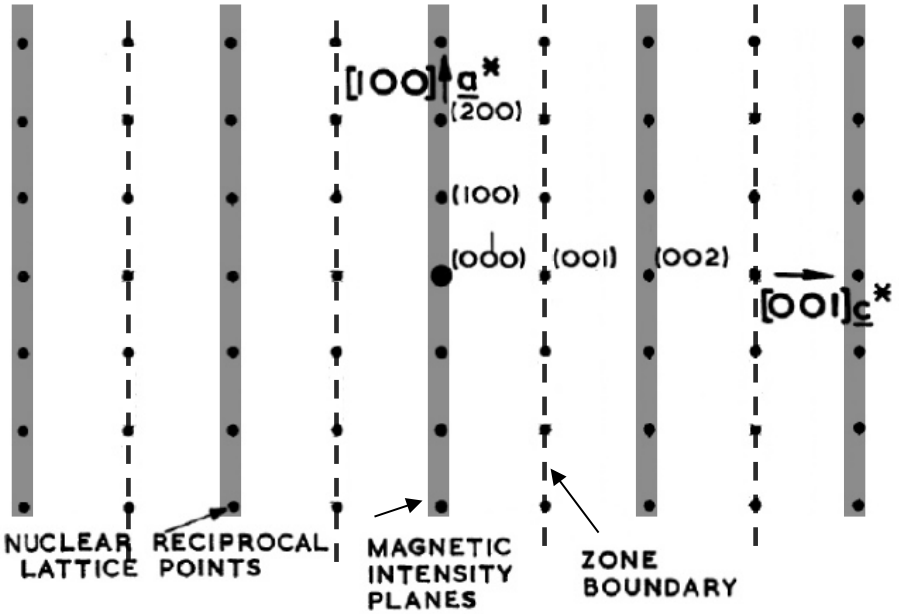

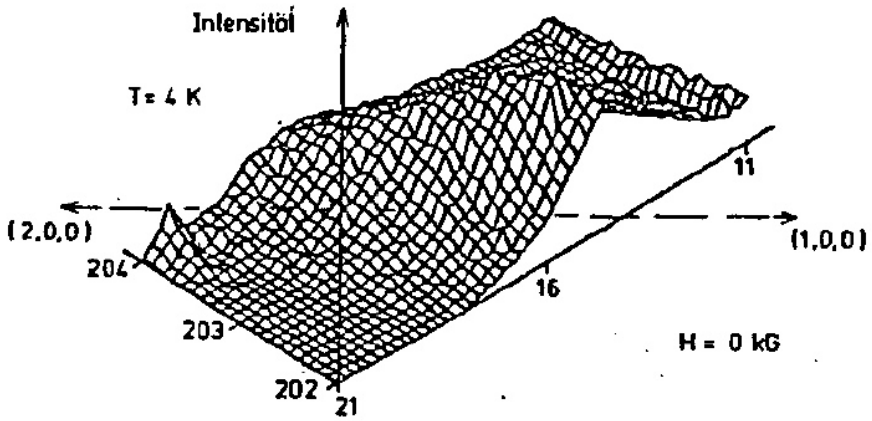

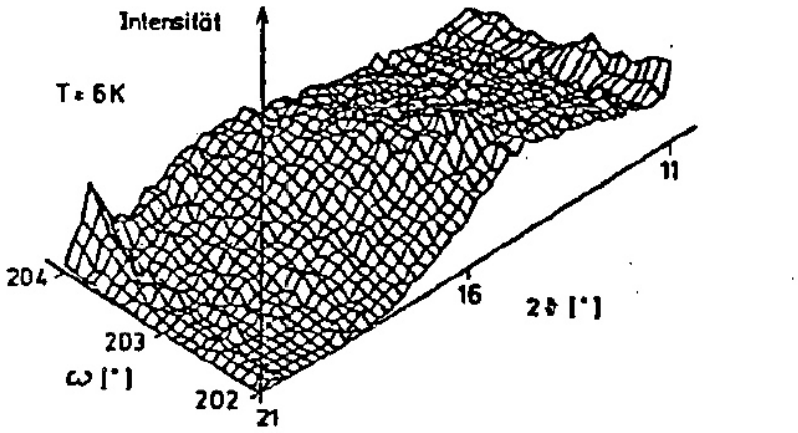

Neutron magnetic cross section (for the localized spin-only magnetic moments)

$$S(\mathbf{q},\omega)\sim\frac{d^2\sigma}{d\Omega\,d\omega}=\frac{|\mathbf{k}_f|}{|\mathbf{k}_i|}\left(1{\cdot}91\,\frac{e^2}{mc^2}\right)^2\sum_{ij}F_j^*(q)F_i(q)\cdot\frac{1}{2\pi}\int dt\;\exp(i\omega t)\,\langle S_{i\perp}(0)S_{j\perp}(t)\rangle\exp[i\mathbf{q}(\mathbf{R}_i-\mathbf{R}_j)]$$

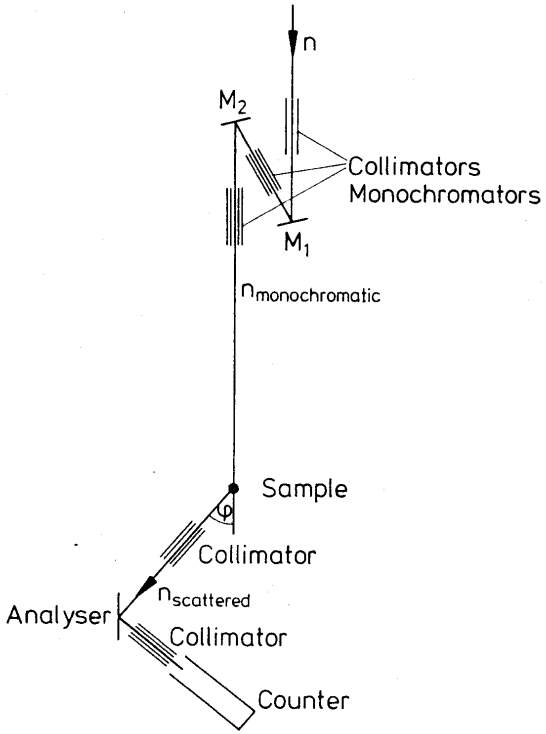

Experimental set-up of a triple axis spectrometer for inelastic neutron scattering (e.g. IN2 of ILL Grenoble).

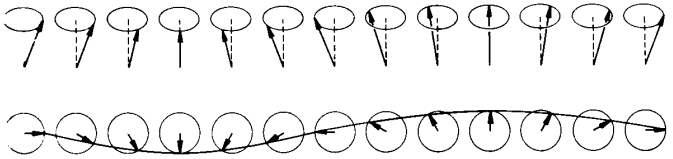

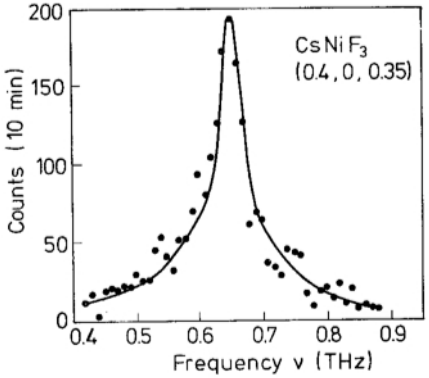

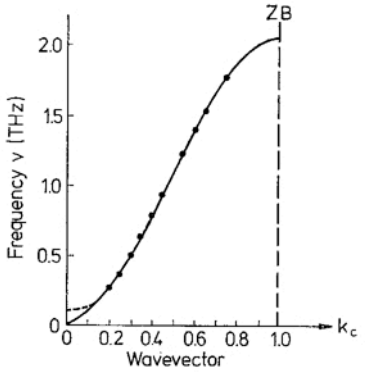

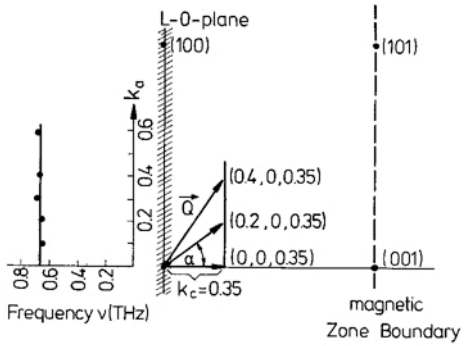

$J/k = 11.8\ \mathrm{K};\ A/k = 9.5\ \mathrm{K}$

M. Steiner, B. Dorner: Spin Wave Measurements in the One Dimensional Ferromagnet $CsNiF_3$. Solid State Communications 12, S. 537-540 (1973)

Solitons in easy-plane ferromagnet $CsNiF_3$

Mapping on sine-Gordon system

H.J. Mikeska, J. Phys. C 11(1978)

$$\boldsymbol{S}_n = S\{\sin\theta_n \cos\phi_n, \sin\theta_n \sin\phi_n, \cos\theta_n\}.$$

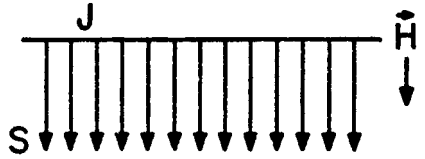

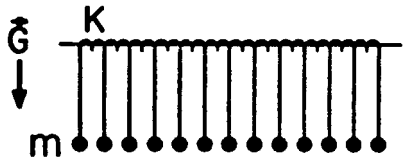

$$\mathscr{H} = -J\sum_n \boldsymbol{S}_n . \boldsymbol{S}_{n+1} + A\sum_n (S_n^z)^2 - g\mu_B B \sum_n S_n^x.$$

$$\frac{\partial^2\phi}{\partial z^2} - \frac{1}{c^2}\frac{\partial^2\phi}{\partial t^2} = m^2 \sin\phi$$

$$\theta = \frac{1}{2AS}\frac{\partial\phi}{\partial t}.$$

$J/k = 11.8$ K; $A/k = 9.5$ K

$$c = aS\,(2AJ)^{1/2}$$

$$m = \{g\mu_B B/JS\,a^2\}^{1/2}$$

s-G system represents a completely integrable Hamiltonian system with the following solutions:
free oscillations, soliton and breathers

Evidence for Soliton Modes in the One-Dimensional Ferromagnet $CsNiF_3$

J. K. Kjems
Risø National Laboratory, DK-4000 Roskilde, Denmark

and

M. Steiner
Hahn-Meitner-Institut für Kernforschung, D-1000 Berlin 39, Germany
(Received 24 July 1978)

Evidence for solitons moving along the ferromagnetic chains in $CsNiF_3$ has been obtained by inelastic neutron scattering. As predicted by Mikeska the scattering is found at low q, around zero energy. The soliton activation energy, $8m$, is determined via the temperature and field dependence of the intensities (m is the effective mass of the quasiparticle soliton). At $H = 5$ kG we find $8m/k_B = 27$ K in reasonable agreement with the predicted value, as is the energy width at $q = 0.1$.

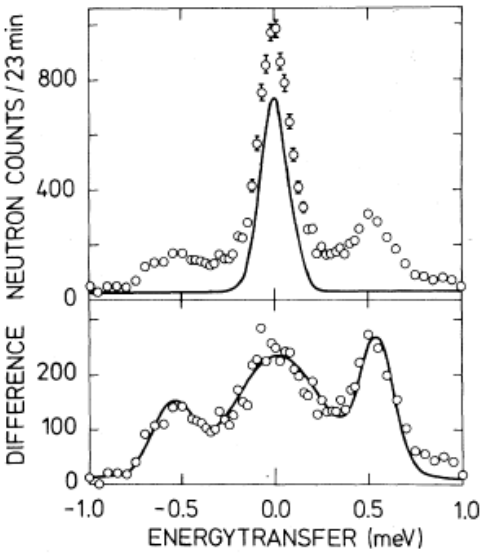

Upper: Observed inelastic spectrum at (0, 0, 1.9) at $T = 9.3$ K and $H = 5$ kG (circles). The full line is the observed profile at $T = 3.1$ K and 30 kG which is assumed to be the background. Lower: Difference between the two spectra in the upper part of the figure. The full line is the result of a least-squares fit as described in the text.

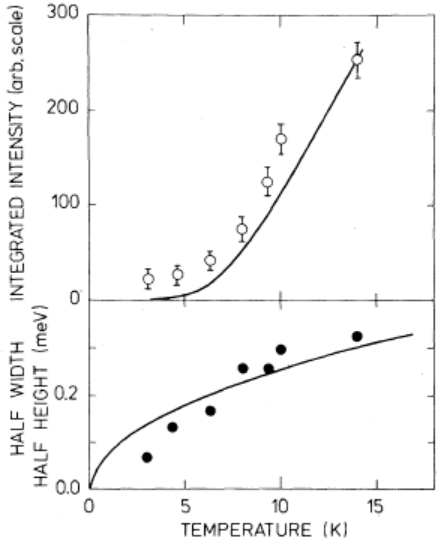

Temperature dependence of the integrated intensity (upper) and energy half-width at half-maximum (lower) of the quasielastic component at $H = 5$ kG and $q = (0, 0, 1.0)$. The values are derived from the least-squares fitting procedure described in the text. The full lines are the results predicted by Mikeska with no adjustable parameter for the energy width and only a scale factor for the intensity.

$$S_{sol}(q,\omega) \propto \frac{\beta e^{-8m\beta}}{cq} \times$$

$$\exp\left(-\frac{4\beta m\omega^2}{c^2q^2}\right)\left(\frac{\pi q/2m}{\sinh(\pi q/2m)}\right)^2$$

experiment on TAS-7, Risø March 1979

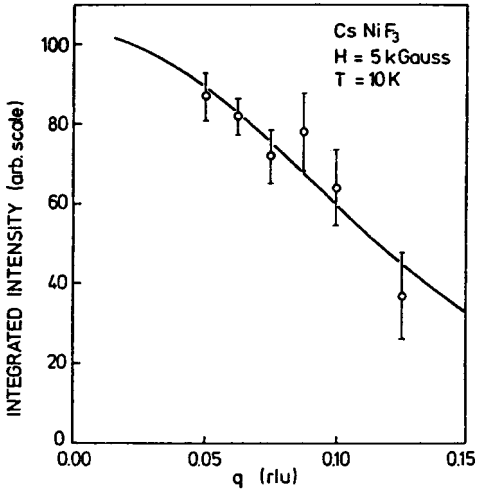

8m=69K

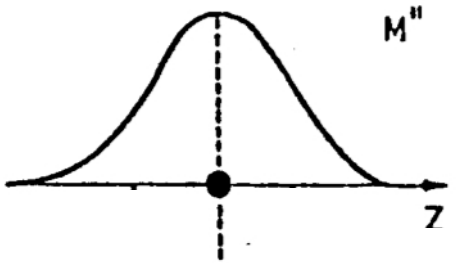

H vertical ⊙

$\mathbf{Q}_1$: $\langle S^x S^x \rangle + \langle S^z S^z \rangle$: I

$\mathbf{Q}_2$: $\langle S^x S^x \rangle + \langle S^y S^y \rangle$: II

H horizontal →

$\mathbf{Q}_1$: $\langle S^z S^z \rangle + \langle S^y S^y \rangle$: III

$\mathbf{Q}_2$: $\langle S^x S^x \rangle + \langle S^y S^y \rangle$: II

mass of the soliton

$$m = \{g\mu_B B/JS\,a^2\}^{1/2}$$

different by factor 2!

$$8m_{\text{theor}} = 34\ \text{K},$$

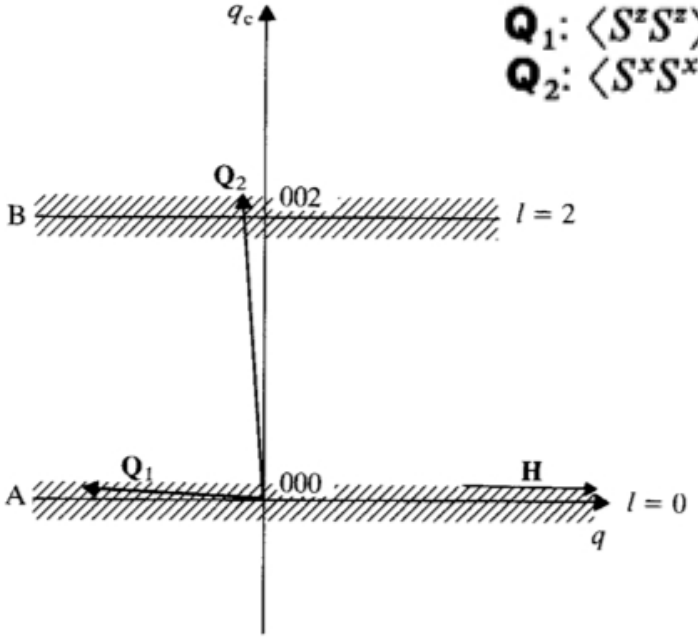

Controversial points

a) Validity of sine-Gordon mapping in $CsNiF_3$ case

b) Two magnon contribution in the central peak

Validity of sine-Gordon mapping in $CsNiF_3$ case

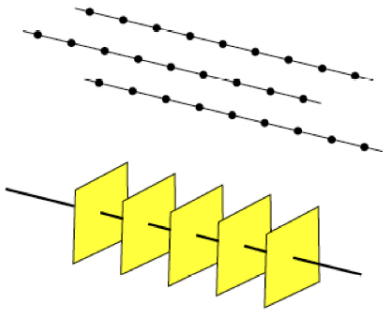

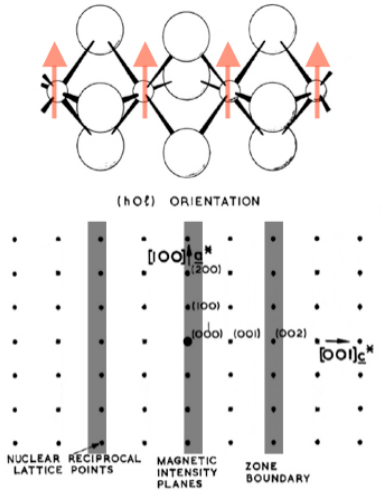

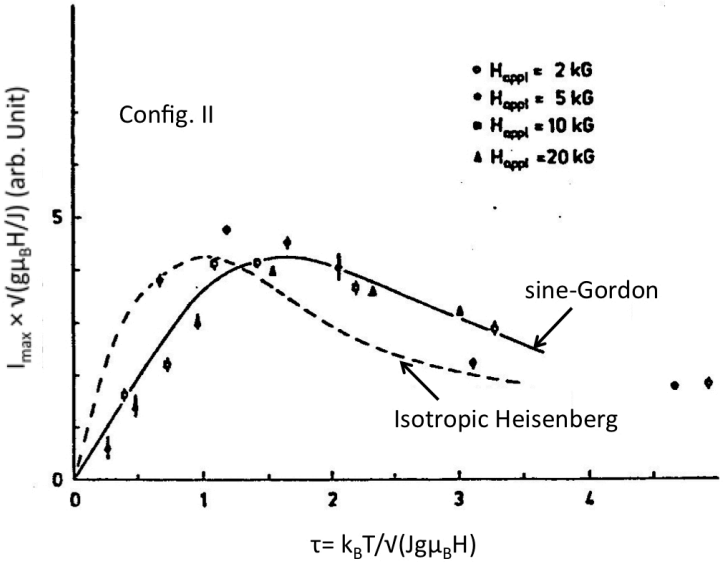

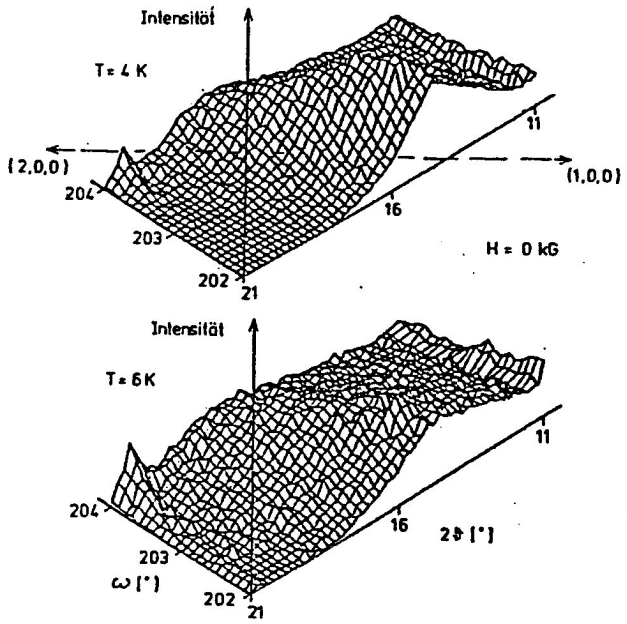

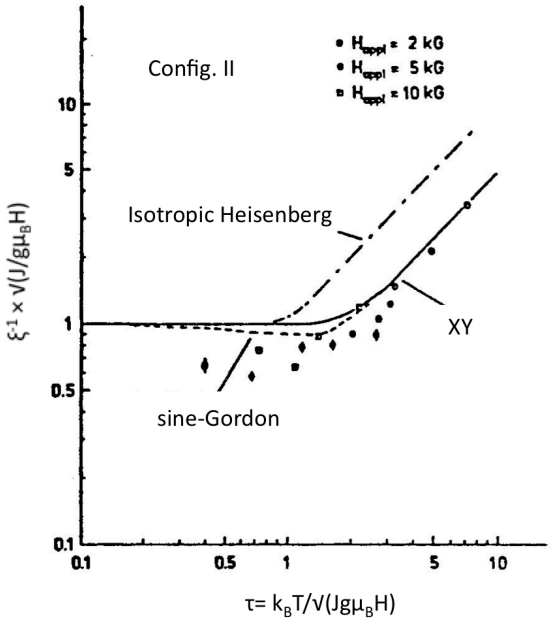

Looking for pure soliton contribution

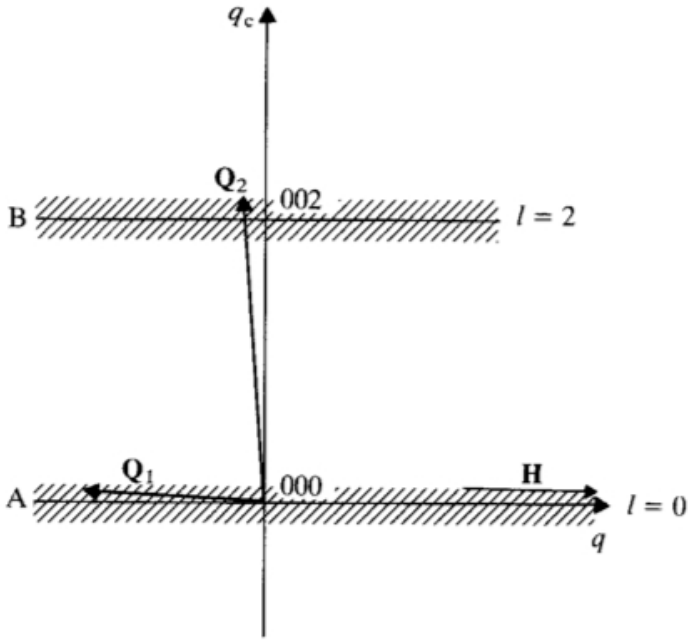

H vertical ⊙

$\mathbf{Q}_1$: $\langle S^x S^x \rangle + \langle S^z S^z \rangle$: I

$\mathbf{Q}_2$: $\langle S^x S^x \rangle + \langle S^y S^y \rangle$: II

H horizontal →

$\mathbf{Q}_1$: $\langle S^z S^z \rangle + \langle S^y S^y \rangle$: III

$\mathbf{Q}_2$: $\langle S^x S^x \rangle + \langle S^y S^y \rangle$: II

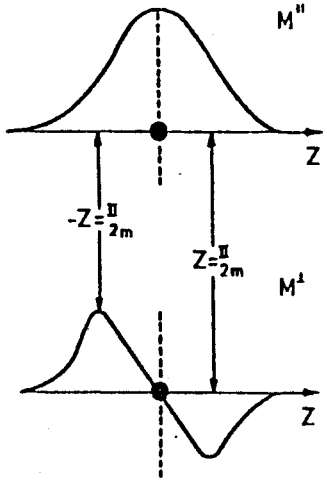

$\propto (Q/\sinh Q)^2$

$\propto (Q/\cosh Q)^2$

where $Q=\pi q/(2m)$

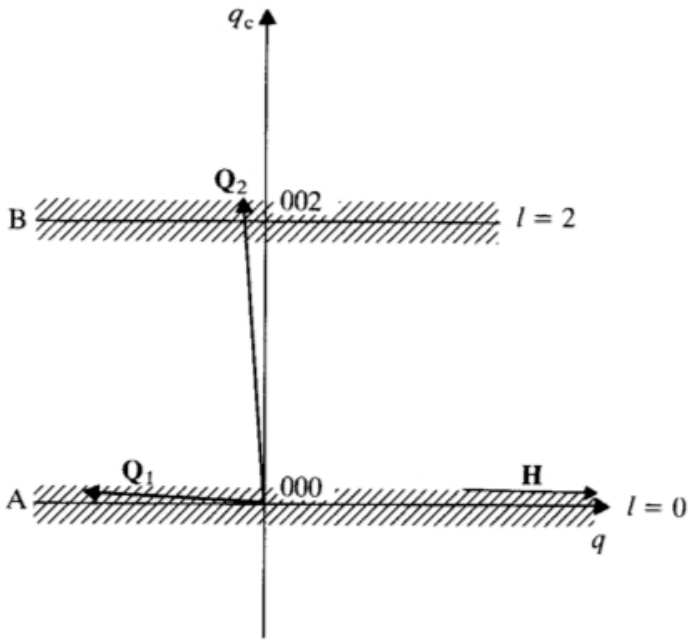

H vertical ⊙

$\mathbf{Q}_1$: $\langle S^x S^x \rangle + \langle S^z S^z \rangle$: I

$\mathbf{Q}_2$: $\langle S^x S^x \rangle + \langle S^y S^y \rangle$: II

H horizontal →

$\mathbf{Q}_1$: $\langle S^z S^z \rangle + \langle S^y S^y \rangle$: III

$\mathbf{Q}_2$: $\langle S^x S^x \rangle + \langle S^y S^y \rangle$: II

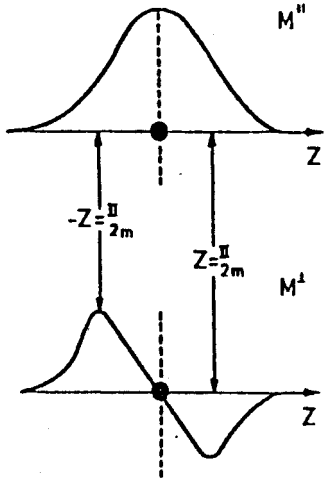

$\propto (Q/\sinh Q)^2$

$\propto (Q/\cosh Q)^2$

where $Q=\pi q/(2m)$

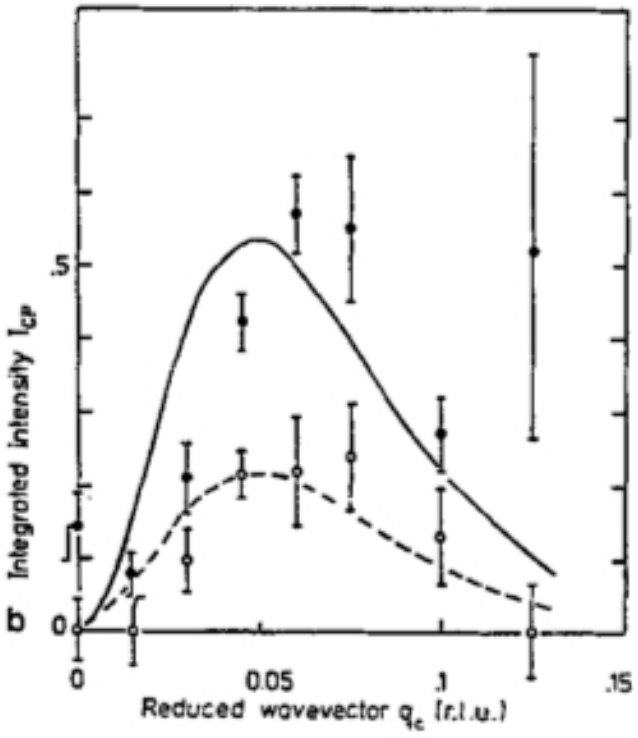

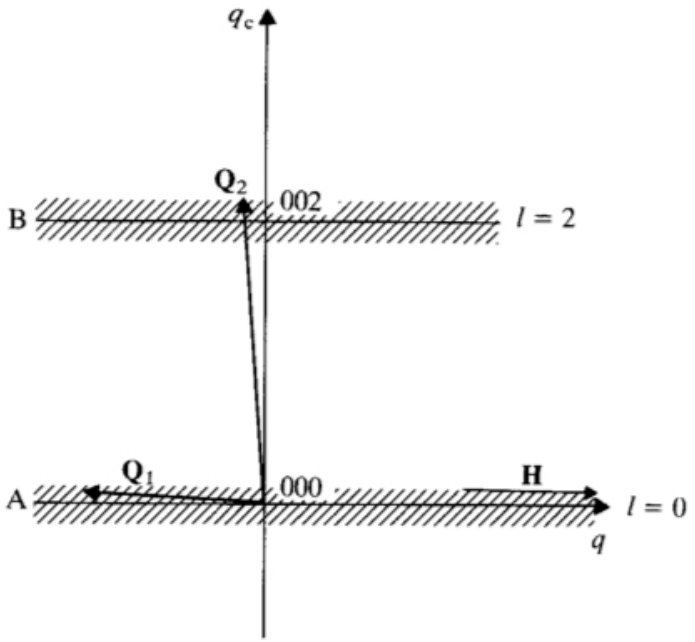

H vertical ⊙

Q_1: $\langle S^x S^x \rangle + \langle S^z S^z \rangle$: I

Q_2: $\langle S^x S^x \rangle + \langle S^y S^y \rangle$: II

H horizontal →

Q_1: $\langle S^z S^z \rangle + \langle S^y S^y \rangle$: III

Q_2: $\langle S^x S^x \rangle + \langle S^y S^y \rangle$: II

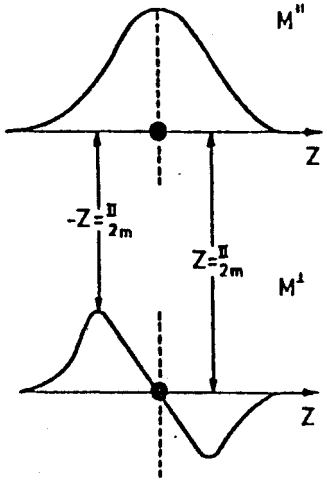

$\propto (Q/\sinh Q)^2$

$\propto (Q/\cosh Q)^2$

where $Q=\pi q/(2m)$

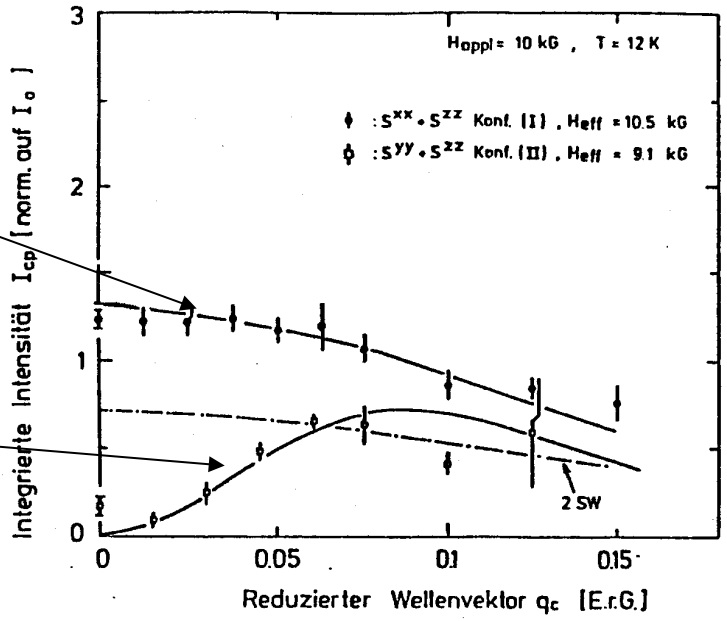

ADVANCES IN PHYSICS, 1991, VOL. 40, NO. 3, 191–356

Solitary excitations in one-dimensional magnets

By H.-J. MIKESKA
Institut für Theoretische Physik, University of Hannover, Germany

and M. STEINER
Institut für Physik, University of Mainz, Germany

[Received 6 November 1990]

Abstract

The present status of theoretical and experimental investigations of solitary excitations in one-dimensional magnetic systems is reviewed. A survey of exact solutions to the nonlinear equations of motion for pertinent classical chain systems (sine–Gordon chain and ferromagnetic Heisenberg chains with various anisotropies) is given. Particular emphasis is devoted to the role of solitons in the thermodynamics of such systems. Models corresponding to real quasi-one-dimensional magnets are broadly discussed to demonstrate the properties of their solitary excitations. The experimental significance of such nonlinear excitations in the static and dynamic quantities of such systems is discussed in detail. The models and model substances are the easy-plane ferromagnet (model substances $CsNiF_3$ and $(C_6H_{11}NH_3)CuBr_3$), the easy-plane antiferromagnet $(CH_3)_4NMnCl_3$) and the $S=\frac{1}{2}$ Ising chain with transverse interactions ($CsCoCl_3$). The quantum aspects of solitary excitations are treated in some theoretical detail. Finally, open questions and possible future investigations are discussed.

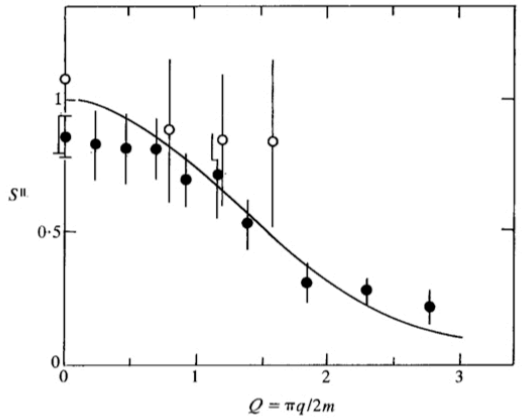

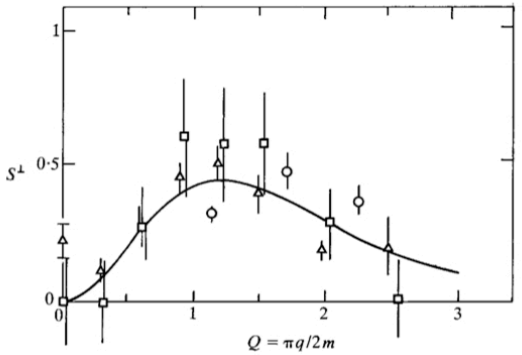

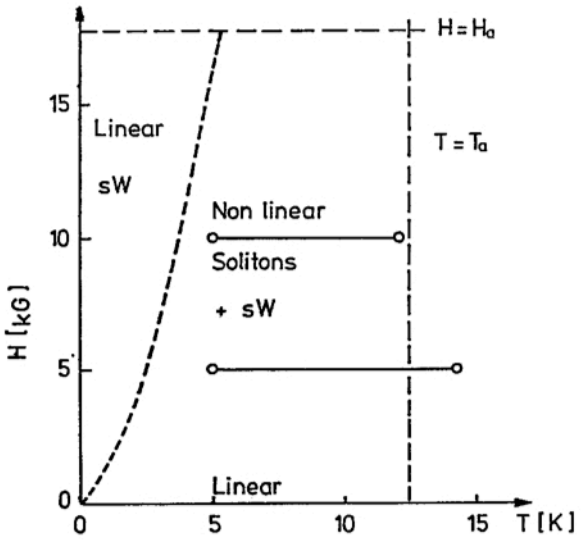

'The fundamental question for the existence of sine-Gordon-like solitons in one-dimensional magnets, as suggested by the theory, appears to have been answered positively by the experiments.'

Spin Excitations in Quantum Magnets

Example: Quasi 1-D AF system TMMC

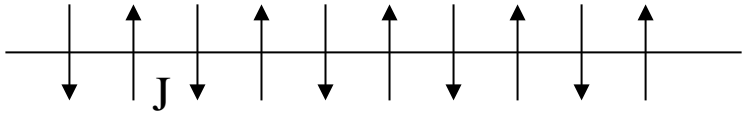

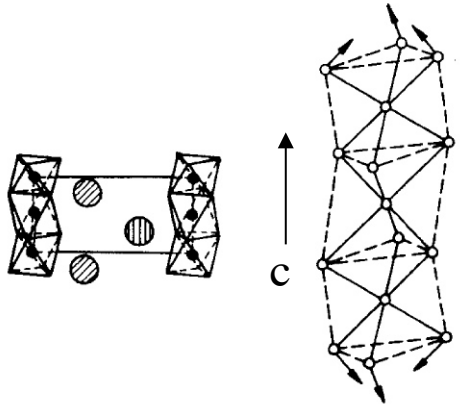

$$H = J\sum_{n.n.} S_i S_j$$

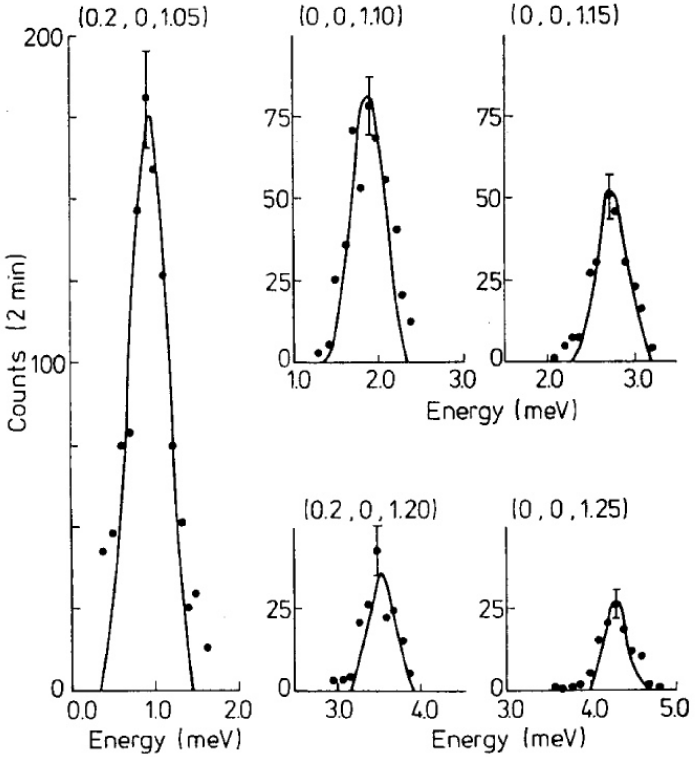

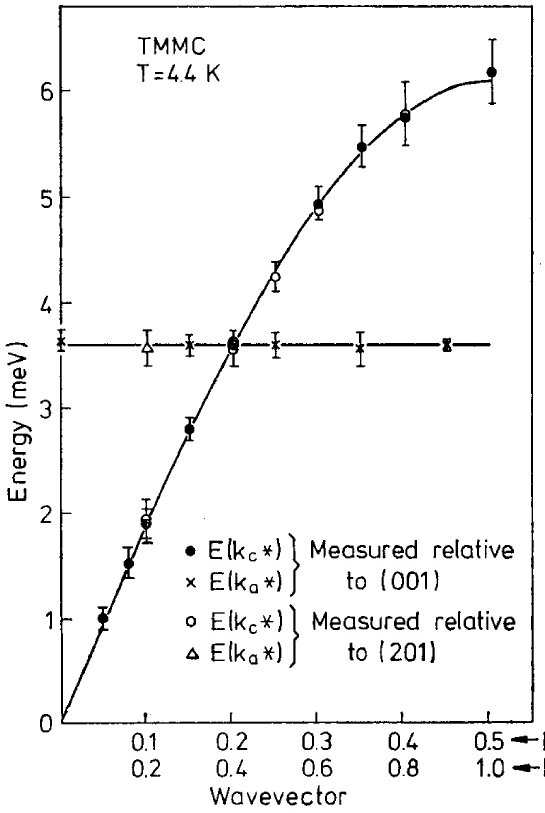

$\hbar\omega_k = 4S|J\sin(\pi k)|$
along the chain direction

flat perpendicular to the chain direction

M.T. Hutchings et al. PRB 5 (1972) 1999

low-dimensional character of the magnetic exchange

Quantum spin systems: dimer, Haldane, ladder systems

in contrast to the classical isotropic AF system without gap

Singlet ground state with a gap in spin excitation

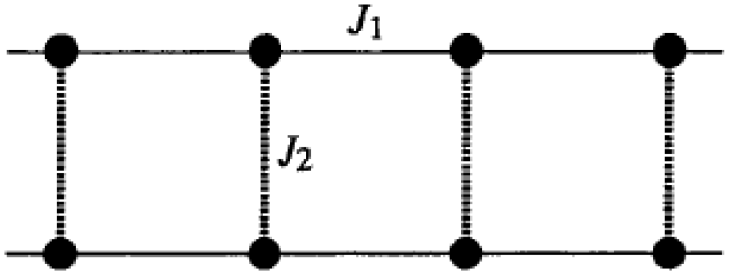

dimer case:

$|S\rangle = 1/\sqrt{2}\,(\,|\uparrow\downarrow\rangle - |\downarrow\uparrow\rangle)$

$|t\rangle = |\uparrow\uparrow\rangle,\ 1/\sqrt{2}\,(\,|\uparrow\downarrow\rangle + |\downarrow\uparrow\rangle),\ |\downarrow\downarrow\rangle$

The case of $KCuCl_3$

Weakly coupled dimer system with a singlet ground state

in collaboration with

T. Kato[1)], K. Takatsu[2)], W. Shiramura[2)], H. Tanaka[2)], K. Nakajima[3)]

[1)]Chiba University; [2)]Tokyo Institute of Technology; [3)]ISSP, Univ. of Tokyo

$KCuCl_3$

a = 4.029 Å
b = 13.735Å
c = 8.736 Å

monoclinic; $P2_1/c$

β = 97.3°

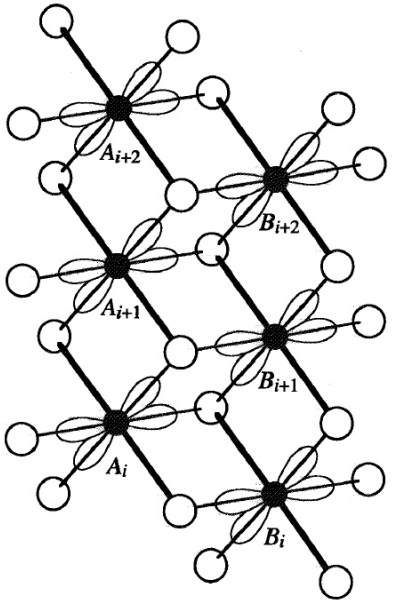

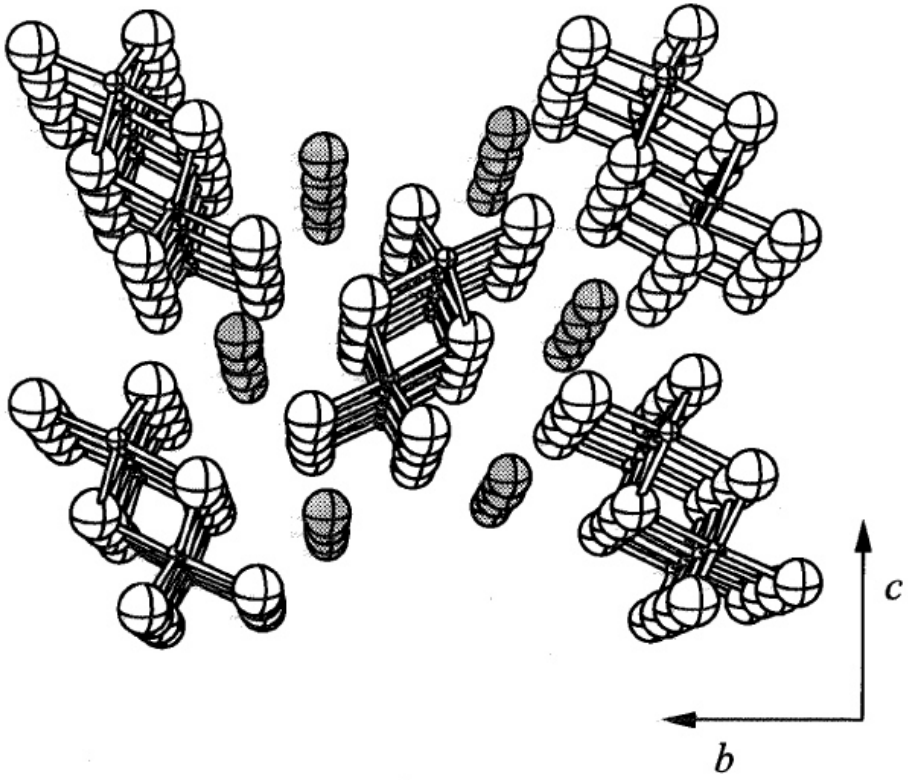

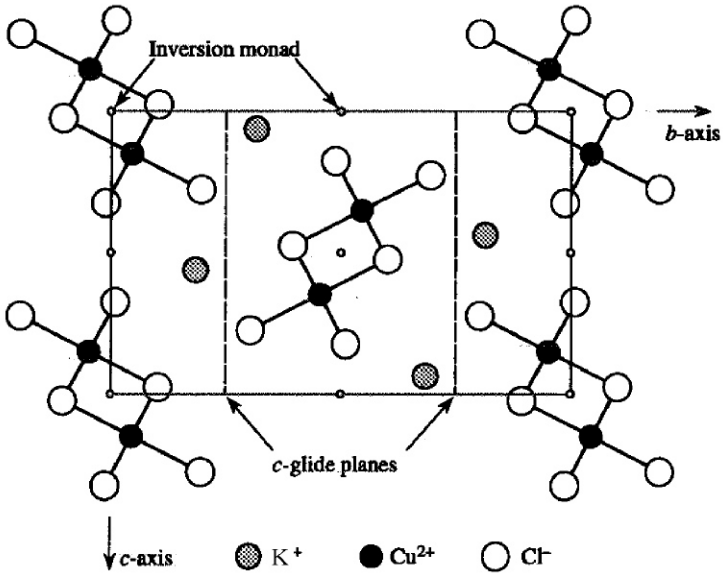

K^+ Cu^{2+} Cl^-

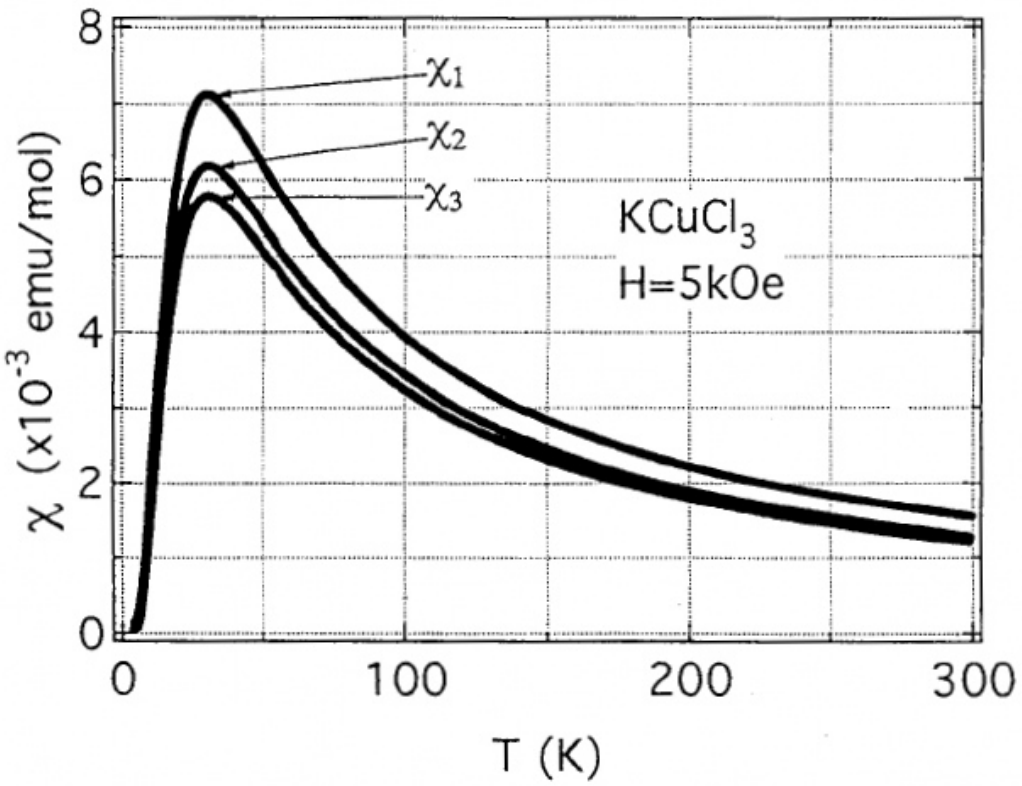

Susceptibility

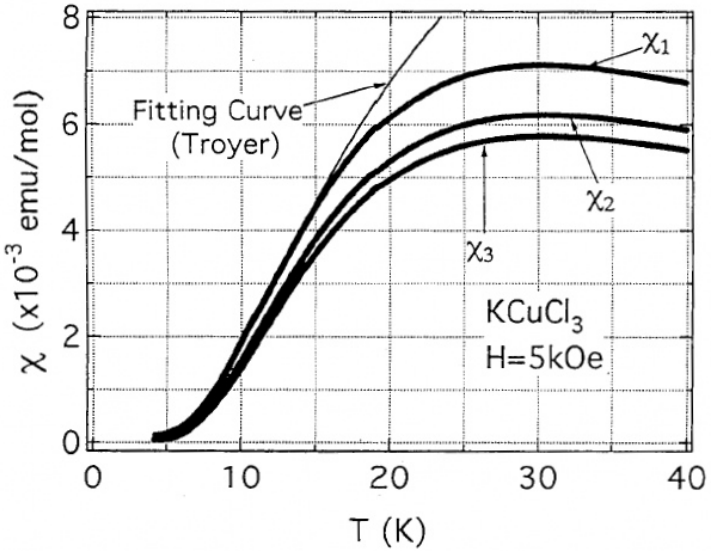

$$\chi \propto \frac{1}{\sqrt{T}} \exp\left(-\frac{\Delta}{k_B T}\right)$$

$$\frac{\Delta}{k_B T} \approx 35\ K$$

Magnetization: existence of critical field (zero-field plateau)

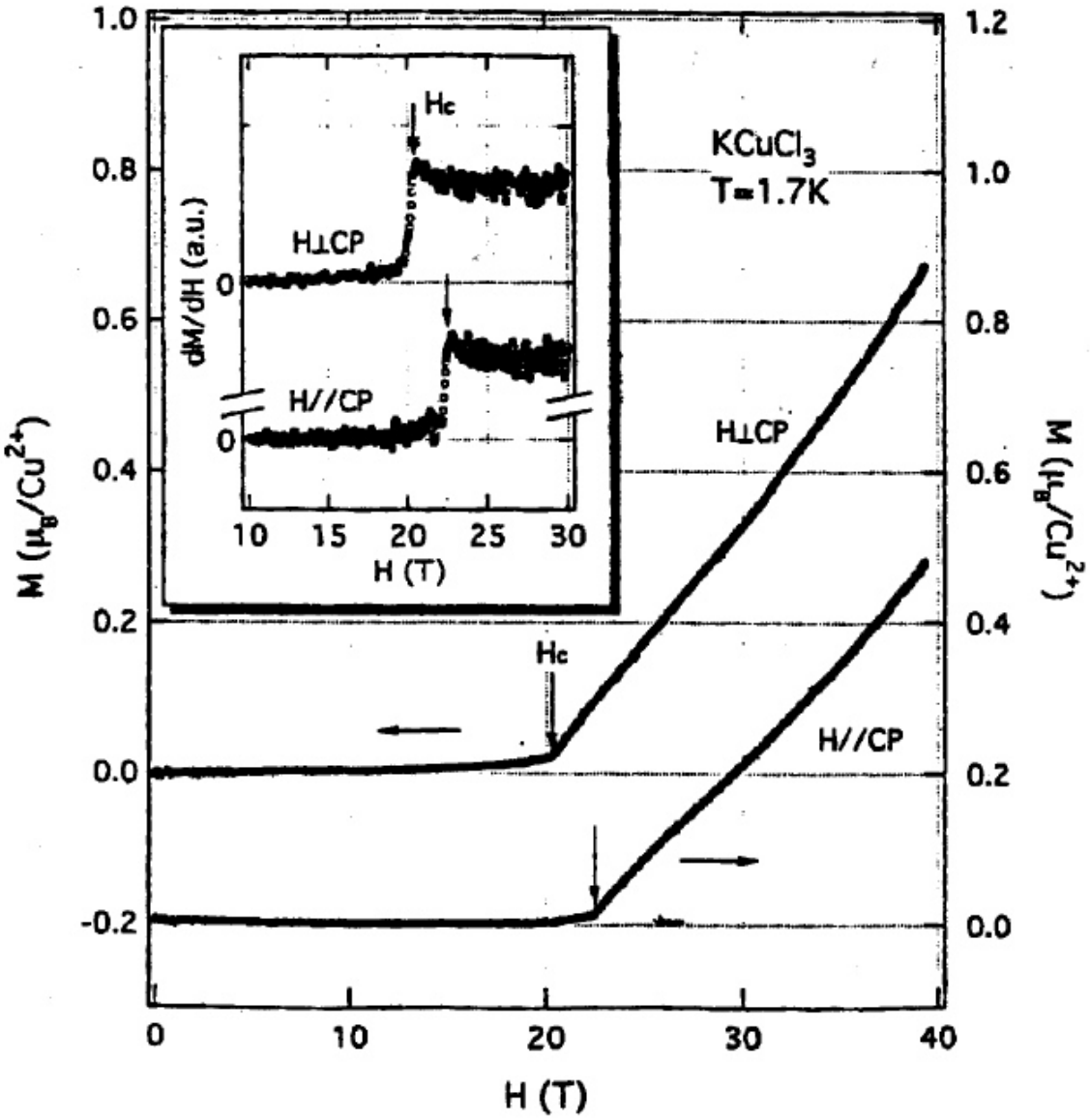

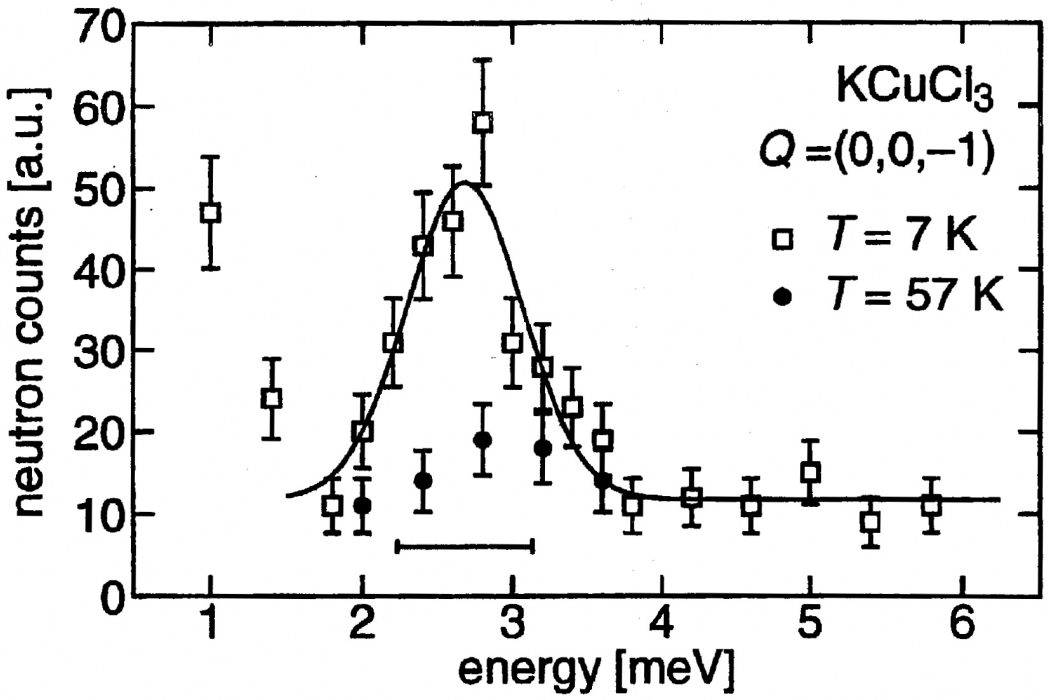

Fig. The constant-Q scans of the inelastic neutron scattering for $KCuCl_3$ at $Q = (0, 0, -1)$ at $T = 7$ and 57 K.

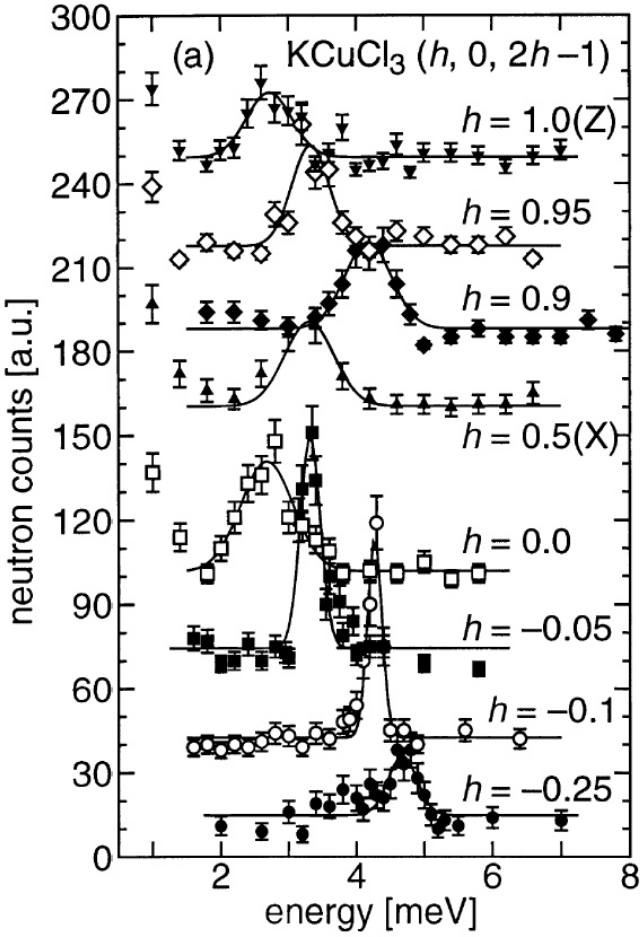

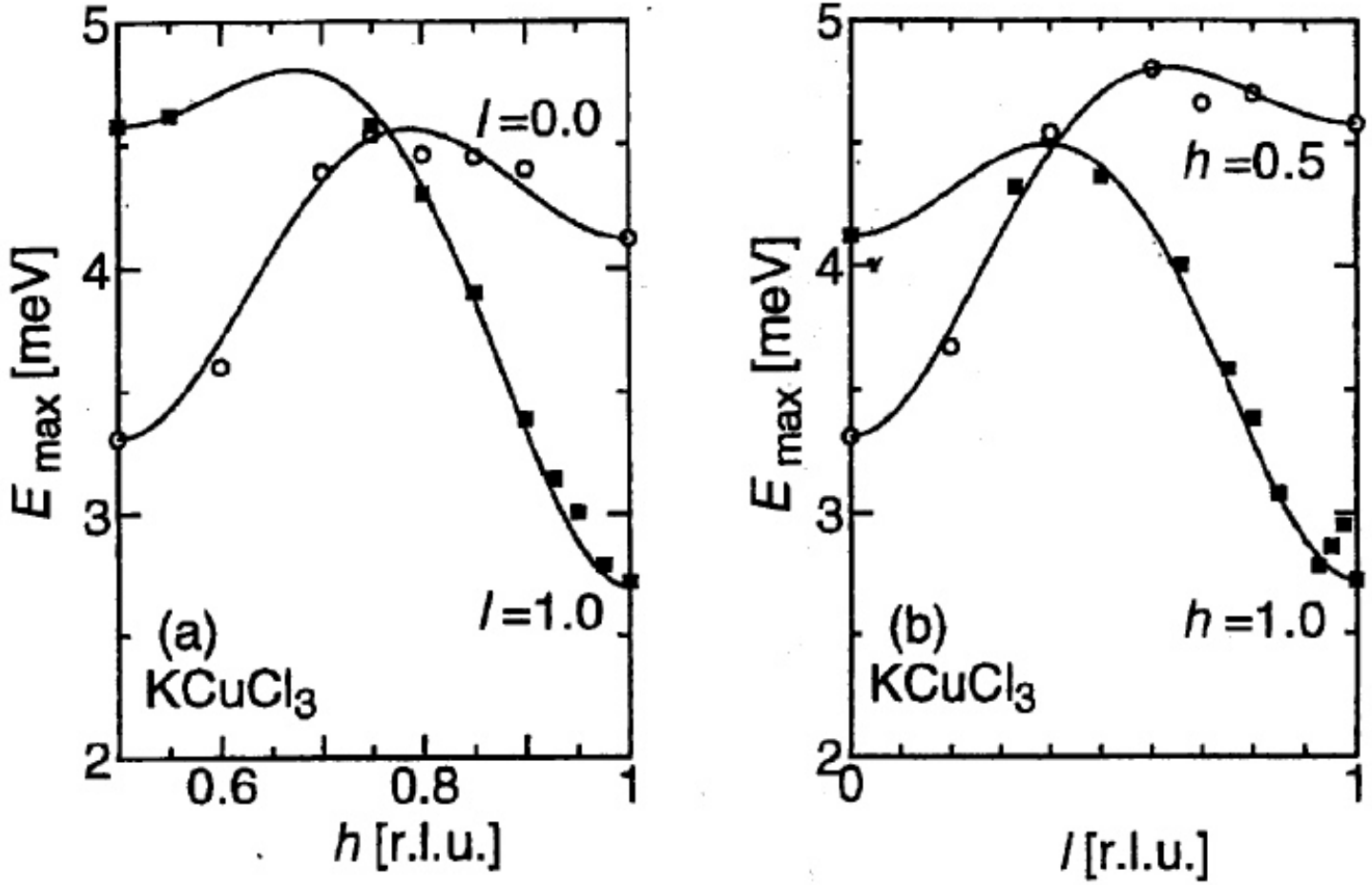

Fig. 4. The dispersion relation $\omega(k)$ of $KCuCl_3$ for k changing (a) parallel and (b) perpendicular to the double chain.

Example: Quasi 1-D AF system TMMC

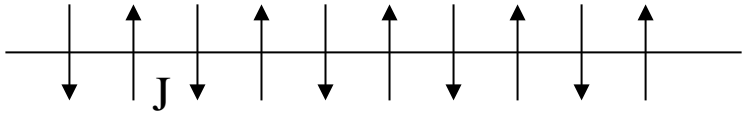

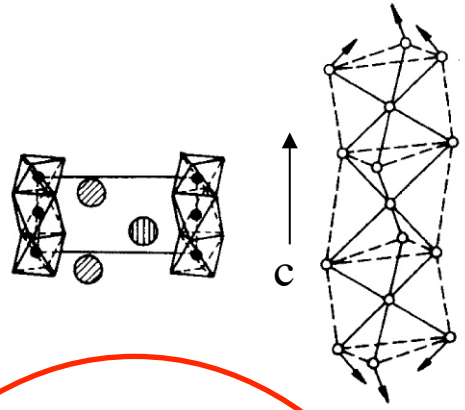

$$H = J\sum_{n.n.} S_i S_j$$

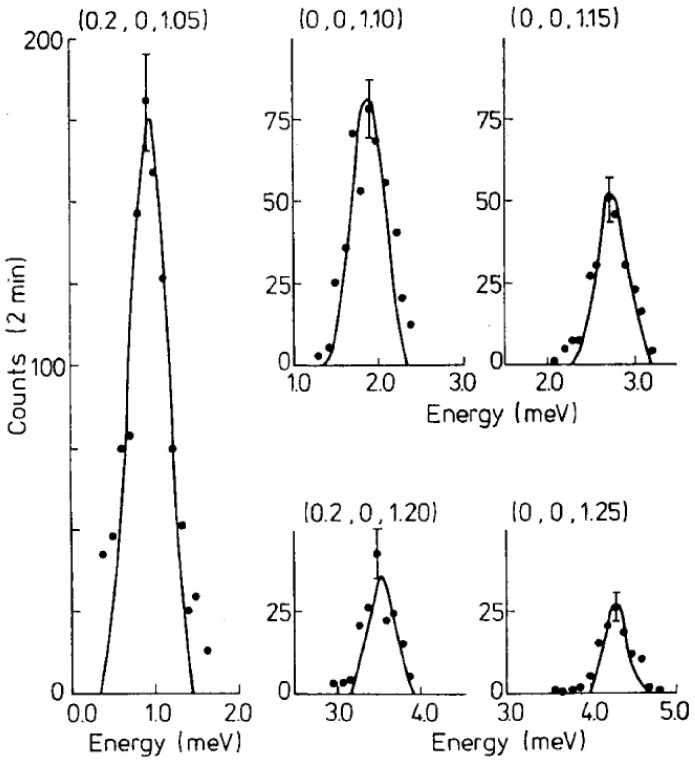

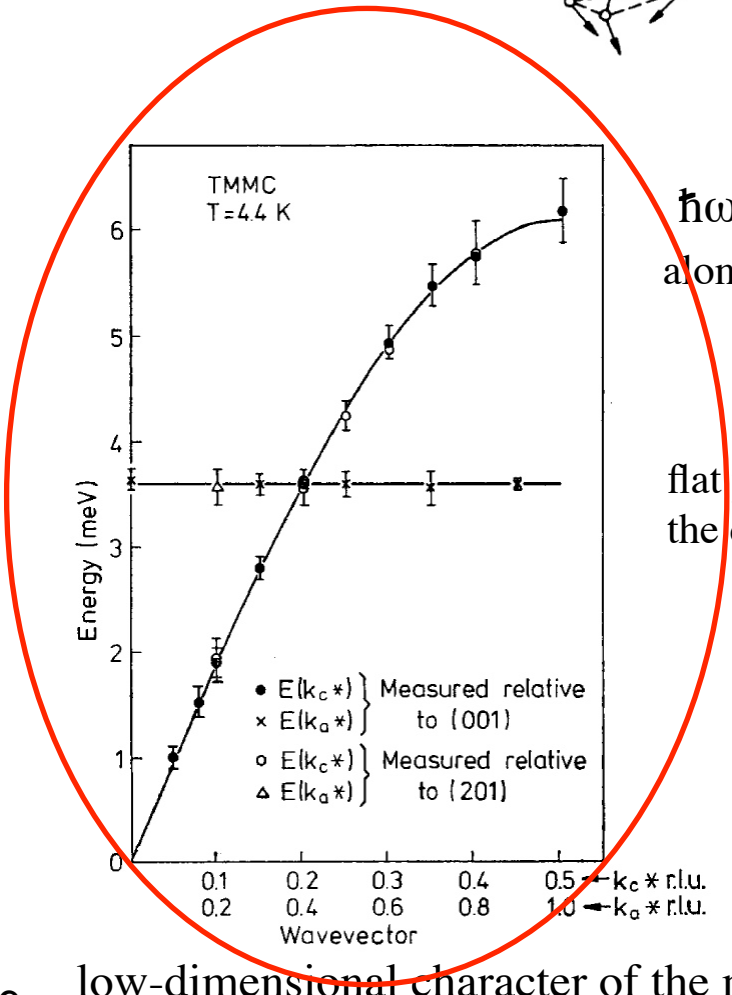

$\hbar\omega_k = 4S|J\sin(\pi k)|$
along the chain direction

flat perpendicular to the chain direction

low-dimensional character of the magnetic exchange

M.T. Hutchings et al. PRB 5 (1972) 1999

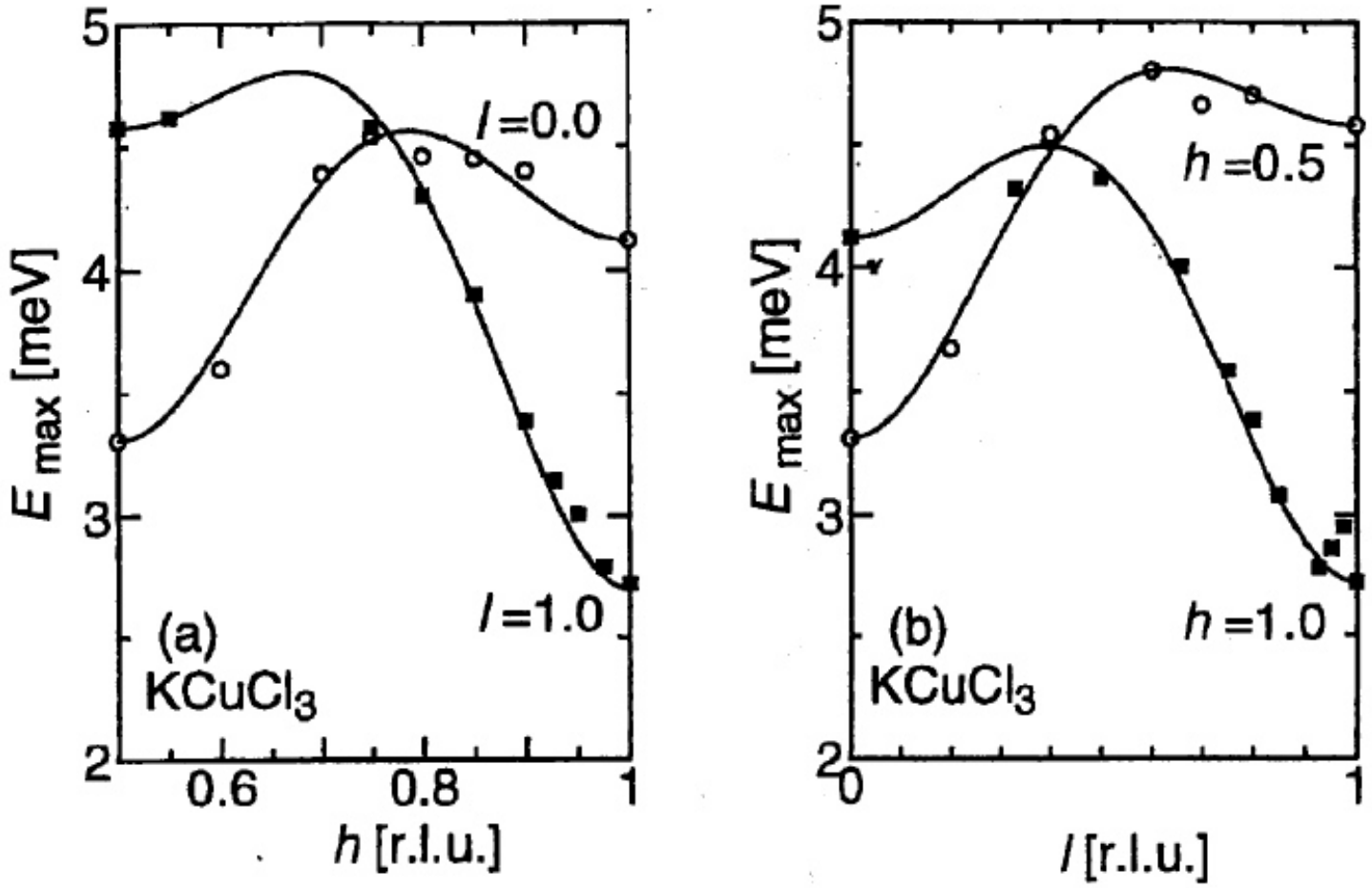

Fig. 4. The dispersion relation $\omega(k)$ of $KCuCl_3$ for k changing (a) parallel and (b) perpendicular to the double chain.

Not very strong 1-D (ladder) character

Weakly coupled dimers

RPA : $E = \sqrt{J^2 - J\,J(q)}$

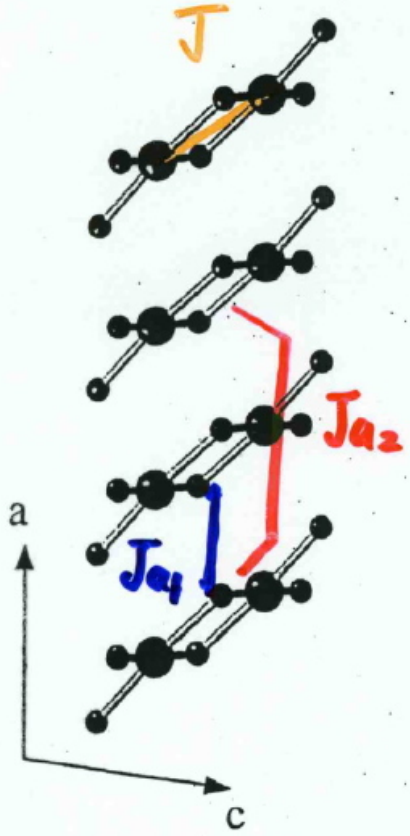

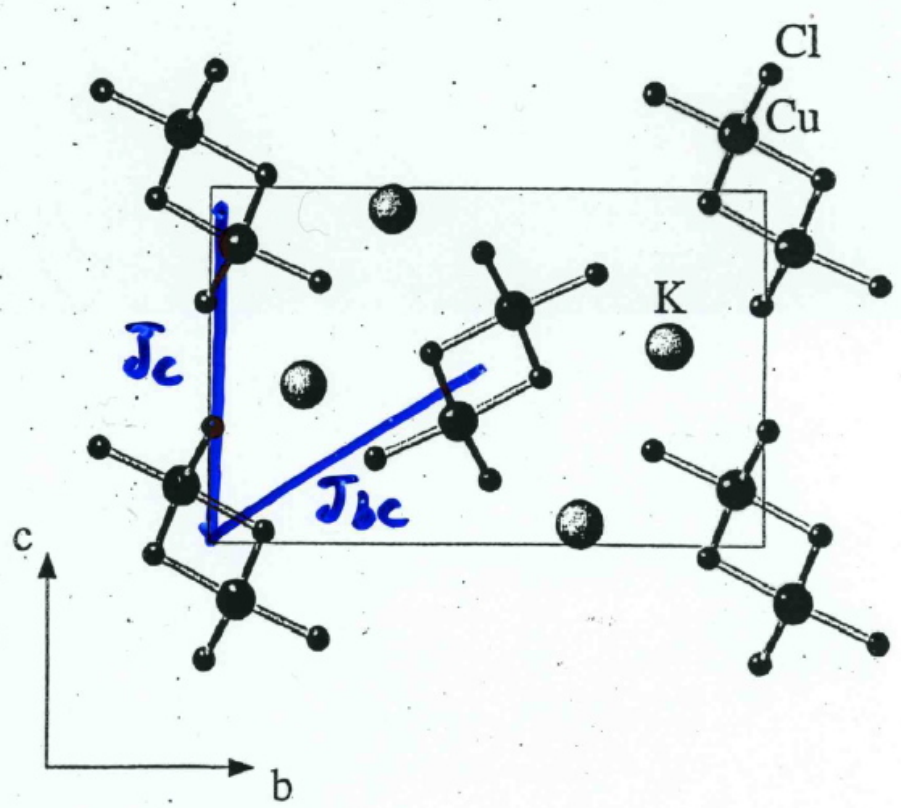

Random Phase Approximation

$$E = \sqrt{J_d^2 - J_d J(\boldsymbol{q})}$$

$$J(\boldsymbol{q}) = 2J_{a2c}\cos\{4\pi(h+l/2)\}$$
$$+4J_{abc}\cos\{2\pi(h+l/2)+\pi k\}$$
$$+2J_{a2}\cos\{4\pi h\}$$
$$+2J_{a}\cos\{2\pi h\}$$
$$+2J_{bc}\cos\{\pi l+\pi k\}$$

$J(r_0-r_i)$	r_i	meV
J_{a1}	(1 0 0)	0.222(6)
J_{a2}	(2 0 0)	0.389(6)
J_c	(0 0 1)	0.352(6)
J_{bc}	(0 ½ ½)	0.014(2)
J_{abc}	(1 ½ ½)	-0.326(4)
J = -4.638(6) meV		

Summary

Inelastic neutron scattering investigation unequivocally shows that $KCuCl_3$ is a weakly coupled dimer system with a singlet ground state and first triplet excited state, which propagates due to the inter-dimer coupling.

Inelastic neutron scattering is an unique and important tool to investigate the microscopic nature of the quantum magnets

Concluding remark

Versatility of the triple axis spectrometer

Importance of the neutron magnetic scattering investigation on the spin dynamics by means of triple axis spectroscopy

Complementarity to the ToF spectroscopy at pulsed neutron source, i.e. flexibility in the choice of the sample environment and utilization of the advanced polarized neutron techniques such as neutron polarimetry

Thank you for your attention!